

UNIVERSITÄTSKLINIKUM HAMBURG-EPPENDORF

Institut für Klinische Chemie und Laboratoriumsmedizin

Director: Prof. Dr. med. Dr. rer. nat. Thomas Renné

Efficiency of tissue homogenization via picosecond infrared Laser (PIRL) and mechanical homogenization as sample preparation step for proteomics

Dissertation

zur Erlangung des Doktorgrades PhD
an der Medizinischen Fakultät der Universität Hamburg.

vorgelegt von:

Refat Nimer
aus Amman-Jordan

Hamburg 2016

Angenommen von der

Medizinischen Fakultät der Universität Hamburg am: 21.02.2017

Veröffentlicht mit Genehmigung der

Medizinischen Fakultät der Universität Hamburg.

Prüfungsausschuss, der/die Vorsitzende: Prof. Dr. Hartmut Schlüter

Prüfungsausschuss, zweite/r Gutachter/in: Prof. Dr. med. Tobias Lange

*Dedicated to
my beloved mother and Father
and to my beloved wife Feda'
and my sweet sons Laith & Omar*

Part of this work was published in Journal of Proteomics 134 (2016): 193-202[1]

Table of Contents

Dedication.....	iii
Table of Contents	v
1 Introduction	1
1.1 Proteomics	1
1.1.1 Mass spectrometry in proteomics.....	2
1.1.2 Proteomics approaches.....	3
1.1.3 Sample preparation in proteomics.....	4
1.1.4 Protein species.....	6
1.2 Homogenization of biological samples.....	7
1.2.1 Protein stability during the homogenization process	8
1.3 Picosecond infrared laser (PIRL)-Desorption by impulsive excitation of intramolecular Vibrational states (DIVE)	11
1.3.1 Laser overview	11
1.3.2 Homogenization tissue via PIRL-DIVE.....	11
1.4 Hypothesis	13
1.5 Aims	13
2 Materials and Methods	14
2.1 Materials.....	14
2.1.1 Laboratory devices	14
2.1.2 Chemicals, reagents, and kits	16
2.1.3 Biological materials	17
2.1.4 Consumables	18
2.1.5 Software	19
2.2 Methods	19
2.2.1 Sample collection	19

2.2.1.1 Porcine muscle tissue	19
2.2.1.2 Rat pancreas	20
2.2.2 Histology	20
2.2.3 PIRL-DIVE homogenization	20
2.2.3.1 PIRL-DIVE homogenization of porcine muscle tissue and protein extraction	22
2.2.3.2 PIRL-DIVE homogenization of rat pancreas sample and protein extraction	22
2.2.3.3 PIRL-DIVE homogenization of rat pancreas spiked with alpha-casein and protein extraction.....	23
2.2.4 Mechanical homogenization	23
2.2.4.1 Mechanical homogenization and protein extraction of porcine muscle tissue	23
2.2.4.2 Mechanical homogenization and protein extraction of rat pancreas.....	23
2.2.4.3 Mechanical homogenization of rat pancreas spiked with alpha-casein and protein extraction.....	23
2.2.5 Determination of protein concentration	24
2.2.5.1 Bicinchoninic acid (BCA) assay	24
2.2.5.2 UV spectrophotometric protein quantification.....	24
2.2.5.3 2-D Quant Kit.....	25
2.2.6 Two-dimensional gel electrophoresis (2DE)	26
2.2.6.1 Image analysis of two-dimensional electrophoresis gels.....	26
2.2.7 Sodium Dodecyl Sulfate Polyacrylamide Gel Electrophoresis (SDS-PAGE).....	26
2.2.8 Tryptic in-gel digestion	27
2.2.9 LC-MS/MS analysis.....	27
2.2.9.1 LC-MS/MS analysis from mechanical and PIRL homogenates from porcine muscle tissue	27

2.2.9.2 LC-MS/MS analysis from mechanical and PIRL homogenates	
from rat pancreas and spiked rat pancreas with alpha-casein	28
2.2.10 Bioinformatic data analysis.....	29
2.2.10.1 LC-MS/MS raw data from 2DE of PIRL and mechanical	
homogenates from porcine muscle tissue	29
2.2.10.2 LC-MS/MS raw data from SDS-PAGE of PIRL and mechanical	
homogenates from rat pancreas and spiked experiment with	
alpha-casein.....	29
3 Results.....	30
3.1 Comparison of the protein composition in picosecond infrared laser	
(PIRL) homogenate (PH) and in mechanical homogenate (MH).....	30
3.1.1 Comparison between two-dimensional gel electrophoresis (2DE)	
patterns of the PIRL homogenate (PH) and mechanical	
homogenate (MH) of porcine muscle tissue	31
3.2 Comparison of the protein composition in the picosecond infrared	
laser (PIRL) homogenate (PH) and in the mechanical homogenate (MH)	
in the presence of Laemmli buffer	35
3.2.1 Histological examination, comparison between tissue samples used	
for PIRL tissue homogenization (PTH) and mechanical	
tissue homogenization (MTH)	40
3.2.2 Comparison of the protein composition in the PIRL homogenate (PH)	
and in the mechanical homogenate (MH) by one-dimensional gel	
electrophoresis.....	42
3.2.3 Construction of protein species migration profiles of the SDS-PAGE	
of the PIRL homogenate (PH) and the mechanical homogenate (MH)	44
3.2.4 Examination of migration profiles of the SDS-PAGE of the	
PIRL homogenate (PH) and the mechanical homogenate (MH)	48

3.2.5 Global statistical analysis of the LC-MS/MS data from the SDS-PAGE of the PIRL homogenates (PH) and the mechanical homogenates (MH) from rat pancreas (n=3)	66
3.3 Comparison of the recovery rate of alpha casein spiked in rat pancreas and homogenized via PIRL-DIVE and mechanical in the presence of urea and thiourea as lysis buffer	75
3.3.1 Histological examination, comparison between tissue samples used for PIRL- DIVE and mechanical tissue homogenization.....	75
3.3.2 Separation of proteins in PIRL homogenate (PH) and mechanical homogenate (MH) by one-dimensional gel electrophoresis	77
3.3.3 Comparison of the degradation, recovery rate and the number of identified phosphopeptides between PIRL homogenates (PH) and in mechanical homogenates (MH)	79
4 Discussion	89
5 Summary-Zusammenfassung.....	103
a) Summary	103
b) Zusammenfassung.....	105
6 Abbreviations.....	106
7 References	109
8 Appendix	121
9 Acknowledgement	126
10 Curriculum Vitae	128
11 Eidesstattliche Versicherung.....	131

1 Introduction

1.1 Proteomics

Proteins are organic molecules, consisting of amino acids linked to each other by peptide bonds [2]. Proteins have a diversity of functions, playing crucial roles in all biological processes such as catalysis of chemical reactions in the cell, transportation and storage of other molecules, generation of movement, and control of growth and differentiation [2-5].

The starting point of the proteomics field was in 1975 by the invention of two-dimensional gel electrophoresis and mapping of proteins from the bacterium *Escherichia coli* [6, 7]. Also, Klose et.al in his study on mouse tissue was able to map the proteins based on the 2D PAGE technique [8].

In 1995 the term „proteomics“ was coined by Marc Wilkins while doing his Ph.D. [9]. This term describes the complete set of proteins which is expressed and modified by the entire genome in the lifetime of the cell, throughout the lifetime of the organism [9-12]. This means that if we want to study the proteome of the particular organ, we have to describe all proteins in each cell type with respect to a time frame.

Since 1995, the field of proteomics started to grow rapidly due to the progress in the area of molecular biology. On the other hand, this led to a large body of sequence data due to the development of new techniques in the analysis of proteins, in particular mass spectrometric techniques [11, 12]. Also, the scope of what was summarized under the term proteomics widened since its invention. According to Fields et.al [13] proteomics includes not only the identification and quantification of the proteins, but also the determination of their localization, modifications, interactions, activities, and, ultimately, their function.

The significance of the field of proteomics is a result of the overwhelming importance of proteins, which have a leading role in all biological processes in the cell.

In the past, researchers focused on individual genes to study the function proteins [14]. However, the investigation of the gene by which a protein is coded is not sufficient to understand the actual function of a protein [15]. By looking only at the gene, lots of information about the protein for which that particular gene is coding remains missing. In order to obtain information like the cellular distribution and concentration of proteins, in which organ and part of the organism and compartment of the cell they are present and which functions they may have, we have to look at the proteome, which provides directly information on the structure and usually hints at the function of the proteins [7].

Contrary to the genome, which is static, the proteome is highly dynamic. The protein expression pattern in the cells of an organism varies depending on the intra- and extracellular environmental events. For instance, heat stress on certain strains of bacteria leads to the synthesis of proteins, which let these types of bacteria survive under the heat stress [16]. In addition, alternative splicing of mRNAs and a broad range of posttranslational modifications (e.g., phosphorylation, glycosylation, and ubiquitination) increase the proteome complexity [15, 17].

Nowadays, it's obvious that proteomics techniques are the methods of choice in various applications such as in the analysis of post-translational modifications (PTM), identifications [18-20], protein-protein interactions [21, 22], analysis of protein expression [23, 24] and in the search for new biomarkers [25, 26].

1.1.1 Mass spectrometry in proteomics

One of the most popular, powerful and comprehensive tools in large-scale proteomics is mass spectrometry (MS) [27, 28].

Basically, as shown in figure 1, this analytical instrument is made up of an ion source, which is responsible for ionizing the molecules, a mass analyzer to separate ions in the gas phase according to their mass-to-charge ratio, a detector and finally a data entry to process the data. At the end, the results are visualized by an m/z vs intensity plot in a mass spectrum. This experimental mass spectrum can be compared to theoretical spectra from a database of known sequences to find the sequence that matches best, using a variety of popular database search tools [29].

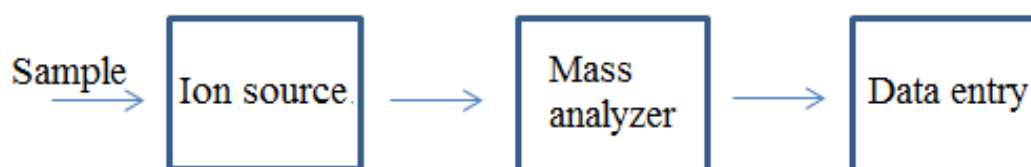


Figure 1: Basic scheme of a mass spectrometer

A revolution in the use of mass spectrometry, which opened the door for starting proteomics research, occurred by the invention of soft ionization techniques, which enabled the transfer of proteins and peptides into gas phase without fragmentations of ions. Thereby these biomolecules can be analyzed by mass spectrometry [30, 31].

By coupling two mass analyzers (called tandem mass spectrometer) it became possible to isolate ions with a particular m/z ratio out of a mixture, fragment it by various techniques and acquire the fragment spectrum. This so called MS/MS spectrum provides information on the mass of the intact molecule and its fragments [32]. This information can be used to identify the molecule with high accuracy, either by comparison with a database or by manual inspection.

Nowadays mass spectrometry has become the dominant and indispensable tool used in virtually all proteomics applications such as protein identification, detection of post-translational modifications, and in the assessment of the quality of recombinant proteins [33].

1.1.2 Proteomics approaches

In proteomics, we have two classical approaches; bottom-up and top-down proteomics.

Even though the full information of a protein is not obtained in the bottom-up proteomic approach, it is still widely used in proteomics because of its practical advantages [34, 35].

The workflow of a bottom-up experiment starts with the extraction of the proteins from the biological source and proteolytic (typically tryptic) digestion of the proteins. The resulting peptide mixture is separated, typically via reverse phase chromatography and the separated peptides are injected into the mass spectrometry for analysis. Finally, the data obtained from mass spectrometry are searched by database search algorithms for protein identification (Figure 2) [36].

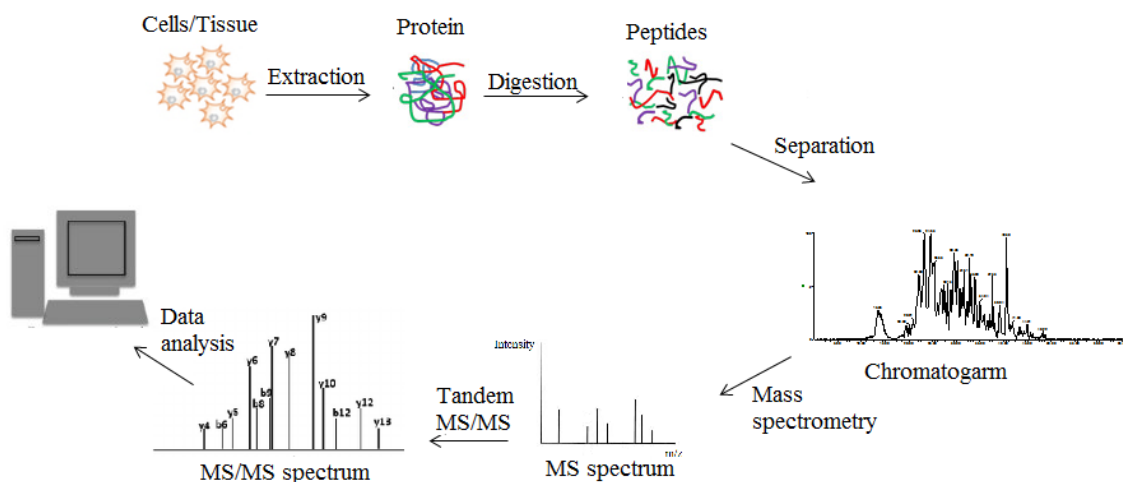


Figure 2: Bottom-up proteomics approach workflow

In top-down proteomics approach on the other hand, intact proteins are analyzed by mass spectrometry. Again starting with the extraction of the proteins from the source, the protein mixture is separated to reduce their complexity without enzymatic digestion. As in the case of the bottom-up proteomics approach, the intact proteins are introduced into the mass spectrometer. The mass data of the intact and, if available, the fragment data are searched against the database to identify the proteins (Figure 3) [35, 37].

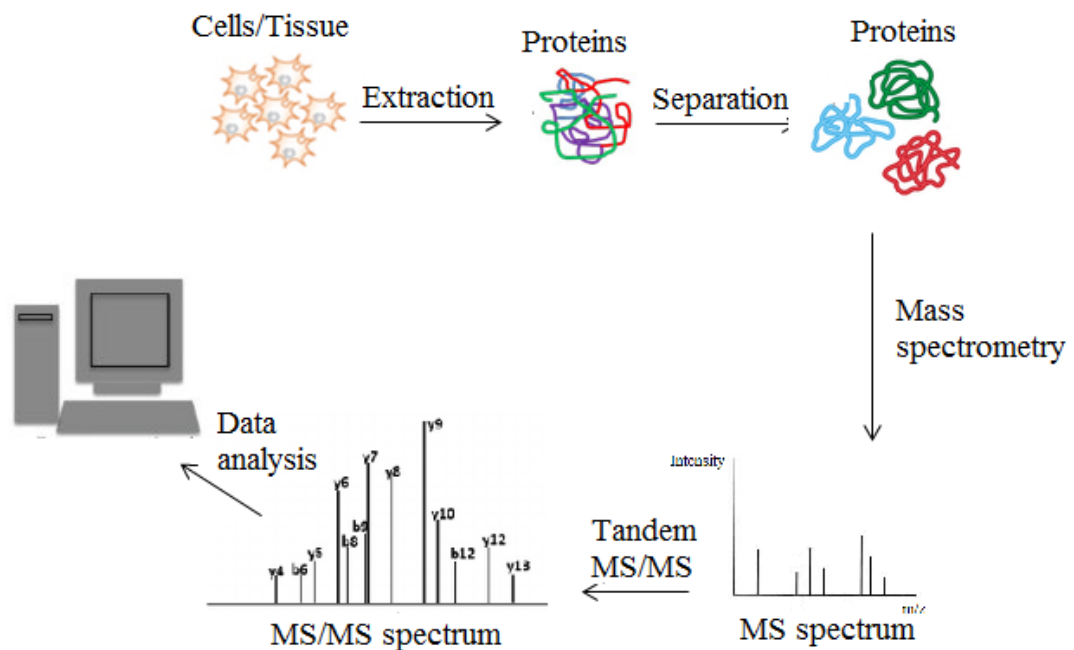


Figure 3: Top-down proteomics approach workflow

1.1.3 Sample preparation in proteomics

Sample preparation constitutes one of the most important steps in a proteomics workflow, because at this stage artifacts can be introduced and often affect the quality of the results [38]. This correlation between sample preparation steps and the quality of results shows why the proper handling of the sample is of utmost importance [39].

The complex nature of proteomes represents one of the most demanding challenges in proteomics in general and especially in sample preparation. Due to this complexity and variability of proteomes, it is at present not possible to name a single method as the „gold standard“ for proteomics sample preparation.

Proteins can be extracted from various biological sources such as cells, body fluids, tissue, etc. The extracted proteins have variations in their properties depending on the composition of

their amino acids, thereby making it more complicated to study the proteome than the genome. The chemical structures of all genes are polyanionic polymers with the negative charge because of a phosphate group; this means that DNA and RNA behave very similar, unlike the proteins.

We can't deal with all properties of proteins at the same time: some proteins are hydrophilic and highly soluble in water, others are hydrophobic like membrane proteins anchored in the lipid bilayer and may be lost during preparation, and some may precipitate because they stick together and can be kept in solution only in the presence of detergents.

Another challenge in proteomics is the huge dynamic ranges of proteins [40, 41]. The abundance of proteins can differ widely, for example, dynamic ranges vary from less than 50 to more than 10^6 molecules per cell in yeast [42] or in the case of plasma proteins by more than 10^{10} [42].

Proper preparation of samples in proteomics is necessary to reduce the complexity of the sample and the dynamic range of proteins to facilitate the access to less abundant proteins [43].

The improvement in detection of low abundance proteins is essential for the design of new therapeutic biomarkers [44].

Various techniques in pre-fractionation are used to reduce sample complexity before injected to mass spectrometry like chromatography, centrifugation, and electrophoresis [45].

In general, sample preparation includes many procedures and workflows starting from obtaining the samples from their sources, homogenization, extraction, digestion, and various chromatographical techniques for fractionation and enrichment.

Basically, it is essential to keep the sample as clean as possible by avoiding contaminations like keratin as they may result in the suppression of peptides of interest during mass spectrometry measurement. In any case, unwanted contaminations will increase the complexity of the mass spectrum [46].

In addition, it's highly recommendable to avoid using detergents if you plan to measure your samples by mass spectrometry. The use of detergents may interfere with the HPLC separation and the peptide ionization and also add to the chemical noise or background in the mass spectra [39].

1.1.4 Protein species

The term protein species was proposed in 1996 by Jungblut et al. to describe different forms of proteins in connection with their exact chemical composition [47-49]. To better and comprehensively understand how cellular processes function in health and disease states, we should analyze the proteome at the level of protein species. Contradictory to the old central dogma of molecular biology, it is now known that one gene encodes many protein species that differ in their function. These protein species result from protein post-translational modifications, alternative mRNA splicing, and proteolytic processing due to a disease condition or drug treatment [50, 51].

A nice example how different protein species with different functions can be derived from a single gene product is given in the review of Schlüter et.al [49], which highlights the importance of knowing the exact chemical compositions of protein species. The protein angiotensin-converting enzyme (ACE) is present in two different species in the cell and fulfills different functions. Germinal ACE (gACE) has a role in the regulation of blood pressure, and somatic ACE (sACE) is involved in male fertility.

We are able by a high-resolution method known as two-dimensional electrophoresis (2DE) to resolve more than 10,000 spots per gel and to separate one protein into its different protein species [52]. Due to the different chemical composition of these protein species, a change in molecular mass and charge leads to the appearance of different spots in 2DE [51]. However, 2DE is unable to resolve all proteins in a sample such as hydrophobic membrane proteins [53-55] and proteins with a very high or low molecular weight [56].

By using 2DE Jungblut et al. [57] were able to detect about 1,800 protein species of *Helicobacter pylori* cellular proteins. Rosal-Vela et al. [58] were able to identify six serotransferrin protein species using 2DE-MS. However, the study of protein species in consideration to their exact chemical composition still a challenge.

The analysis of protein species using a bottom-up proteomics approach is problematic, since the tryptic peptides released from proteins species, which are all coded for by one gene are mixed together and we cannot assign the peptide to a particular protein species. Thus the information, which post-translation modification occurred in a particular protein species, is lost [34, 59, 60].

Alternatively, in the top-down proteomics approach, intact proteins are subjected to mass spectrometry, which retains their individual post-translation modification status [35, 60, 61].

However, the limitations of this approach are on the one hand the technical difficulties in the handling of complex protein samples, and on the other hand the elaborate analysis of the fragment patterns of whole protein species. The ability of the bioinformatics tools to interpret these data is still limited [62].

In general, with all limitations and challenges, a complete analysis of protein species is still not reachable. Further improvement and new development of protocols and methods in proteomics, starting from the first step of sample preparation to the bioinformatics analysis tools is in high demand.

1.2 Homogenization of biological samples

The first step in proteomics experiments is the homogenization of the biological samples.

Because proteins are contained by the cytoplasmic membrane and many are further packed in various intracellular compartments, the extraction and solubilization of these safely packed proteins inside the cell requires the disruption of the cells and cellular compartments. Homogenization covers several meanings such as mixing, stirring, dispersing, emulsifying, but in general, it means transferring a sample into a solution with the same composition and structure in the whole volume [63].

Homogenization methods used for the proteomics purposes can be divided into five major types: 1. pressure; 2. ultrasonic; 3. mechanical; 4. freeze–thaw; 5. osmotic and detergent lysis [64]. The homogenization method of choice varies according to the type of samples. This variation in choosing the appropriate methods represents one of the limitations of classical homogenization methods. In the case of different cell lines, for example, one should optimize different homogenization processes according to the variations in the cytoplasmic and cytoskeletal organization of different tissue culture cells [65]. Pressure homogenizer, also called a French press, is an optimal and efficient system for homogenization of eukaryotic cells as well as microorganisms in suspension [63, 64].

Freeze–thaw homogenization depends on the effect of ice crystals forming in the tissue during the freezing process and is applicable for most of the bacterial, plant and animal cells in water solution. It can also be used as a final step after mechanical or ultrasonic homogenization [64, 66].

Osmotic and detergent lysis methods of disruption of cells depend on the action of osmotic pressure or detergent interactions to destroy the cell walls and membranes [64, 67].

Ultrasonic homogenization depends on shock waves to disrupt the cell, but is not appropriate for solid samples like tissues [68, 69].

For most types of tissue such as liver, bone, and muscle, the method of choice is mechanical homogenization [70-72]. The most common devices used for mechanical homogenization are rotor–stator homogenizers, bead-based disruptors and open blade mills [63, 68].

The ideal homogenate is obtained if all proteins are released from the organelles and other cellular constituents as a free suspension of intact and individual components [73, 74].

Afterwards, clarifying the samples to get rid of cell debris and insoluble components must be carried out by centrifugation or precipitation methods [75, 76]. This has limitations due to loss of proteins by adsorption to the surface, during homogenization, centrifugation, and precipitation [77]. In addition, in the case of incomplete homogenization, the sample usually needs to be processed by another method, which increases the risk of sample loss and may affect the integrity of proteins [78].

1.2.1 Protein stability during the homogenization process

The quality of homogenates is important not only to ensure the absence of organelle particles but also to preserve the exact chemical composition of protein and reduce the effect of endogenous enzymes on cellular protein during homogenization process.

Basically, applying a homogenization procedure leads to disruption of the compartment in the cell and liberates the endogenous enzymes, which comes in direct contact with cellular proteins, potentially susceptible to degradation or modification. If this is the case one can assume, that the exact chemical composition of the proteins is changed due to the action of these endogenous enzymes. An example of the effect of endogenous enzymes on the integrity of proteins during the homogenization process is the degradation which occurred in estrogen and progesterone receptors during mechanical homogenization of human breast tumor tissue and calf uterus [79].

Several endogenous enzymes play a role in changing the chemical composition of proteins in vitro such as proteases and phosphatases.

The proteolytic enzymes such as proteases cleave the proteins by a hydrolysis reaction, leading to the addition of a molecule of water to a peptide bond as shown schematically in figure 4 [2].

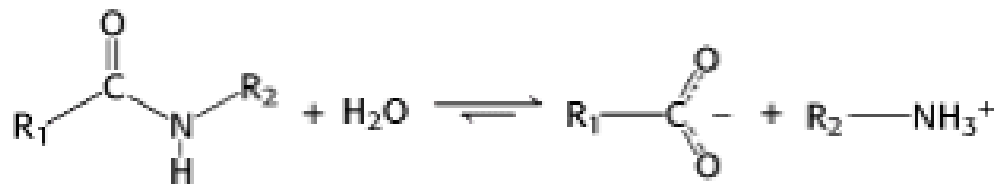


Figure 4: hydrolysis reaction[2]

The proteases enzymes can be classified into[80]:

1. Serine proteases - using a serine alcohol
2. Cysteine proteases - using a cysteine thiol
3. Threonine proteases - using a threonine secondary alcohol
4. Aspartic proteases - using an aspartate carboxylic acid
5. Glutamic proteases - using a glutamate carboxylic acid
6. Metalloproteases - using a metal, usually zinc

These enzymes are present in all tissue with variation in their activities and between the tissue types. Therefore the susceptibility to degradation by endogenous enzymes depends on the type of protein and the type of tissue. For instance contains liver tissue higher protease levels than others [81].

The other important endogenous enzymes that affect the integrity of proteins are phosphatases. Phosphatases catalyze the hydrolytic removal of a phosphate group attached to protein [2].

Reducing possible protein degradation and changes in the exact chemical structure of the proteins are vital if we want to have profound knowledge about protein species. In addition, the action of liberated endogenous enzymes after cell disruption may create new artifacts that will lead to further complications in the analysis of a proteome [63]. Therefore, many protocols and methods have been applied in an attempt to prevent sample degradation catalyzed by the endogenous enzymes.

Protease and phosphatase inhibitors are used to help preventing degradation and dephosphorylation of proteins during protein preparation [82]. However, care should be taken that by such inhibitors adducts and charge trains are not introduced [24].

Olivieri et.al [82] compared the effect of proteases on red blood cell membranes before and after adding protease inhibitor. Significant differences between the 2D patterns of red blood cell membranes were shown with reduced recovery of high molecular weight proteins in the case of the sample without added protease inhibitor [82].

The commercial proteases inhibitor cocktails inhibit a broad range of protease. However, it has been recommended to add specific protease inhibitors beside commercial inhibitor cocktails, such as Phenylmethylsulfonyl fluoride (PMSF), to enhance the range of the inhibition [63].

Another example to prevent degradation by endogenous enzymes during the homogenization process is using strong acidic or basic conditions [83, 84].

Further methods for inhibiting the action of enzymatic degradation are available such as use of organic solvents [85], microwave irradiation [86, 87], incorporation of thiourea with urea for the inhibition of the proteolysis [88], boiling the sample in SDS buffer with high-pH Tris base, or by lowering the pH and performing ice-cold (20% TCA) precipitation [89], and boiling in water [90]. However, the diversity of the proteases, which may be present in the sample, further complicates the inhibition process [88, 91] and make choosing the proper method for the inhibition of degrading enzymes difficult.

An additional limitation in the choice of buffers and chemicals use to stop the action of endogenous enzyme is their compatibility with the intended downstream processing steps. For example, SDS denatures and inactivates most proteins and enzymes, including proteases, it is, however, not suitable for functional studies because it denatures proteins, nor is it suitable for analysis by reverse phase chromatography (RPC) because of its interference with the separation [92].

The delay in the time required to obtain the samples from their sources, sample preparation, homogenization and protein extraction is considered one of biggest challenges and the related problems need to be resolved in order to determine the exact structure and chemical composition of proteins *in vitro*.

For example, obtaining the samples after surgery is associated with loss of vascular supply, resulting in a progressive increase of endogenous protease activity, protein degradation, and tissue autolysis [93].

The effect of time has been shown in brain tissue where significant changes in the level of several PTMs within minutes post mortem have been demonstrated [86].

Several protocols and techniques like laser-capture microdissection were proposed to improve the quality of sample tissue by a decrease in the time during sample collection in order to preserve the molecular integrity of the proteins [94-97].

In general, time is critical in the gathering and preparing samples. Therefore the preanalytical procedures must be standardized to a maximum with minimizing the time of process to avoid degradation or dephosphorylation in protein samples [98].

1.3 Picosecond infrared laser (PIRL)-Desorption by impulsive excitation of intramolecular Vibrational states (DIVE)

1.3.1 Laser overview

The term Laser is the acronym for „light amplification by stimulated emission of radiation.“ The first laser sources were built by Maiman in 1960 and almost directly their clinical use was demonstrated [99, 100].

The term amplification in laser physics means a process where the medium transfers part of its energy to the emitted electromagnetic radiation, leading to an increase in optical power.

Based on the gain medium, lasers are categorized into: gas lasers such as nitrogen laser, chemical lasers such as deuterium fluoride laser, dye lasers, metal-vapor lasers such as helium–selenium, and solid-state lasers such as Nd: YAG (Neodymium-doped Yttrium Aluminium Garnet) laser.

1.3.2 Homogenization tissue via PIRL-DIVE

The application of lasers in clinical use is still limited due to the side effect of thermal energy by damaging the surrounding tissue.

Recently, Prof. Dwayne Miller and his group have developed a new concept of laser system called picosecond infrared laser (PIRL) [101, 102].

This laser system is a solid-state laser using medium Neodymium-doped yttrium lithium fluoride (Nd: YLF).

This new laser technology has several advantages in surgical applications compared to conventional lasers or cold instruments. PIRL laser enables precise ablation in the cellular

dimension, causes less cellular damage of surrounding tissue and therefore nearly avoids the formation of scars [103].

The ablation process via PIRL is based on a mechanism called Desorption via Impulsive Vibrational Excitation (DIVE).

The principle behind PIRL-DIVE is that the infrared laser beam is directed on tissue which has water content of about 70%, for an extremely short pulse duration (300 ps) at the wavelength $\lambda = 2.96 \mu\text{m}$, tuned to excite the OH vibration stretch band in water [103]. In the range of Infrared (IR), the hydrogen bonds of the water molecules take up the energy from the laser. Because of very fast pulses of the IR laser, the energy absorbed by the hydrogen bonds in the water molecules and turned into translational energy causes the water molecules to burst out of the tissue, forming an aerosol of droplets and taking along all the contents of the cell. Since this process occurs very fast before nucleation growth can take place, the translational energy cannot be converted to thermal energy and diffuse to adjacent tissue [104]. Water with biomolecules from inside of the tissue are transferred into the gas phase in an ablation plume within a picosecond time scale [101].

The possibility of ultra-fast tissue ablation by PIRL-DIVE is not only relevant in surgery, where it allows a more accurate and gentle removal of tissue, which is less damaging to the surrounding tissue, but also provides an opportunity to obtain material for biochemical analysis by a gentle procedure. Because the PIRL ablation is ultrafast, no diffused heat energy is generated, which otherwise would potentially affect the conformation or even the chemical structure of the proteins. Within the PIRL plume the native enzymatic activity and the nature of extracted biological are preserved. Therefore, this whole process guarantees a soft extraction of biomolecules [105, 106].

The homogenization of tissue via PIRL is highly efficient for tissue with a high content of water [1, 106, 107]. However, successful attempts have also been made at hard tissue. Jowett et.al [108] demonstrated for bone, Franjic et.al in his study on tooth [102], that no significant thermal effect by using PIRL were observed.

1.4 Hypothesis

Previous work from Bottcher et al. [109] has shown, that it is possible to cut tissues via Picosecond infrared laser (PIRL) for surgery and according to Kwiatkowski et al. [106] PIRL can release proteins from tissues in intact form.

Based on the previous work by Kwiatkowski et al. [106] it can be hypothesized that because of the ultrafast homogenization process of the tissues via PIRL; the proteins are exposed to the enzymatic action of proteases only for a very short time interval, which would enable a soft extraction of proteins from tissues.

1.5 Aims

The main aim of our study is to investigate this hypothesis through three main experiments: First, to investigate if we have fewer changes of the in-vivo protein composition in PIRL homogenates (PH) compared to mechanical homogenates (MH). For this purpose tissue are homogenized either with PIRL or mechanically and both protein extracts analyzed via two-dimensional gel electrophoresis (2DE).

Secondly, to investigate how PIRL and mechanical homogenates behave in hot Laemmli buffer and to study the degree of differences between both homogenates.

Thirdly, to validate previous results regarding protein degradation, determine a recovery rate and to get a first hint concerning the behavior of phosphoproteins in the PIRL process.

2 Materials and Methods

2.1 Materials

2.1.1 Laboratory devices

Instrument	Supplier
Ablation box (dimensions : 9 cm x 7.5 cm x 10.5 cm)	Built by Wesley Robertson (Max Planck Institute for Structure and Dynamics of Matter, Hamburg, Deutschland)
ACQUITY UPLC PST C18 nanoACQUITY Column 10K psi, 130Å, 1.7 µm, 75 µm X 200 mm	Waters (Manchester, UK)
ACQUITY UPLC PST C18 nanoACQUITY Trap 10K psi MV, 100Å, 5 µm, 180 µm X 20 mm	Waters (Manchester, UK)
Analytical balance ALS 120-4	Kern & Sohn GmbH (Balingen-Frommern, Germany)
Bandelin Sonopuls HD 2070 ultrasonic homogenizer	Bandelin Electronic(Berlin, Germany)
Cooling trap RCT90	Thermo Scientific (Waltham, USA)
Gel Doc XR+	Bio-Rad Laboratories (Munche, Germany)
Lyophilizer (model Christ Alpha 1-4)	(B. Braun Biotech International, Germany),
Membrane pump MZ 2C VARIO	VACUUBRAND GmbH & CO KG, Wertheim, Deutschland
nanoACQUITY UPLC System	Waters (Manchester, UK)

Nanodrop® ND-1000	NanoDrop (Wilmington, USA)
New Objective SilicaTip™ Emitter	New Objective (Woburn, USA)
Orbitrap fusion mass spectrometer	Thermo Scientific (Waltham, USA)
pH-Meter Φ 72	Beckmann Coulter (Krefeld, Deutschland)
Pico second-Infrared-Laser PIRL-HP2-1064 OPA-3000	Attodyne, Toronto, Canada
Q-TOF Premier	Micromass/Waters (Manchester, UK)
Refrigerated centrifuge 4-16K	Sigma (Osterode, Deutschland)
Speed Vac concentrator 5301	Eppendorf AG (Hamburg, Deutschland)
Table Centrifuge	Sigma-Aldrich (Steinheim, Deutschland)
Table Centrifuge Eppendorf 5415 C	Eppendorf 8Hamburg, Germany)
Thermo mixer 5320	Eppendorf AG (Hamburg, Deutschland)
Vacuum centrifuge Jouan RC1010	Thermo Scientific (Waltham, USA)
Vacuum pump ValuPump VLP120	Thermo Scientific (Waltham, USA)
Vacuum pump CVC 2000	Vacuubrand (Germany)

2.1.2 Chemicals, reagents, and kits

Substance	Supplier
10% Criterion™ XT Bis-Tris Gel, 18 well, 30 µl	Bio-Rad Laboratories (Germany)
2-beta mercaptoethanol	Bio-Rad Laboratories (Germany)
2x Laemmli Buffer	Bio-Rad Laboratories (Germany)
2D Quant-Kit	GE Healthcare Life Sciences(Freiburg, Germany)
Acetonitril (LiChrosolv®)	Merck (Darmstadt, Germany)
Ammonium bicarbonate	Merck (Darmstadt, Deutschland)
BCA test kit	Thermo Scientific (Germany)
Complete protease inhibitor cocktail	(Roche Diagnostics Ltd, Mannheim, Germany)
Dithiotrietol	Sigma-Aldrich (Steinheim, Germany)
Dulbecco phosphate buffered saline	Bio-Rad Laboratories (Germany)
Ethanol (LiChrosolv®)	Merck (Darmstadt, Germany)
Formic acid	Merck (Darmstadt, Germany)
Glycerol	Sigma-Aldrich (Steinheim, Germany)
Iodoacetamide	Sigma-Aldrich (Taufheim, Germany)
Methanol (LiChrosolv®)	Merck (Darmstadt, Germany)
See blue plus 2 prestained standard	Invitrogen (Kahlsruhe, Germany)
Sodium dodecyl sulfate (SDS)	Fluka
Sodium hydrogen carbonate	Merck (Darmstadt, Germany)

Trifluoroacetic acid	Sigma-Aldrich (Steinheim, Germany)
Trizma base	Sigma-Aldrich (Steinheim, Germany)
Tris	Bio-Rad Laboratories (Munche, Germany)
Trypsin Resuspension buffer	Promega (Mannheim, Germany)
Thiourea	Sigma-Aldrich (Steinheim, Germany)
Urea	Amersham (Freiburg, Deutschland)
Water (LiChrosolv®)	Merck (Darmstadt, Germany)
XT MES 4x	Bio-Rad Laboratories (Munche, Germany)
XT Reducing agent 20x	Bio-Rad Laboratories (Munche, Germany)

2.1.3 Biological materials

Material	Supplier
Alpha-S1/S2-Casein	Sigma-Aldrich (Steinheim, Germany)
Pancreas tissues	Dr. Hannes Petersen (UKE, Klinik und Poliklinik für Hals-, Nasen- und Ohrenheilkunde)
Porcine muscle tissue	slaughter-house
Trypsin	Sigma-Aldrich (Steinheim, Germany)

2.1.4 Consumables

Material	Supplier
Centrifuge filter(10 kDa cut-off)	(Merck Millipore, Darmstadt,Germany)
Centrifuge tubes 15 mL, 50 mL	Greiner (Melsungen, Germany)
Eppendorf tube(0.5 ml , 1.5 ml ,2 ml)	Eppendorf (Hamburg, Germany)
Fused-Silica-Kapillaren O.D. 360 µm, I.D. 75 µm	Postnova Analytics GmbH (Landsberg am Lech, Germany)
GeLoader pipette tip 10 µL	Eppendorf (Hamburg, Germany)
Pipette tips 10 µL, 200 µL, 1000 µL	Eppendorf (Hamburg, Germany)

2.1.5 Software

Software	Supplier
Andromeda	Thermo Scientific, Bremen, Germany
eulerAPE v3	http://www.eulerdiagrams.org/eulerAPE/
Graph Pad Prism 4	Graph Pad Software, Inc. (San Diego, USA)
Image Lab™ 5.0	Bio-Rad Laboratories
Magellan version 5.0	Tecan(Männedorf, Switzerland)
MassLynx 4.1	Waters (Manchester, UK)
MaxQuant (version 1.5.2.8)	http://maxquant.org
Microsoft Excel, word, power point 2010	Microsoft Corporation
ProteinLynx 2.5.2 Waters	(Manchester, UK)
Wolfram Mathematica 9.0.1.0	Wolfram Research (Oxfordshire, UK)
Xcalibur™ 2.1	Thermo Scientific, Bremen, Germany

2.2 Methods

2.2.1 Sample collection

2.2.1.1 Porcine muscle tissue

Porcine (*Sus scrofa domestica*) muscle tissues used for this experiment were obtained commercially from the public slaughterhouse and directly treated after the animal was killed to minimize postmortem tissue changes. Fresh pieces of muscle (5 cm x 5cm) were cut and transferred directly to liquid nitrogen, then later stored at -80°C for proceeding the experiments.

2.2.1.2 Rat pancreas

The pancreas was taken from six different Wistar rats directly after proper euthanasia by carbon dioxide inhalation. All animal experiments were supervised by the institutional animal welfare officer at the University Hospital Hamburg-Eppendorf (UKE) and approved by the local licensing authority (Amt für Gesundheit und Verbraucherschutz; Billstr. 80, D-20539 Hamburg, Germany).

Each pancreas tissue was cut in half, and tiny pieces were again cut from their edges for histological examination.

The pieces were frozen in liquid nitrogen immediately after preparation and stored at -80°C for further experiments.

2.2.2 Histology

The incised pieces from pancreas tissue samples were fixed in phosphate buffered 3.5% formaldehyde. Specimens were then embedded in paraffin, cut into 4- μm thick sections, and stained with hematoxylin and eosin (H.E., Merck, Darmstadt, Germany) [110]. Scanning of stained samples was performed using the MIRAX SCAN (Carl Zeiss Microimaging GmbH, Jena, Germany) [107].

2.2.3 PIRL-DIVE homogenization

The ablation experiments were performed by adapting a laser system (PIRL-HP2-1064 OPA-3000, Attodyne Inc., Toronto, Canada). The parameters were set up for this laser system under supervision of the physical staff from the group of Prof. R.J. Dwayne Miller (Max Planck Institute for the structure and dynamics of matter, Hamburg, Germany).

The generated wavelength was 3 μm with a pulse width of 300 ps and repetition rate of 1 kHz.

The samples were placed on a cold copper block inside a home-built chamber box; this cold copper block will maintain a low temperature of the sample to minimize the effect of protease enzymes. This ablation box was designed to minimize the loss of ablation plume, humidity effect and for safety purpose, then the laser beam was guided via a set of mirrors and focused on the surface of samples. Approximately 450 mW optical power was reached at the sample surface. The optical energy density at the sample surface was 3.4 J/cm^2 and the average optical power density was $3.4 \times 10^3 \text{ W/cm}^2$.

The laser started the ablation process over the samples with scanning speed 130 mm/s, square scan pattern of a dimension of approximately 5 mm x 5 mm and 2 mm in depth, and a focal spot diameter of 190 μm . The PIRL set up parameters are shown in table 1.

Table 1: PIRL settings and beam characteristics

Parameter	Value
Wavelength	3 μm
Pulse width	300 ps
Repetition rate	1 kHz
Average power	0.45 W
Optical energy density	3.4 J/cm ²
Average optical power density	3.4x 10 ³ W/cm ²

The generated plume via laser ablation on the surface of the sample was transferred and condensated in a wash bottle immersed in a Dewar flask containing liquid nitrogen to keep the ablated material frozen and minimize the effect of proteases enzymes. The process the ablation plume was done by a vacuum pump connected to the ablation box via metal tubes and PTFE tubes which are also connected to a washing bottle. The frozen condensates were kept at -80 °C for further experiments (Figure 5).

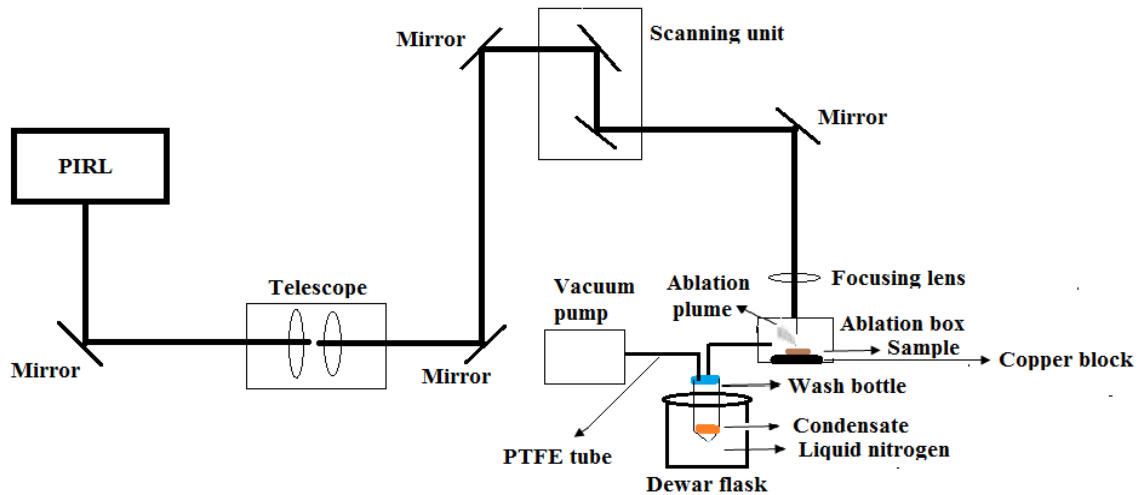


Figure 5: Schematic structure of PIRL and capturing ablation plume

2.2.3.1 PIRL-DIVE homogenization of porcine muscle tissue and protein extraction

Porcine muscle tissues were homogenized with PIRL according to Kwiatkowski et al. [111].

The samples were irradiated by picosecond infrared laser (PIRL). The ablation plume was collected as described above, mixed with 50 μ L 10X phosphate buffer solution (PBS, PH7.4), including Roche Complete protease inhibitor cocktail in a wash bottle. The volume was adjusted with HPLC-grade water to 500 μ L then the sample was ultrasonicated for 1 minute at magnitude 25-30%, centrifuged at 4°C for 10 minutes at 14000 rpm, the supernatant was collected in 2 ml Eppendorf tube. The sample was transferred to a 10 kDa cut-off centrifuge filter, centrifuged at 4°C for 20 minutes at 14000 rpm for removing fragmented DNA and then the retentate was collected in a two mL Eppendorf tube for further experiments.

2.2.3.2 PIRL-DIVE homogenization of rat pancreas sample and protein extraction

The rat pancreas tissue samples were homogenized via PIRL-DIVE according to Kwiatkowski et al. [111] and the ablation plume was captured in a wash-bottle. A volume of 100 μ L of 5X hot Laemmli buffer (0.225 M Tris-HCl, pH 6.8; 50% glycerol; 5% SDS; 0.05% bromophenol blue; 0.25 M DTT, T= 95°C) was added to the frozen condensates then directly transferred in a boiling water bath [1].

HPLC-grade water was added to adjust the final volume to 500 μ L, and the PIRL homogenates (PH) were incubated in the boiling water bath for 5 minutes. PIRL homogenates (PH) were centrifuged at 15000 x g for 3 min. The supernatants were transferred into a 2 mL Eppendorf tube for further experiments [1].

2.2.3.3 PIRL-DIVE homogenization of rat pancreas spiked with alpha-casein and protein extraction

The rat pancreas tissue samples for the spiking experiment were ablated via PIRL. The ablation plume was captured in a wash-bottle containing a powder of urea (m= 210.21 mg), thiourea (m= 76.12 mg), Tris-HCl (m= 1.82 mg) and 180 µg alpha-Casein (c= 1.8 µg/µL, dissolved in HPLC-grade water) [1].

After the ablation had been performed, HPLC-grade water was added to the PIRL condensates and adjusted to a total volume of 500 µL resulting in a final concentration of 7 M urea, 2 M thiourea, 30 mM Tris-HCl (pH 6.8). PIRL homogenates (PH) of spiked rat pancreas with alpha-casein were centrifuged at 15000 x g for 3 min. The supernatants were transferred into a two mL Eppendorf tube for further experiments.

2.2.4 Mechanical homogenization

2.2.4.1 Mechanical homogenization and protein extraction of porcine muscle tissue

Porcine muscle tissue was lyophilized in a bench top freeze-dryer (B. Braun Biotech International, model Christ Alpha 1-4, Germany), coupled to a Savant VLP 200 Vacuum Pump for two days. Lyophilized tissue was grounded to a fine powder with a mortar and a pestle, mixed with 1X phosphate buffer saline (PBS) including protease inhibitors. The homogenate was sonicated by a Bandelin Sonopuls HD 2070 ultrasonic homogenizer (Bandelin Electronic, Berlin, Germany) for 1 minute with a magnitude of 25-30%. The lysate was centrifuged for 10 minutes at 4°C at 14000rpm and the supernatant transferred to a 2 ml Eppendorf tube for further experiments.

2.2.4.2 Mechanical homogenization and protein extraction of rat pancreas

The comparable frozen piece of rat pancreas tissue samples was transferred to a 2 ml Eppendorf tube containing 500 µL lysis buffer (45mM M Tris-HCl, pH 6.8; 10% glycerol; 1% SDS; 0.01% bromophenol blue; 0.05 M DTT), then homogenized via a bead mill (TissueLyser II) with a 3mm stainless steel bead for 3.5 minutes at a frequency of 25/s[1].

Mechanical homogenates (MH) of rat pancreas were centrifuged at 15000 x g for three minutes; then the supernatants were transferred into a 2 mL Eppendorf tube for further experiments.

2.2.4.3 Mechanical homogenization of rat pancreas spiked with alpha-casein and protein extraction

For the spiking experiment, the comparable frozen piece of rat pancreas tissue samples was transferred to a 2 ml Eppendorf tube, which contained 500 µL lysis buffer (7 M urea, 2 M

thiourea, 30 mM Tris-HCl, pH 6.8) and 180 μg alpha-casein, then the homogenization was performed using a bead mill (TissueLyser II) with a 3mm stainless steel bead for 3.5 minutes at a frequency of 25/s [1].

Mechanical homogenates (MH) were centrifuged at 15000 x g for three minutes, then the supernatants were transferred into 2 mL Eppendorf tubes for further experiments.

2.2.5 Determination of protein concentration

2.2.5.1 Bicinchoninic acid (BCA) assay

The BCA assay is a colorimetric detection assay, which depends on the reduction of Cu^{2+} ions from the copper (II) sulfate to Cu^+ by the peptide bonds of the proteins. The Cu^+ ions are chelated by two molecules of bicinchoninic acid (BCA) in a temperature dependent reaction, forming a purple-colored complex that absorbs light at a wavelength of 562 nm [112].

Protein concentration from mechanical homogenization (MH) and PIRL homogenization (PH) of porcine muscle tissue was determined by a BCA protein assay kit purchased from Pierce (Thermo Scientific).

The working reagent, samples and serial dilutions of bovine serum albumin standards were prepared and measured according to kit instructions.

Figure (42) in the appendix shows the calibration curve of the BCA test constructed by different BSA standard concentrations and their corresponding absorbance at 595 nm and in addition the calculated protein concentration of PIRL and mechanical homogenate from porcine muscle tissue.

2.2.5.2 UV spectrophotometric protein quantification

For the UV spectrophotometric determination of the protein concentration and purity the Nanodrop® ND-1000 spectrophotometer device developed by Thermo Fischer Scientific was used. It is a full spectrum (220 nm – 750 nm) spectrophotometer which enables the measurement of highly concentrated samples and volumes as small as 1 μL without dilution with high accuracy and reproducibility [113, 114].

A 1 μL sample is pipetted onto the end of a fiber optic cable (the receiving fiber). A second fiber optic cable (the source fiber) is then brought into contact with the liquid sample causing the liquid to bridge the gap between the fiber optic ends. The gap is controlled to both 1mm and 0.2 mm paths [115]. The light source was provided by a pulsed xenon flash lamp, the light passing through the sample was analyzed by a spectrometer utilizing a linear CCD array.

The device is controlled by PC-based software, and the data is logged in an archive file on the PC [113, 114].

The device was cleaned by deionized water and 70% ethanol. The protein absorbance was measured at 280 nm (A₂₈₀), and the concentration calculated after a set of blanks and standards were measured. 260/280 values were calculated which represents a ratio of sample absorbance at 260 and 280 nm [113, 114].

2.2.5.3 2-D Quant Kit

The 2-D Quant Kit was developed by GE Healthcare for the accurate determination of protein concentration. This kit circumvents the limitations in protein determination such as interfering or contaminating substances and those which are incompatible with protein assays [116].

The principle of this assay is based on the specific binding of copper ions to protein. Precipitated proteins are resuspended in a copper-containing solution and unbound copper is measured with a colorimetric agent. The color density is inversely related to the protein concentration [116].

In this protocol, a combination of a unique precipitant and co-precipitant is used to precipitate sample proteins while leaving interfering contaminants in solution. To each tube of the sample and standard 500 μ L of a "precipitant" was added and the tubes were briefly vortexed and incubated for 2-3 minutes at RT. A "co-precipitant" (500 μ L) was then added to each tube and vortexed. The protein was pelleted by centrifugation, the supernatant decanted and the pellet resuspended in 100 μ L alkaline solution of cupric ions and 400 μ L of Milli-Q water. Next, 1 mL of a color reagent (prepared according to manufacturer's instructions) was added to each tube. The tubes were incubated for 15 to 20 min at room temperature and the absorbance was measured at 480 nm.

This technique was used for protein precipitation and determination from both mechanical and PIRL homogenates from rat pancreas and rat pancreas spiked with alpha-casein. All reagents, samples, and standards were prepared according to the manufacturer's instruction.

The spectrophotometric analysis of the BSA standards and the samples from PIRL and mechanical homogenate of both rat pancreas and spiked experiment were performed at 480 nm in polystyrene cuvettes (10 \times 10 \times 45 mm³ purchased from Sarstedt (Numbrecht, Germany) using a spectrophotometer model Utrospec 2000 (Pharmacia Biotec, Piscataway, NJ, USA) (Figures 43-46, appendix).

2.2.6 Two-dimensional gel electrophoresis(2DE)

Two-dimensional electrophoresis (2DE) was performed by Proteome Factory AG (Berlin) based on the protocol by Klose and Kobalz [117]. Isoelectric focusing (first dimension) was made in vertical rod gels containing 9 M urea, 4% acrylamide, 0.3% piperazine diacrylamide, 5% glycerine, 2% carrier ampholyte (pH 2-11), 0.06% TEMED, and 0.08% ammonium persulfate. For each sample 200 µg of the protein extract was focused at 8820 Vh. SDS-PAGE (second dimension) was performed in gels (0.1 cm, 20 cm, 30 cm; 15% acrylamide, 0.2% bisacrylamide, 375 mM Tris-HCl (pH 8.8), 0.1% SDS, 0.03% TEMED, and 0.08% ammonium persulfate). 2DE gels were stained with FireSilver (Proteome Factory, Berlin, Germany) [117].

2.2.6.1 Image analysis of two-dimensional electrophoresis gels

Images of 2D gels were analyzed using a conventional method which was based on printing the gel images on plastic transparency sheets. Images of the 2D gels of the PIRL homogenate (PH) and the mechanical homogenate (MH) of every biological sample were warped against each other to correct positional spot variations. The comparison was performed based on the spot intensities and the position of these spots.

2.2.7 Sodium Dodecyl Sulfate Polyacrylamide Gel Electrophoresis (SDS-PAGE)

The samples were first mixed with 5 µL 4x sample buffer (Bio-Rad, Munich, Germany) which contains SDS, 1 µL 20x reducing agent (Bio-Rad, Munich, Germany) and the total volume of the mixture adjusted to 20 µL with HPLC-grade water. The mixture was incubated for 5 minutes at 95°C and cooled to room temperature and then loaded onto 10% Criterion™ XT Bis-Tris precast polyacrylamide gel with a 30-well (Bio-Rad, Munich, Germany) where a total of 30 µg of protein was applied to each well. 7.5 µL of Precision Plus Protein™ Dual Color (Bio-Rad, Munich, Germany) was loaded onto the gel as protein marker.

Electrophoresis was carried out at a constant voltage (120 V) and approximately 30 mA for 45 minutes until the bromophenol blue front reached the bottom of the gel. The gel was stained using a Coomassie solution (40% MeOH, 10% acetic acid, 0.025 % Coomassie blue-250, dissolved in H₂O) for two hours at RT on a shaker and destained with 40% MeOH for decolorizing the gels at RT.

2.2.8 Tryptic in-gel digestion

The tryptic digestion was performed according to the method described by Shevchenko et al. [118]. Briefly, the selected protein bands in SDS-PAGE and protein spots in 2DE were cut out of the gel using a razor blade, cut into small pieces approximately 1x1 mm and transferred to 1.5 ml Eppendorf tubes. Short centrifugation for 1 min was performed to settle down the gel pieces. Several steps of shrinking and swelling for gel pieces were performed with 500 μ L of 100% ACN and 500 μ L of 100 mM NH_4HCO_3 (dissolved in HPLC-grade water). The reduction was carried out with 10 mM dithiothreitol (dissolved in 100 mM NH_4HCO_3 in HPLC-grade water) and alkylation with 55 mM iodoacetamide (dissolved in 100 mM NH_4HCO_3 in HPLC-grade water). The gel pieces were covered completely with a trypsin solution (13 ng/ μ L sequencing-grade trypsin, dissolved in 10 mM NH_4HCO_3 , 10% ACN in HPLC-grade water) and incubated at 37°C overnight for protein digestion. Tryptic peptides were extracted with 5% FA, 50% ACN and evaporated to complete dryness by speed vac. The samples were dissolved in 20 μ L 0.1% FA for further LC-MS/MS analysis.

2.2.9 LC-MS/MS analysis

2.2.9.1 LC-MS/MS analysis from mechanical and PIRL homogenates from porcine muscle tissue

For LC-MS analysis, the samples were injected on a nano-ultra pressure liquid chromatography system (nano-UPLC; nanoACQUITY, Waters, Manchester, UK) coupled via electrospray ionization (ESI) to a quadrupole time-of-flight (QTOF) mass spectrometer (QTOF Premier, Micromass/Waters, Manchester, UK). Samples were applied (5 μ L/min) onto a trapping column (Waters nanoAcquity UPLC PST trap column, C18, 180 μ m \times 20 mm, 5 μ m, 100 Å , Waters, Manchester, UK; buffer A: 0.1% FA in HPLC-H₂O; buffer B: 0.1% FA in ACN) with 2% buffer B, washed for 10 min with 2% buffer B (5 μ L/min) and then the peptides were eluted onto the separation column (nanoAcquity UPLC BEH column, C18, 75 μ m \times 150 mm, 100 Å Waters, Manchester, UK; 200 nL/min, gradient: 2–50% B in 30 min for short gradient).

The spray was generated from a fused-silica emitter (I.D. 10 μ m, New Objective, Woburn, USA) at a capillary voltage of 1.5 kV, a source temperature of 100 °C and a cone voltage of 45 V in positive ion mode. For MS/MS measurements, data were recorded in the data-dependent acquisition mode (DDA). MS survey scans were performed over an m/z range from 300-1500 with a scan time of 0.6 s and an interscan delay of 0.05 s. The two most abundant signals were used for fragmentation. MS/MS spectra were obtained from 100-1800

m/z with a scan time of 1.9 sec and a collision ramp from 20-30 eV. An online exclusion was used to prevent multiple fragmentation events (exclusion time: 20 sec, exclusion window: +/- 2 m/z). For calibration, a lockspray spectrum was recorded every 10 seconds (1 pMol/ μ L [Glu1] Fibrinopeptide B (Sigma, Munich, Germany) over an m/z range from 100-1500 using a collision energy of 22 eV.

2.2.9.2 LC-MS/MS analysis from mechanical and PIRL homogenates from rat pancreas and spiked rat pancreas with alpha-casein

LC-MS/MS measurements were performed by injecting the samples on a nano liquid chromatography system (nanoACQUITY, Waters, Manchester, UK) coupled via ESI to a quadrupole orbitrap mass spectrometer (Orbitrap QExactive, Thermo Scientific, Bremen, Germany). The samples were loaded (5 μ L/min) on a trapping column (nanoACQUITY UPLC Symmetry C18 trap column, 180 μ m \times 20 mm, 5 μ m, 100 Å ; buffer A: 0.1% FA in HPLC-H₂O; buffer B: 0.1% FA in ACN) with 2% buffer B. After sample loading the trapping column was washed for 5 min with 2% buffer B (5 μ L/min) and the peptides were eluted (200 nL/min) onto the separation column (nanoAcquity UPLC column, BEH 130 C18, Waters; 75 μ m \times 250 mm, 1.7 μ m, 100 Å ; 200 nL/min, gradient: 2–30% B in 30 min). The spray was generated from a fused-silica emitter (I.D. 10 μ m, New Objective, Woburn, USA) at a capillary voltage of 1650 V. Mass spectrometric analysis were performed in positive ion mode. LC-MS/MS analysis with the Orbitrap QExactive was performed on MS level over an m/z range from 400-1500, with a resolution of 70000 FWHM at m/z 200 (transient length= 256 ms, injection time= 100 ms, AGC target= 3e6). MS/MS measurements were carried out in DDA mode (Top5), with a HCD collision energy of 30%, a resolution of 17000 FWHM at m/z 200 (transient length= 64 ms, injection time= 100 ms, AGC target= 3e6), an underfill ratio of 10% and an isolation width of 2 m/z [1].

2.2.10 Bioinformatic data analysis

2.2.10.1 LC-MS/MS raw data from 2DE of PIRL and mechanical homogenates from porcine muscle tissue

The LC-MS/MS raw data from the 2DE spots were processed using Protein Lynx Global Server version 2.5.2 (Waters, Manchester, UK) for searching in Mascot. The resulting peak lists were exported as a mzML file and searched against a mammalian decoy database using Mascot (Matrix Sciences, London, UK, www.matrixscience.com). The following parameters were set up in the searching process: precursor mass tolerance: 1.4 Da, fragment mass tolerance: 0.2 Da, one missed tryptic cleavage allowed, a carbamidomethylation on cysteine residues as a fixed modification and an oxidation of methionine residues as a variable modification.

2.2.10.2 LC-MS/MS raw data from SDS-PAGE of PIRL and mechanical homogenates from rat pancreas and spiked experiment with alpha-casein

LC-MS/MS raw data from the SDS-PAGE bands were processed using MaxQuant (version 1.5.2.8) [119]. Andromeda as a search engine was used against a SwissProt database of *Rattus norvegicus* (www.uniprot.org, downloaded November 10, 2015, 7,940 entries; spiked with protein sequences of bovine alpha-S1/S2-casein in the case of spiking experiments) for peptide and protein identification. The following parameters were set up during the searching process: precursor mass tolerance was 20 ppm for Orbitrap QExactive measurements, two miss cleavages were allowed for peptide identification, a carbamidomethylation on cysteine residues as a fixed modification and an oxidation of methionine residues as a variable modification. For spiking experiments, phosphorylation on serine residues was also considered.

In addition, relative quantification of protein was performed using MaxLFQ algorithm [120] with at least 3 ratio count of unique peptides.

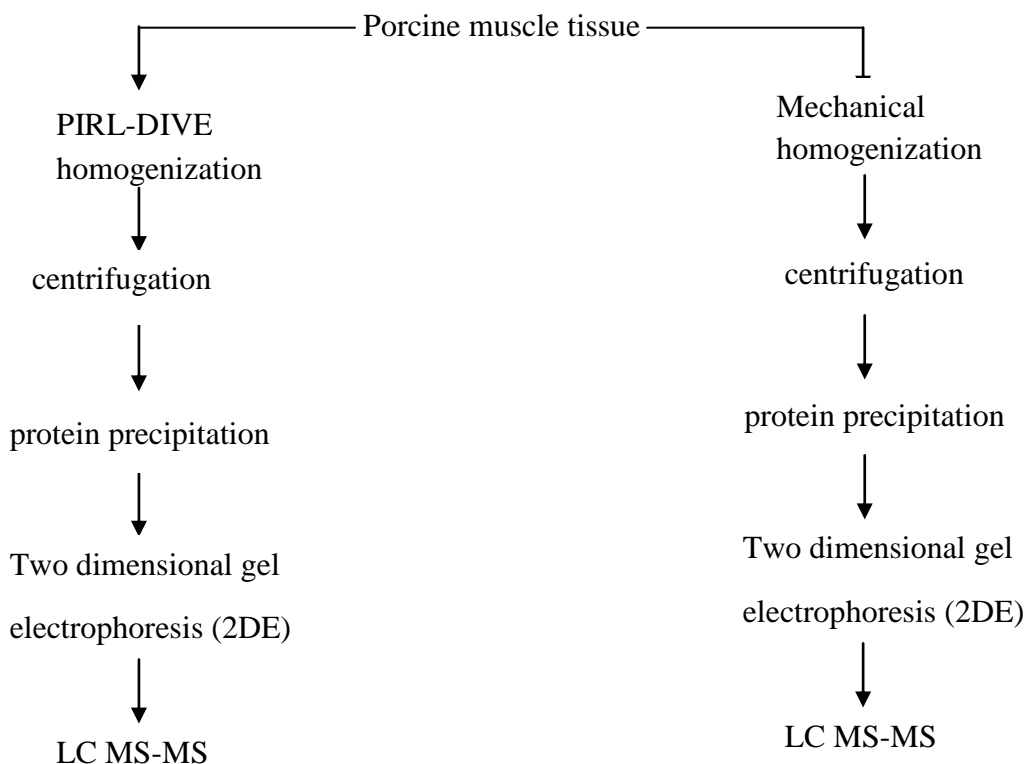
3 Results

3.1 Comparison of the protein composition in picosecond infrared laser (PIRL) homogenate (PH) and in mechanical homogenate (MH)

In order to investigate if we can observe changes in the in-vivo protein species composition between tissue homogenized by PIRL-DIVE compared with tissue homogenized by standard mechanical homogenization, porcine muscle tissue was chosen as model tissue because it is almost homogenous. The workflow proposed and followed is presented in scheme 1.

Porcine muscle tissue samples were homogenized by either picosecond infrared laser (PIRL) according to Kwiatkowski et al. [111] or by the mechanical homogenization method. From PIRL homogenate (PH) and mechanical homogenate (MH), equal amounts of protein ($m=90\ \mu\text{g}$) were applied to high-resolution two-dimensional gel electrophoresis (2DE, Figure 6, Figure 7, Scheme 1).

The image of 2DE-protein pattern from both homogenates was analyzed, and the marked spots from both gels were identified by liquid chromatography-mass spectrometry/mass spectrometry (LC-MS/MS) (Figure 6, Figure 7, Scheme 1).



Scheme 1: Experimental workflow (details in material and methods section). PIRL: Picosecond-infrared laser. LC-MS/MS: liquid chromatography- mass spectrometry/mass spectrometry

3.1.1 Comparison between two-dimensional gel electrophoresis (2DE) patterns of the PIRL homogenate (PH) and mechanical homogenate (MH) of porcine muscle tissue

Two-dimensional gel electrophoresis (2DE) of porcine muscle tissue homogenized via PIRL-DIVE (Figure 6), and the mechanical method (Figure 7) showed protein spots separated in gel arrays using the apparent standard pH range from 3 to 11 and a standard molecular mass range from 10 to 150 kDa.

By comparing spots patterns of the 2DE gel from PIRL homogenate (PH) gel (Figure 6) and mechanical homogenate (MH) gel (Figure 7), more spots were observed in the low molecular weight region (less than 29 kDa) in the MH gel than in the PH gel. In the corresponding region, four spots were detected (spot no. 9 in PH gel, figure 6) (spots no. 6-8 in MH gel, figure 7).

Also, eight spots from the PIRL homogenate (PH) gel (spot no. 1-8, figure 6) and five spots from the mechanical homogenate (MH) gel (spot no. 1-5, figure 7) were identified.

The selected spots were cut out of the gels and the proteins in the gel were digested with trypsin. The resulting peptide mixtures were measured by LC MS-MS. The identified proteins are listed in table 2 and 3, together with the theoretical molecular weight of the proteins.

Adenylate kinase isoenzyme 1 (m=21.6 kDa) was identified in spot no. 9 in PH (Figure 6, Table 2). Spots no. 1-4 in PH (Figure 6, Table 2) and spots no. 1-2,7-8 in MH (Figure 7, Table 3) were identified as fructose bisphosphate aldolase a (m=39.4 kDa). Spots spots no. 5-8 in PH (Figure 6, Table 2) and spots no. 3-6 in MH (Figure 7, Table 3) were identified as creatine kinase m-type (m=43 kDa).

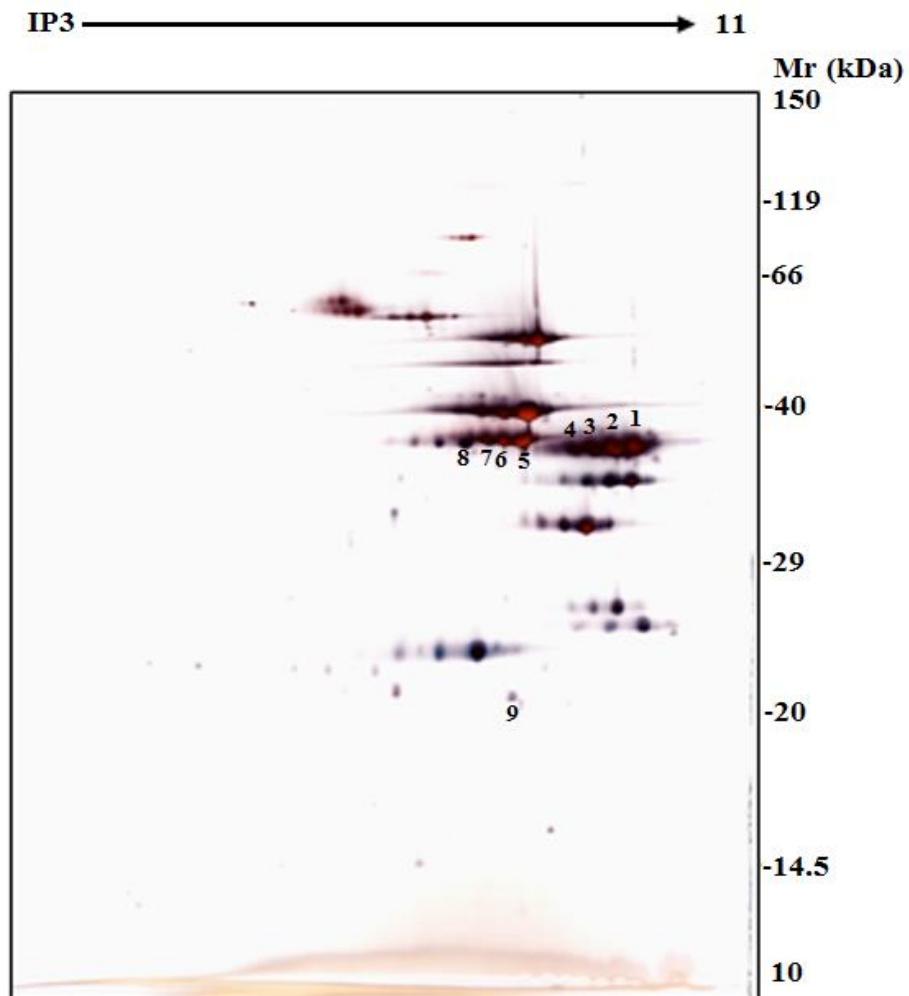


Figure 6: Two-dimensional gel electrophoresis (2DE) of the PIRL homogenate (PH) of porcine muscle tissue ($m=90 \mu\text{g}$). The spots marked with numbers 1-9 were identified by LC-MS/MS, described in text and table 2. PIRL: picosecond infrared laser.

Table 2: Proteins identified in marked spots with numbers 1-9 in the two-dimensional gel electrophoresis (2DE) in (Figure 1) of the PIRL homogenate (PH) with their corresponding theoretical molecular weight.

Spot no.	Protein name	Theoretical Mr (kDa)
1	Fructose-bisphosphate aldolase A	39.4
2	Fructose-bisphosphate aldolase A	39.4
3	Fructose-bisphosphate aldolase A	39.4
4	Fructose-bisphosphate aldolase A	39.4
5	Creatine kinase	43.3
6	Creatine kinase	43.3
7	Creatine kinase	43.3
8	Creatine kinase	43.3
9	Adenylate kinase isoenzyme 1	21.7

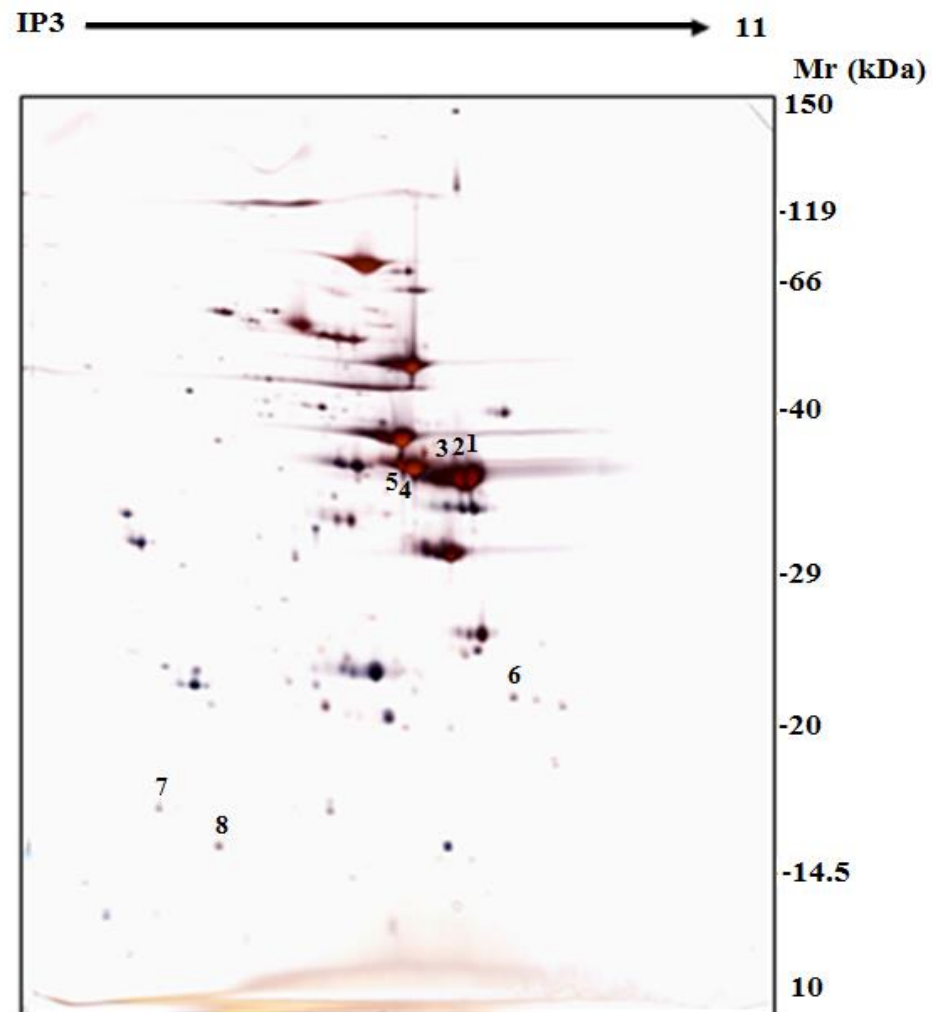


Figure 7: Two-dimensional gel electrophoresis (2DE) of the mechanical homogenate (MH) of porcine muscle tissue ($m=90 \mu\text{g}$). The spots marked with numbers 1-8 were identified by LC-MS/MS, described in the text and table 3.

Table 3: Proteins identified in marked spots with numbers 1-8 in the two-dimensional gel electrophoresis (2DE) in (Figure 2) of the mechanical homogenate (MH) with their corresponding theoretical molecular weight.

Spot no.	Protein name	Theoretical Mr (kDa)
1	Fructose-bisphosphate aldolase A	39.3
2	Fructose-bisphosphate aldolase A	39.3
3	Creatine kinase	43
4	Creatine kinase	43
5	Creatine kinase	43
6	Creatine kinase	43
7	Fructose-bisphosphate aldolase A	39.3
8	Fructose-bisphosphate aldolase A	39.3

3.2 Comparison of the protein composition in the picosecond infrared laser (PIRL) homogenate (PH) and in the mechanical homogenate (MH) in the presence of Laemmli buffer

As described by Kwiatkowski et al. [1] human tonsil tissues were used in previous experiments for the comparison of tissue homogenization by PIRL ablation and by the mechanical method.

According to Kwiatkowski et al. the total number of proteins identified in the three human tonsils samples in the PIRL homogenate was 2085 (+ /- 366) and of the mechanical homogenate (MH) 1850 (+ /- 667) (Figure 8 A). 1343 proteins were identified in all three human tonsil samples in PIRL homogenate whereas in the mechanical homogenate (MH) 974 proteins were identified (Figure 8 A, B, C).

A total of 839 proteins (56.8%) were identified in both homogenates in all three human tonsil samples, 504 proteins (34.1%) were identified only in PIRL homogenate and 135 proteins (9.1%) only in the mechanical homogenate (Figure 8 A) [1].

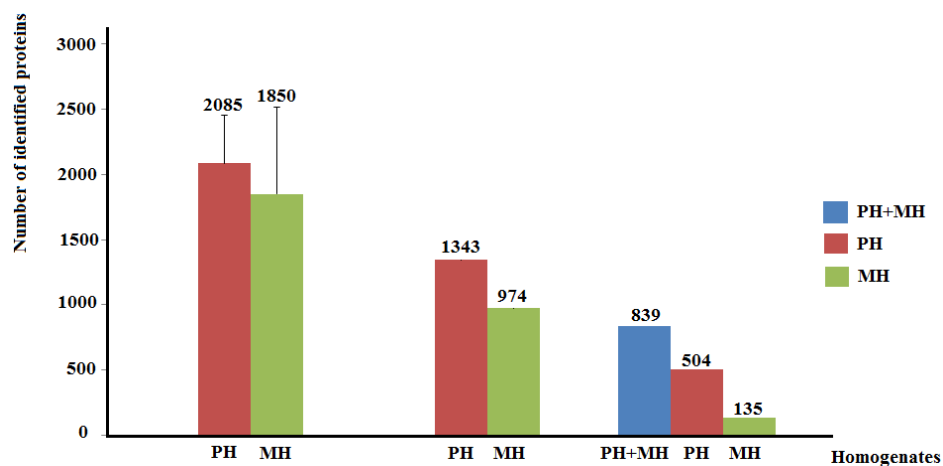
A comparison of identified proteins within PIRL homogenate (PH) between three biological replicates showed the following results: 1343 proteins identified in all three tonsil samples, 68 proteins in samples no. 1 and 2, 305 proteins in samples no. 1 and 3 , 296 proteins in samples no. 2 and 3, 104 proteins only in sample no. 1 ,225 proteins in sample no. 2 ,559 proteins in sample no. 3 (Figure 8 B) [1] .

Accordingly in the mechanical homogenates of the three human tonsil samples, the following results were obtained: 974 proteins identified in all three tonsil samples, 36 proteins only in samples no. 1 and 2, 64 proteins in samples no. 1 and 3 , 649 proteins in samples no. 2 and 3, 39 proteins only in sample no. 1, 363 proteins only in sample no. 2 and 727 proteins only in sample no. 3 (Figure 8 C) [1] .

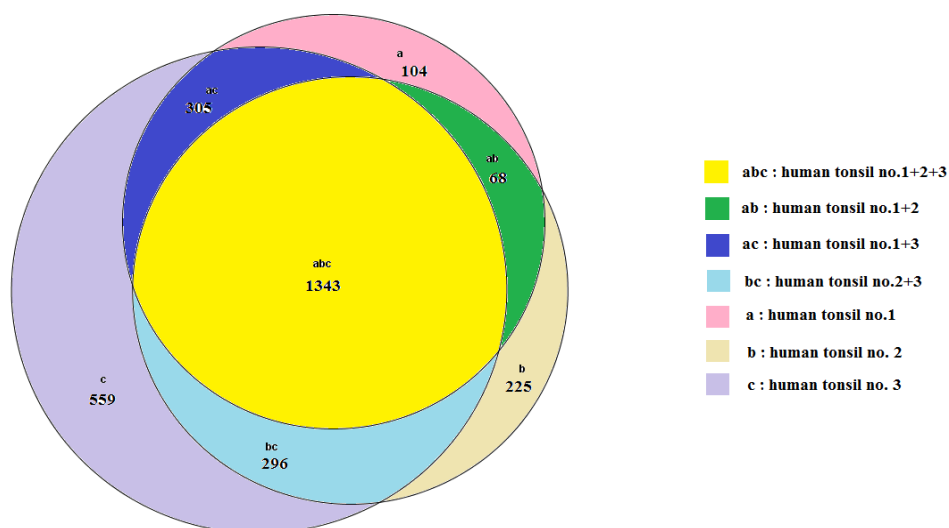
The degree of proteolysis in the three human tonsil samples was shown in (Figure 8 D), 1.92 % in PIRL homogenate and 22.41% in mechanical homogenate (MH) [1].

In summary, the results of tonsils from Kwiatkowski et.al [1] illustrated higher protein identification and lower degree of proteolysis in the case of PIRL homogenate (PH) compared to the mechanical homogenate (MH).

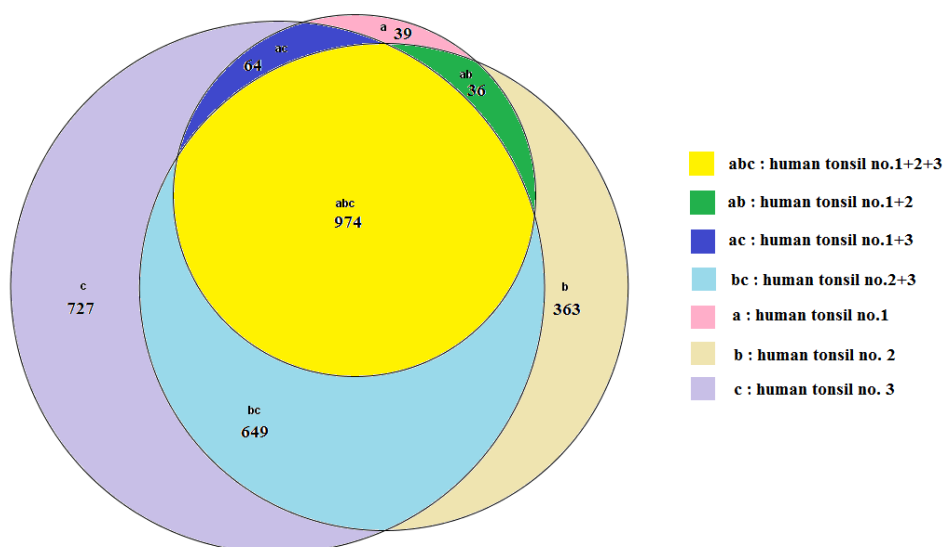
A)



B)



C)



D)

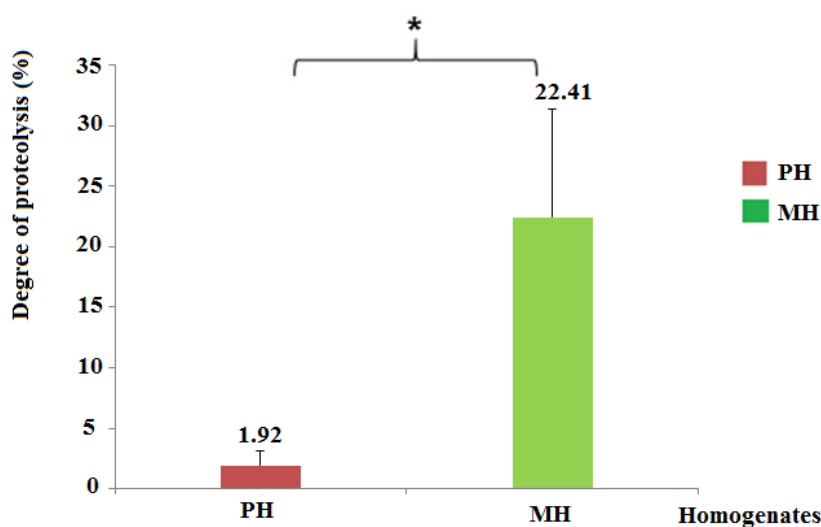


Figure 8: Statistical analysis of the LC-MS/MS data from the SDS-PAGE of the PIRL homogenates (PH) and the mechanical homogenates (MH) from human tonsil samples (n=3). Modified from (Kwiatkowski et al. 2016).

A: Bar graph (mean with standard deviation) showing the total number of proteins identified in the three biological replicates.

Bar graph of the number of proteins identified in all three biological replicates.

Bar graph showing the number of proteins identified in all three biological replicates in both PH and MH, only in PH and only in MH.

B: Venn diagram showing the number of proteins identified in PIRL homogenate (PH) in all three biological replicates (abc), in biological replicates one and two (ab), in biological replicates one and three (ac), in biological replicates two and three, only in biological replicates one (a), only in biological replicates two (b) and only in biological replicates three (c).

C: Venn diagram showing the number of proteins identified in mechanical homogenate (MH) in all three biological replicates (abc), in biological replicates one and two (ab), in biological replicates one and three (ac), in biological replicates two and three, only in biological replicates one (a), only in biological replicates two (b) and only in biological replicates three (c).

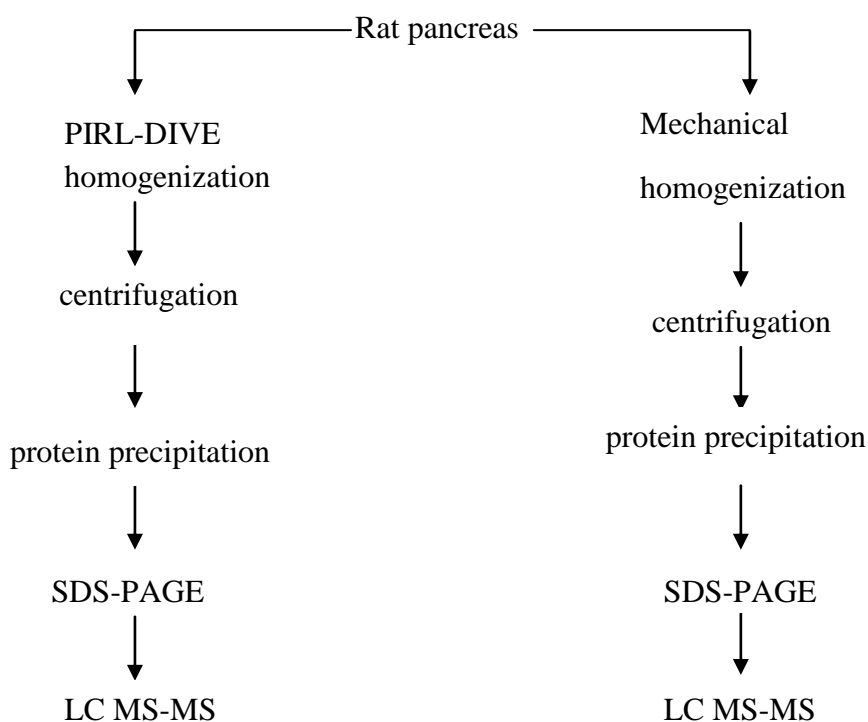
D: Bar graph (mean with SD) showing the global degree of proteolysis in the three biological replicates in PIRL homogenates (PH) and mechanical homogenates (MH), *: $p=0.018$ (t-test). At least two unique peptides had to be identified for a protein to be taken into account.

In this work, a new, different setup of the experiment was performed: Pancreas rat tissue were homogenized via PIRL-DIVE and mechanically. PIRL homogenate (PH) was collected in presence of concentrated Laemmli buffer and immediately transferred to boiling water bath and adjust the volume was adjusted with water(as described in materials and methods section). Mechanical homogenization was performed in presence of hot Laemmli buffer and immediately the MH transferred to boiling water bath (see materials and methods section).

In all other respects the samples were treated as described: the pancreas tissues were homogenized via PIRL-DIVE or the mechanical method, extraction was the same, and the same protein amount was loaded onto the SDS-PAGE (Scheme 2).

Rat pancreas tissue was chosen because it contains huge amounts of enzymes, especially proteases, which directly start to degrade proteins after the animal is killed.

The hot Laemmli buffer was used in this experiment to minimize the degree of proteolytic degradation, in order to make sure that enzymatic degradation was stopped at the earliest time point possible and to analyze if we still see differences regarding proteolytic degradation between both homogenization methods.



Scheme 2: Experimental workflow (details in materials and methods section).

SDS-PAGE: Sodium dodecyl sulfate- polyacrylamide gel electrophoresis

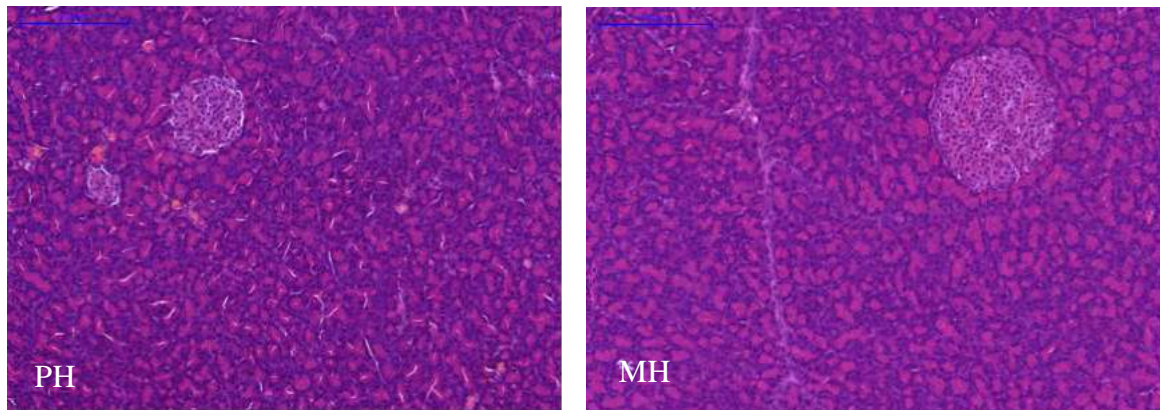
3.2.1 Histological examination, comparison between tissue samples used for PIRL tissue homogenization (PTH) and mechanical tissue homogenization (MTH)

To investigate whether the rat pancreas tissue used for PIRL and mechanical homogenization were comparable, rat pancreas samples were obtained from three different rats. Two equal pieces of tissue were cut for PIRL and mechanical homogenization. Also, from each of the two pieces, a small section was used for histological staining.

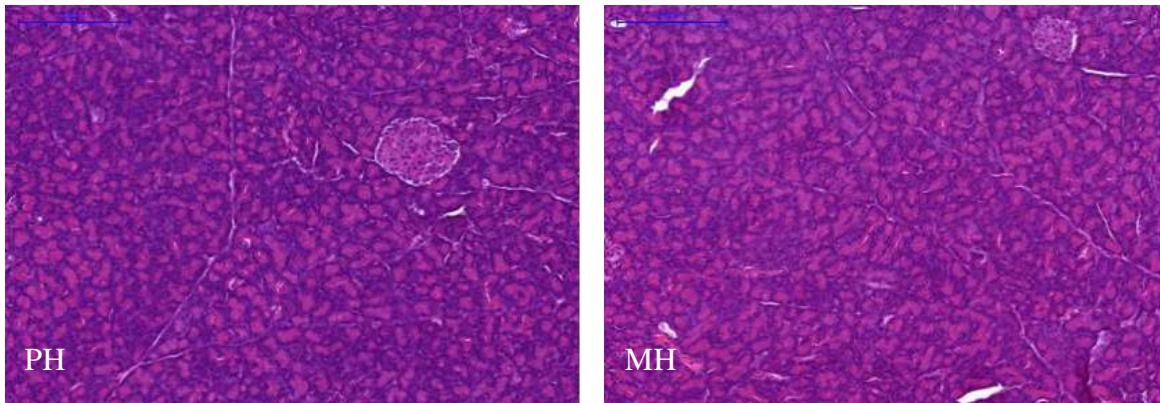
For histological examination (Figure 9) the pancreatic tissue which was used for homogenization via PIRL-DIVE or mechanical homogenization was stained with hematoxylin and eosin.

The histological staining pictures of the tissue samples used for mechanical and PIRL homogenization showed all the pancreas components which involved exocrine and endocrine glandular tissue, lymph and blood vessels, nerves and excretory ducts. The histological examination showed comparable tissue with no hint of the presence of different components.

A)



B)



C)

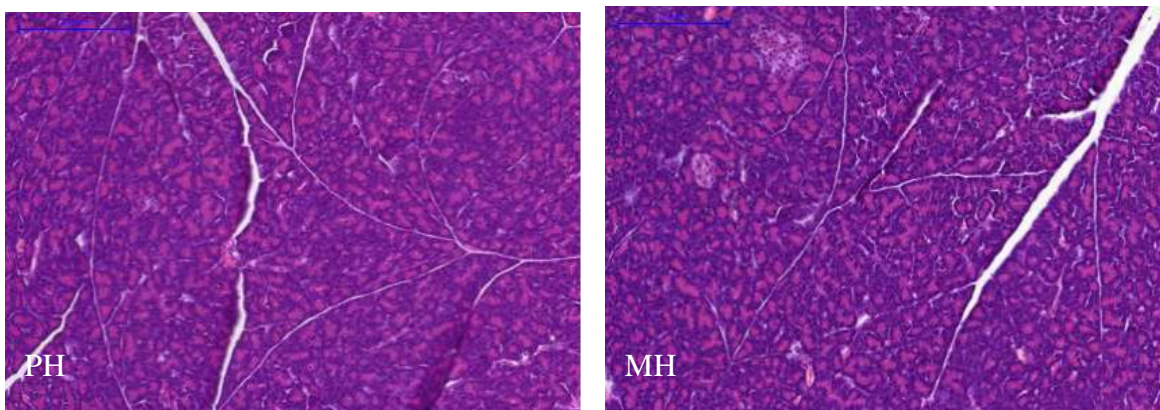


Figure 9: Hematoxylin and Eosin staining (10 x magnification) of pancreas tissue from three rats (A-C), which were homogenized by picosecond-infrared laser (PIRL)-DIVE or mechanically (MH).

3.2.2 Comparison of the protein composition in the PIRL homogenate (PH) and in the mechanical homogenate (MH) by one-dimensional gel electrophoresis

Samples from the PIRL homogenate (PH) and the mechanical homogenate (MH) of all three biological replicates of rat pancreas were applied on the SDS-PAGE shown in (Figure 10). The band patterns of the PIRL (PH) and mechanical homogenate (MH) are rather similar, covering the entire molecular weight range from above 200 kDa down to 6 kDa. Also the color intensity of the bands from each homogenization method in each biological replicate was very similar.

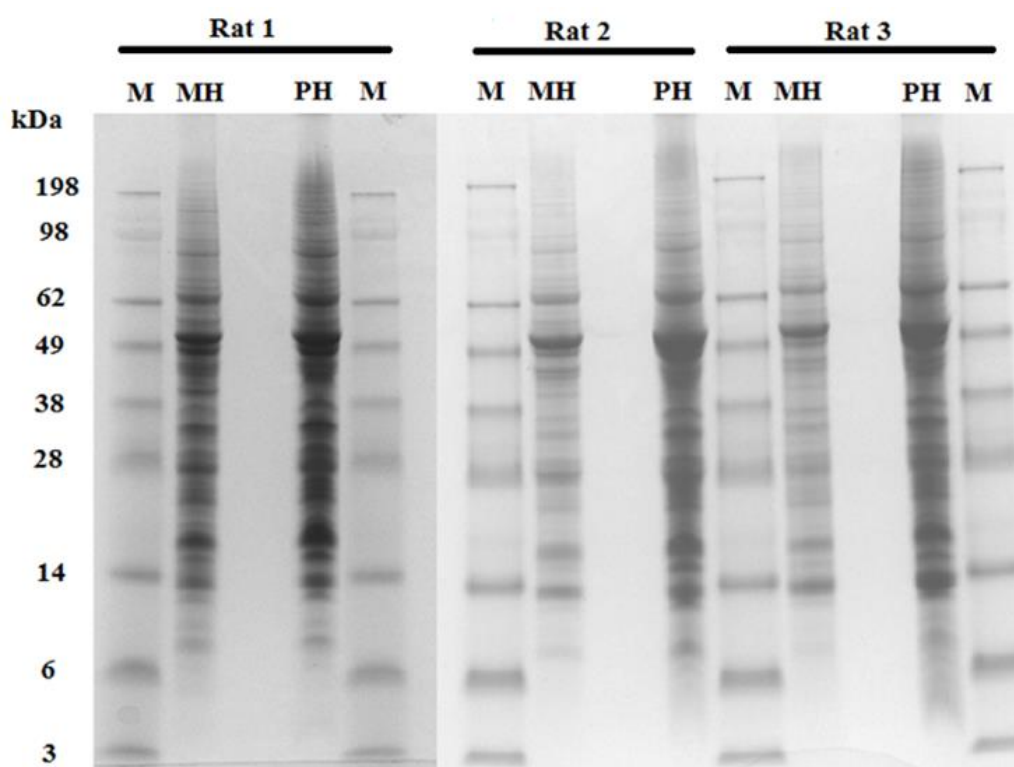


Figure 10: SDS-PAGE of protein homogenates from rat pancreas. M: protein marker. MH: Protein sample of rat pancreas yielded by mechanical homogenization (MH, m= 30 μ g). PH: Protein sample of rat pancreas yielded by PIRL-DIVE homogenization (PH, m= 30 μ g). A: SDS-PAGE of rat pancreas no. 1. B: SDS-PAGE of rat pancreas no. 2. C: SDS-PAGE of rat pancreas no. 3.

For a deeper investigation of the degree of proteolytic degradation, all lanes were divided into comparable bands (Figure 11), every band was cut out of the gel from top to bottom identically for each biological replicate and the proteins in these bands were digested with trypsin (Figure 11).

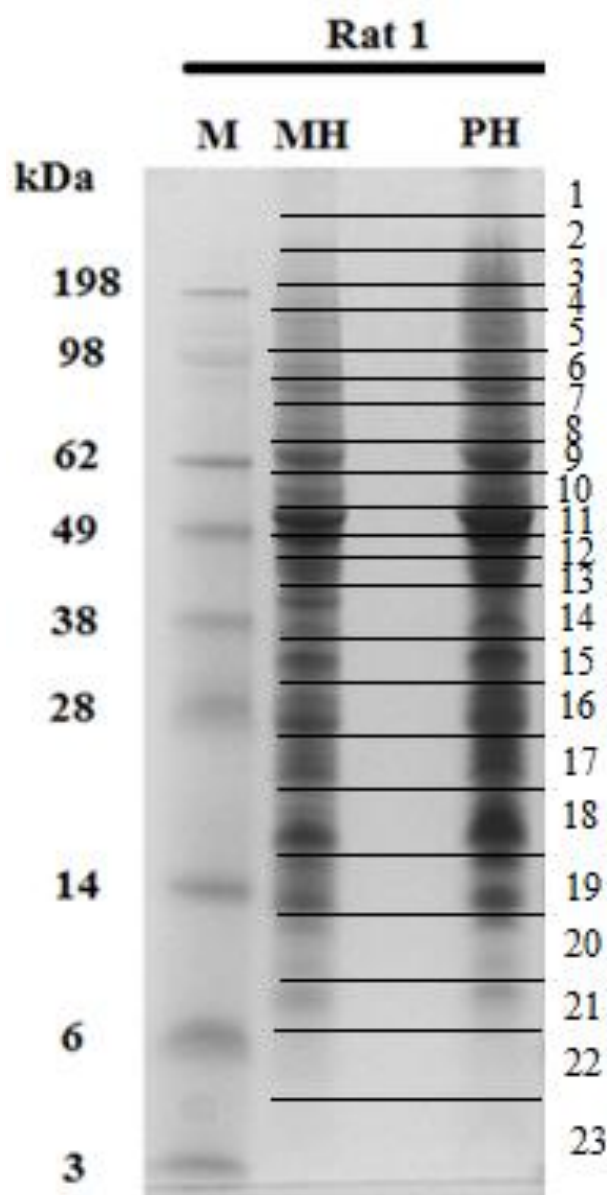


Figure 11: SDS-PAGE of protein homogenates from rat pancreas No.1. M: protein marker. MH: Protein sample of rat pancreas obtained by mechanical homogenization (MH, m= 30 μ g). PH: Protein sample of rat pancreas obtained by PIRL-DIVE homogenization (PH, m= 30 μ g). The drawn lines and numerals mark the bands that were excised for the tryptic digestion and LC-MS / MS analysis. The bands of the SDS-PAGE of rat pancreas no. 2 and no. 3 were divided for tryptic in-gel digestion and LC-MS / MS analysis is according to the above picture.

3.2.3 Construction of protein species migration profiles of the SDS-PAGE of the PIRL homogenate (PH) and the mechanical homogenate (MH)

The resulting tryptic peptide mixtures from proteins in SDS-PAGE bands (Figure 10) were measured by LC MS-MS, the protein composition in every band was analyzed and yielded a huge number of proteomics data.

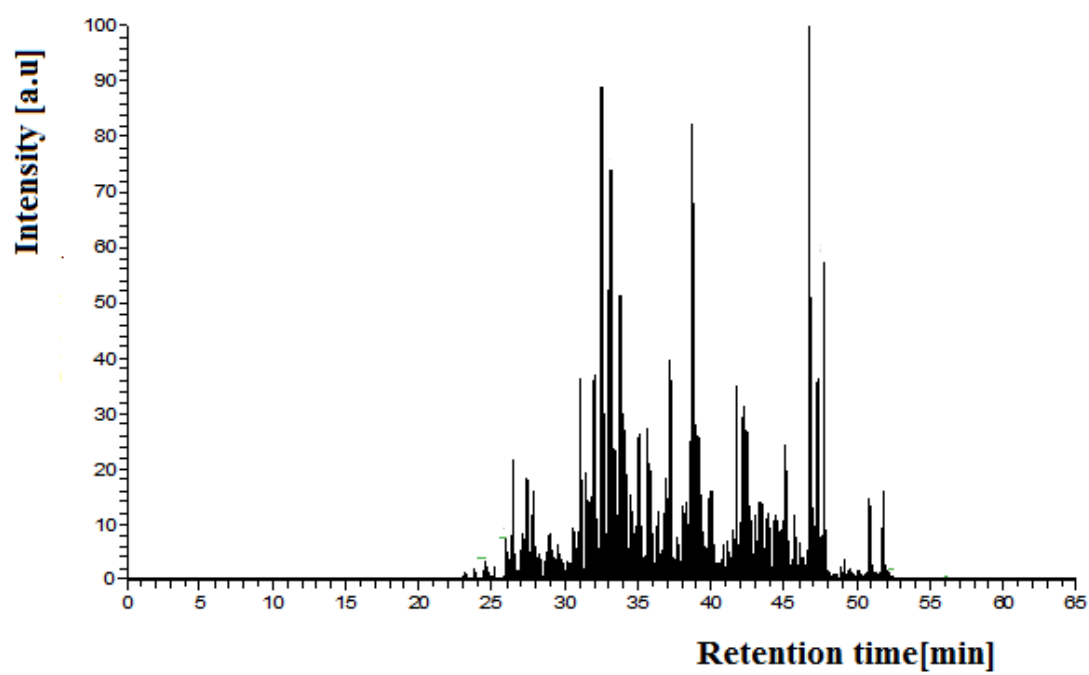
First, the base peak chromatogram of the LC-MS/MS analysis of the tryptic peptides was obtained, constructed by plotting for each data point of the chromatogram the intensity of the the most intense peptide signal against the eluting time at the x-axis (Figure 12 A).

In figure 12, A the base peak chromatogram of the LC-MS/MS analysis of the tryptic peptides in the SDS-PAGE band no.15 (Figure 11) of rat pancreas no. 1 obtained by PIRL-DIVE homogenization is shown. Most peptides were eluted at retention time between 25 min to 55 min.

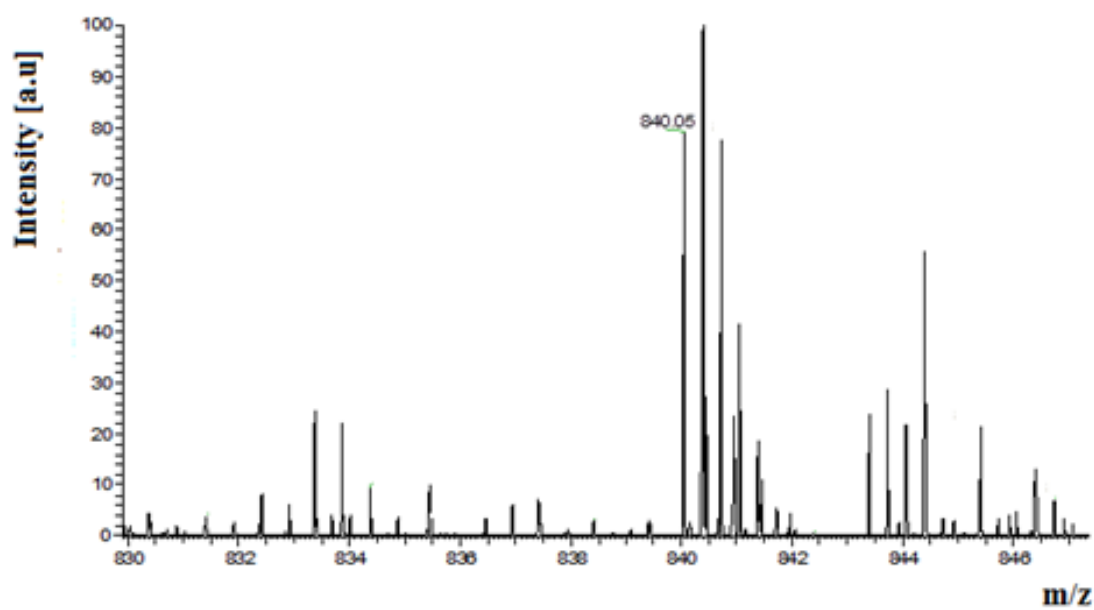
Inspection of the MS spectra at the retention time 36.5 min from the LC-MS /MS analysis of the SDS-PAGE band no.15 (Figure 12 B) of rat pancreas no. 1 showed that the peak is caused by a peptide signal at $m/z = 840.05$; $[M + 3H]^{3+}$. Based on the LC MS-MS analysis, the peptide was identified through MS/MS fragment spectra as a tryptic peptide from the Chloride intracellular channel protein 4 with the sequence DEFTNTCPSDKEVEIAYSVDVAK.

For the signal with $m/z = 840.05$ $[M+3H]^{3+}$ (DEFTNTCPSDKEVEIAYSVDVAK) from Chloride intracellular channel protein 4 in LC MS-MS analysis of rat pancreas no. 1 the extracted ion chromatogram (EIC) was generated (Figure 12 D).

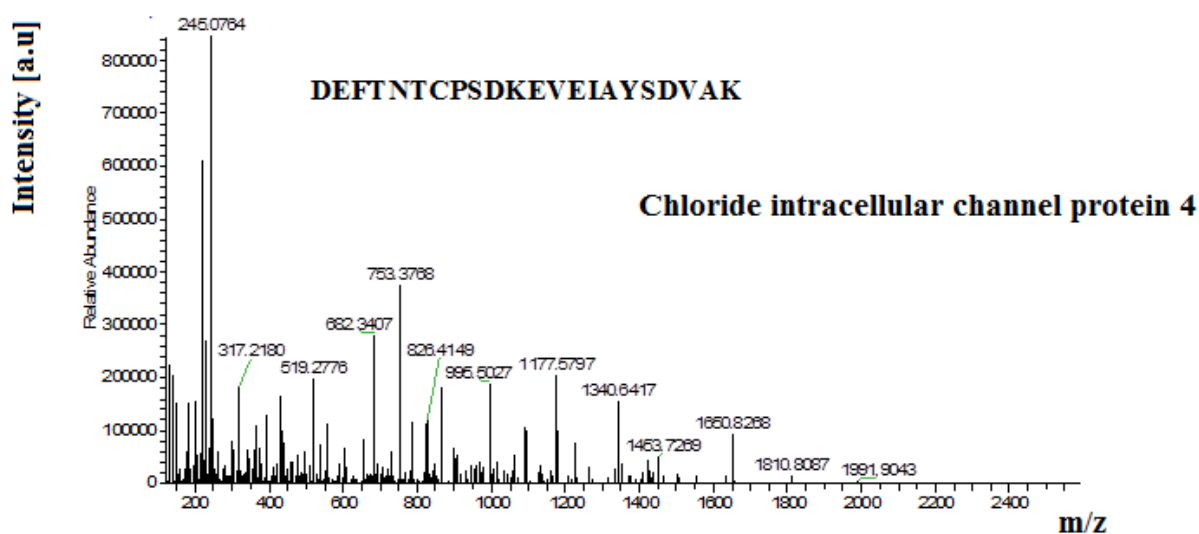
A)



B)



C)



D)

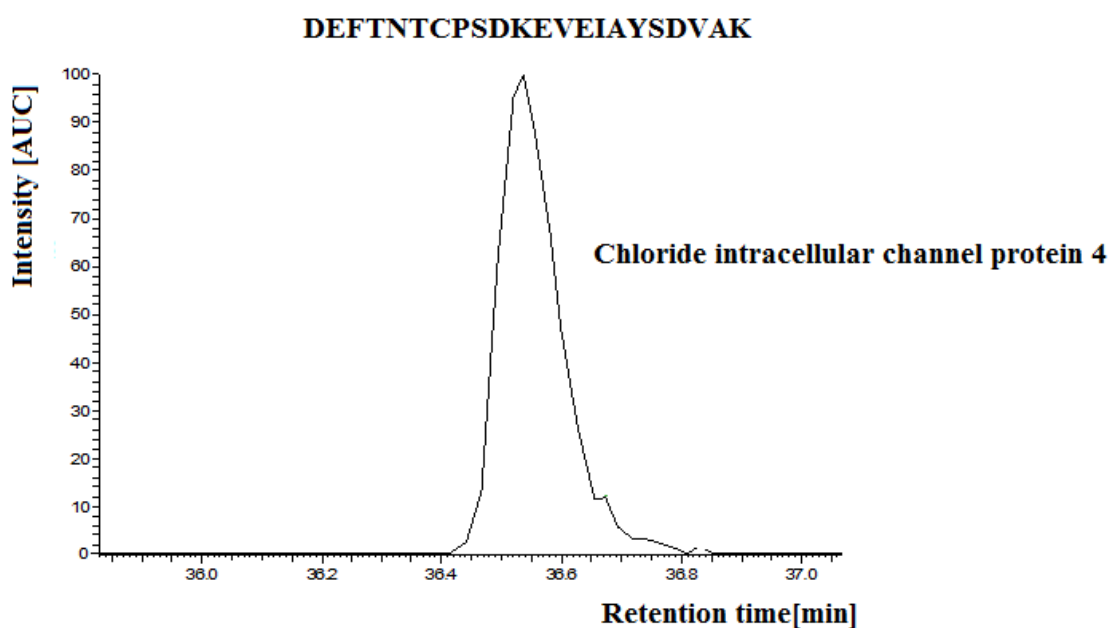


Figure 12: A) Base peak chromatogram (BPC) of the LC-MS/MS analysis of tryptic peptides from SDS-PAGE band no.15 (Figure 6) of rat pancreas no. 1 . Ordinate: Intensity [%]. Abscissa: retention time [min].

B) Section of MS spectrum of the LC-MS analysis of the tryptic peptides from SDS-PAGE band no.15 (Figure 6) of rat pancreas no. 1 at time 36.5 min.

C) MS/MS of fragment spectra from LC MS analysis of the (m/z 840.05; $[M + 3H]^{3+}$, RT 36.5 min).

D) Extracted ion chromatogram for the signal with $m/z = 840.05$ $[M+3H]^{3+}$ (DEFTNTCPDKEVEIAYSDVAK) from the Chloride intracellular channel protein 4 in LC MS-MS analysis of rat pancreas no. 1.

Proteins were quantified with the MaxLFQ algorithm [120] taking in account only proteins with a minimum count of three unique peptides. Protein species migration profiles of the SDS-PAGE of the PIRL homogenate (PH) and the mechanical homogenate (MH) were generated by plotting the label-free quantification (LFQ) intensities for specific proteins against the corresponding fractions on the SDS-PAGE which represents the molecular weight (Figure 13).

Figure 13 demonstrated the SDS-PAGE migration profile of the Chloride intracellular channel protein 4 after mechanical homogenization (MH, blue curve) and PIRL-DIVE homogenization (PH, red curve) of rat pancreas no.1. The LFQ intensity is plotted against the migration distance on the SDS gel. The most intense signal for chloride intracellular channel protein 4 was detected in SDS gel bands 15 (PH) and 20 (MH) (Figure 11). Hence, a shift of the relative migration peak of +5 was determined for the Chloride intracellular channel protein 4.

In general, migration profiles show the quantitative distribution of the protein species over the whole SDS page and thus provide information concerning the degree of enzymatic degradation.

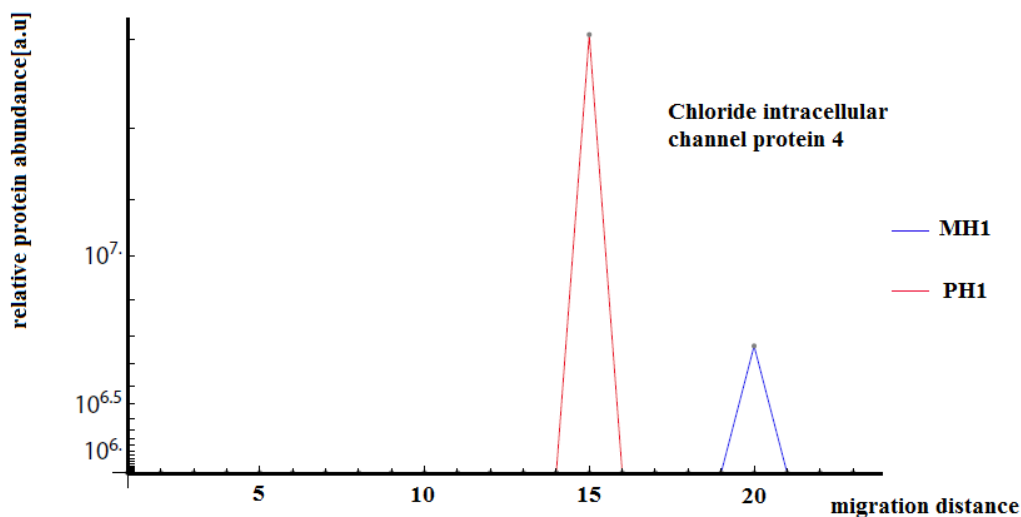


Figure 13: SDS-PAGE-Migration profile of chloride intracellular channel protein 4 after mechanical homogenization (MH, blue curve) and PIRL-DIVE homogenization (PH, red curve) of rat pancreas no.1. The LFQ intensity is plotted against the migration distance on the SDS gel. The most intense signal for Chloride intracellular channel protein 4 was detected in SDS gel bands 15 (PH) and 20 (MH), respectively. Hence, a relative migration peak shift of +5 for Chloride intracellular channel protein 4 was determined.

3.2.4 Examination of migration profiles of the SDS-PAGE of the PIRL homogenate (PH) and the mechanical homogenate (MH)

In order to compare between the protein composition in the PIRL homogenate (PH) and the mechanical homogenate regarding the proteolytic degradation of protein species, migration profiles of the SDS-PAGE of both PIRL and mechanical homogenates were performed and examined.

EH domain-containing protein 1 (Gene: EHD 1, m=60.6 kDa): Migration profiles were constructed for all three biological replicates (Figure 14) and the relative protein abundance of EH domain-containing protein 1 was plotted against the molecular weight, which corresponds to the migration distance of proteins in the SDS gel. This protein was identified at the level of the 62 kDa marker band and the band below this marker in both PH and MH (Figure 11, bands no.9-10).

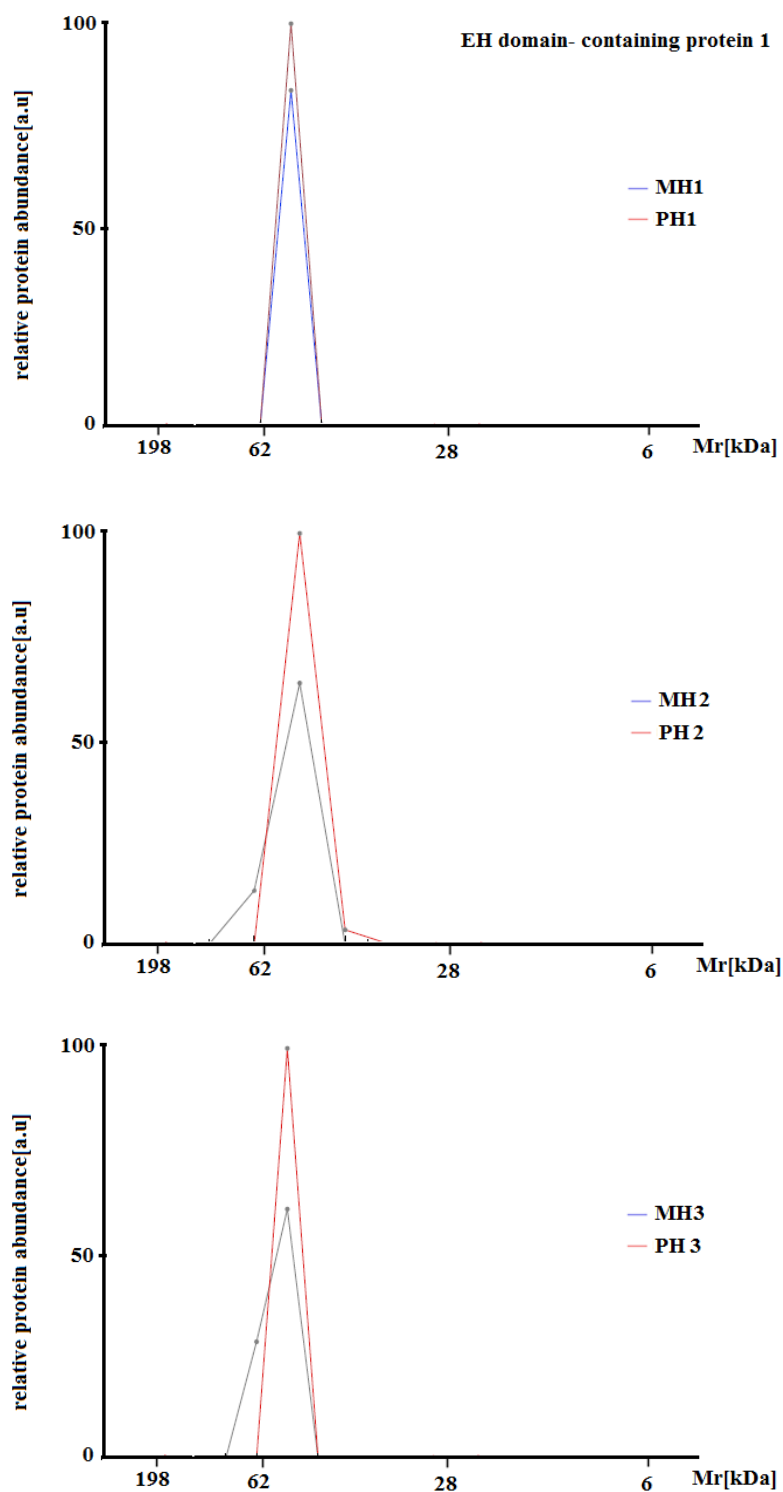


Figure 14: SDS-PAGE-migration profiles of the EH domain-containing protein 1 constructed from the relative quantities of its species, identified by tryptic digestion and following LC-MS/MS analysis in the individual SDS-PAGE bands of the protein extracts from the rat pancreas sample obtained by mechanical homogenization and PIRL-DIVE homogenization. PH1: PIRL homogenate of the first rat pancreas sample, MH1: mechanical homogenate of the first rat pancreas sample. PH2: PIRL homogenate of the second rat Pancreas, MH2: mechanical homogenate of the second rat pancreas sample. PH3: PIRL homogenate of the third rat pancreas sample, MH3: mechanical homogenate of the third rat pancreas sample.

Isocitrate dehydrogenase NAD subunit beta (Gene: IDH3B, m=42.4 kDa): Migration profiles were constructed for all three biological replicates (figure 15) showing, how this protein was distributed. The relative protein abundance of EH domain-containing protein 1 was plotted against the molecular weight, which corresponded to the migration distances of proteins in the SDS gel. This protein was distributed in bands 11-13 at the level of the 38-49 kDa marker bands in both PH and MH (Figure 11).

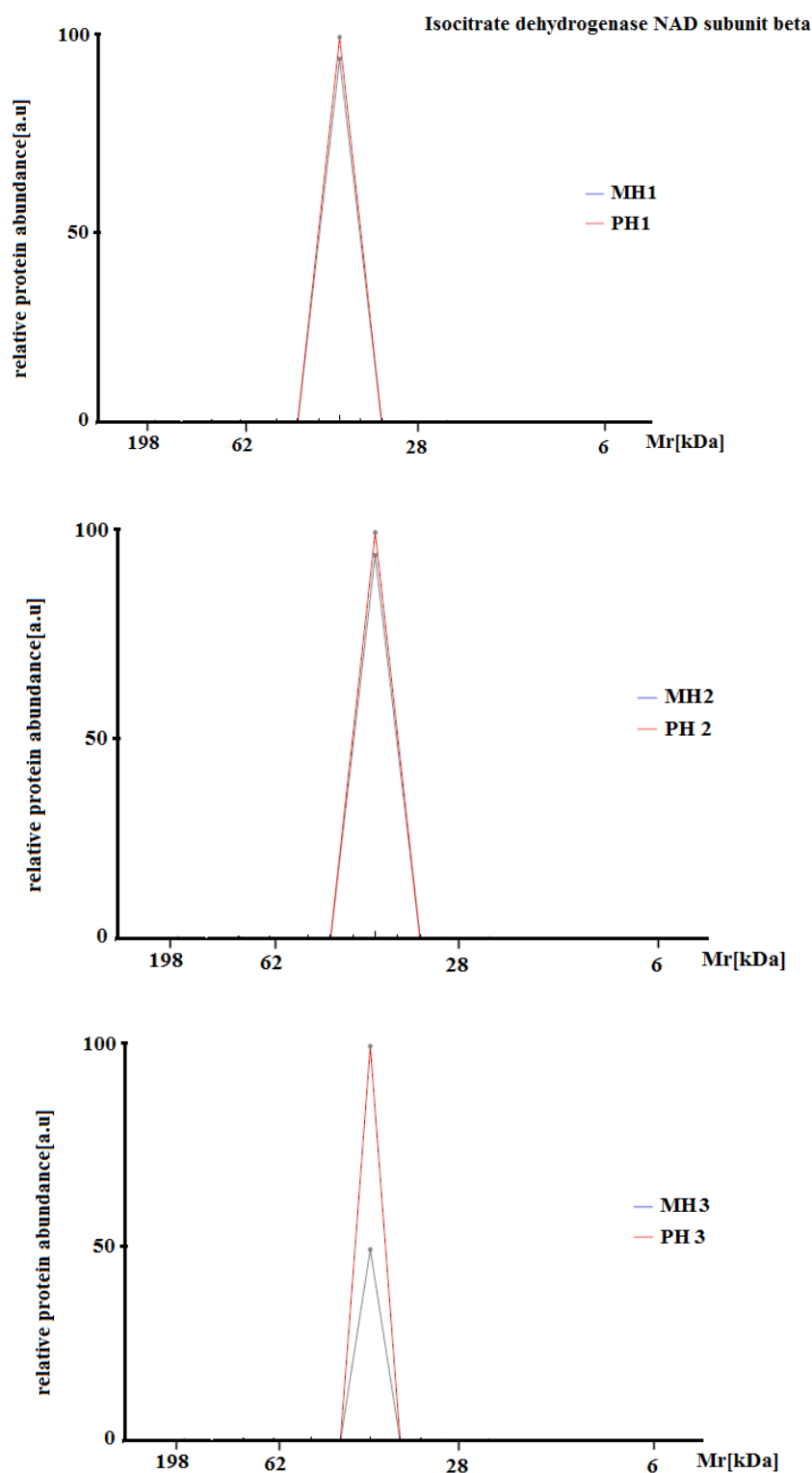


Figure 15: SDS-PAGE-migration profiles of Isocitrate dehydrogenase NAD subunit beta constructed from the relative quantities of its species, identified by tryptic digestion and following LC-MS/MS analysis in the individual SDS-PAGE bands of the protein extracts from rat pancreas sample obtained by mechanical homogenization and PIRL-DIVE homogenization. PH1: PIRL homogenate of the first rat pancreas sample, MH1: mechanical homogenate of the first rat pancreas sample. PH2: PIRL homogenate of the second rat pancreas, MH2: mechanical homogenate of the second rat pancreas sample. PH3: PIRL homogenate of the third rat pancreas sample, MH3: mechanical homogenate of the third rat pancreas sample.

Figure 16 shows the migration profiles of Nucleoside diphosphate kinase A protein (Gene: NDKA, $m=17.2$ kDa). The protein was identified by tryptic digestion and LC-MS/MS analysis in the SDS-PAGE (band no.18, figure 11) of the protein extracts from the third rat pancreas obtained by PIRL-DIVE homogenization at the intense band slightly above the 14 Da marker. In MH it was identified by tryptic digestion and LC-MS/MS analysis in the SDS-PAGE (bands no.18, 22, figure 11) at a molecular weight around 17 kDa and 6 kDa, respectively.

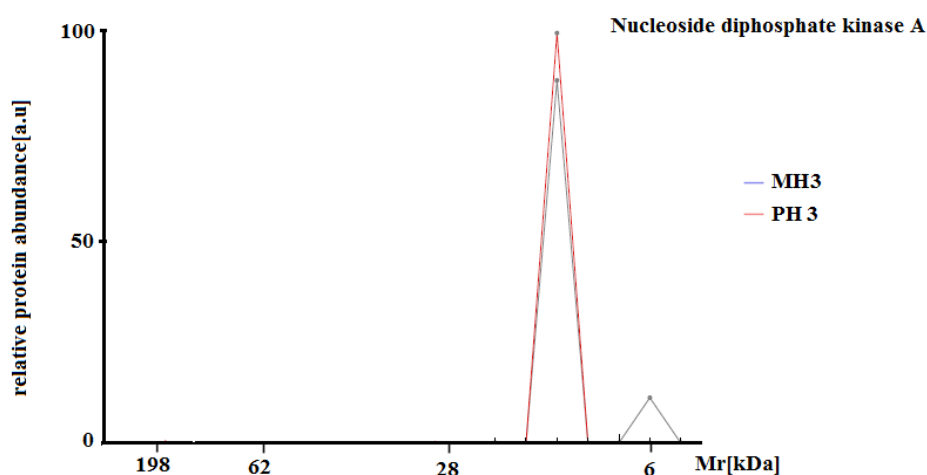


Figure 16: SDS-PAGE-migration profiles of Nucleoside diphosphate kinase A constructed from the relative quantities of its species, identified by tryptic digestion and following LC-MS/MS analysis in the individual SDS-PAGE bands of the protein extracts from the third rat pancreas sample obtained by mechanical homogenization and PIRL-DIVE homogenization. PH3: PIRL homogenate of the first rat pancreas sample, MH3: mechanical homogenate of the first rat pancreas sample.

tRNA-slicing ligase RtcB homolog (Gene: RTCB, $m=55.2$ kDa): SDS-PAGE migration profiles of protein species of this protein was constructed for PH and MH from the third rat pancreas (Figure 17). The protein was identified by tryptic digestion and LC-MS/MS analysis in the SDS-PAGE (band no.11, figure 11) at a molecular weight above the 49 kDa marker in the protein extracts obtained by PIRL-DIVE homogenization. In the MH the protein was identified between molecular weight 55 kDa down to less than 14 kDa (bands no.10-11, 13, 20, figure 11).

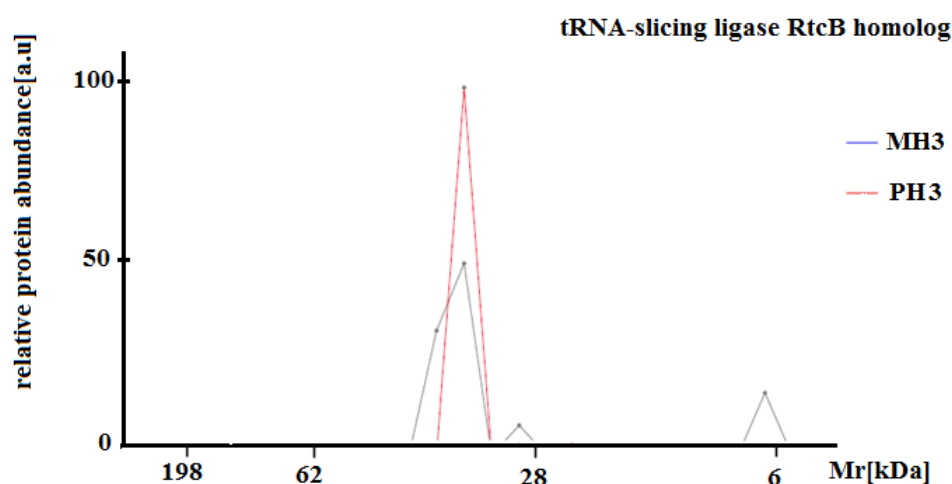


Figure 17: SDS-PAGE-migration profiles of tRNA-slicing ligase RtcB homolog constructed from the relative quantities of its species, identified by tryptic digestion and following LC-MS/MS analysis in the individual SDS-PAGE bands of the protein extracts from rat pancreas sample obtained by mechanical homogenization and PIRL-DIVE homogenization. PH3: PIRL homogenate of the first rat pancreas sample, MH3: mechanical homogenate of the first rat pancreas sample.

Figure 18 illustrates the migration profiles of Septin-2 (Gene: SEPT2, $m=41.6$ kDa). The protein was identified by tryptic digestion and LC-MS/MS analysis in the SDS-PAGE (band no.12, figure 11) at the level below the 49 kDa marker in the protein extracts obtained from the first rat pancreas by PIRL-DIVE homogenization. In the MH extract it was identified by tryptic digestion and LC-MS/MS analysis in the SDS-PAGE (bands no.12, 17, figure 11) at the level below the 49 kDa marker and below the 28 kDa marker, respectively.

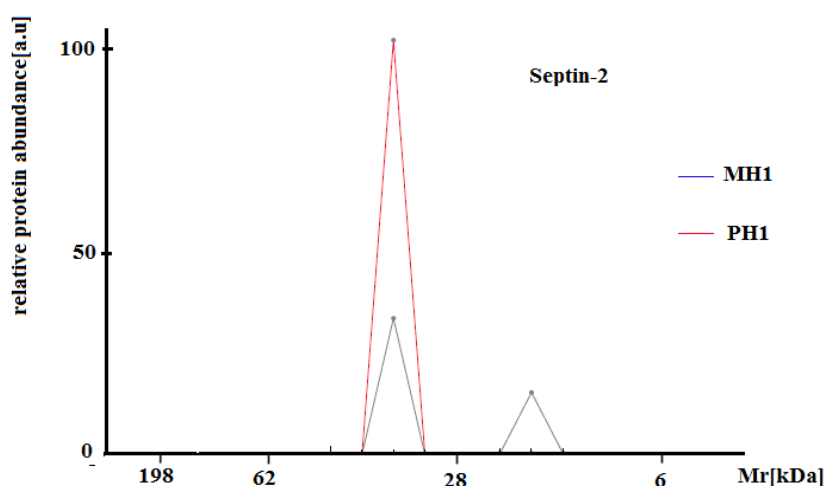


Figure 18: SDS-PAGE-migration profiles of septin-2 constructed from the relative quantities of its species, identified by tryptic digestion and following LC-MS/MS analysis in the individual SDS-PAGE bands of the protein extracts obtained from rat pancreas sample by mechanical homogenization and PIRL-DIVE homogenization. PH1: PIRL homogenate of the first rat pancreas sample, MH1: mechanical homogenate of the first rat pancreas sample.

SDS-PAGE-migration profiles of Alpha-aminoadipic semialdehyde synthase (Figure 19) illustrated that this protein was identified in the PH at band no.7 (figure 11) around the 98 kDa marker, whereas in the MH the protein was distributed over a molecular weight range from 200 kDa down to 6 kDa (bands no.1,7,13,20, figure 11).

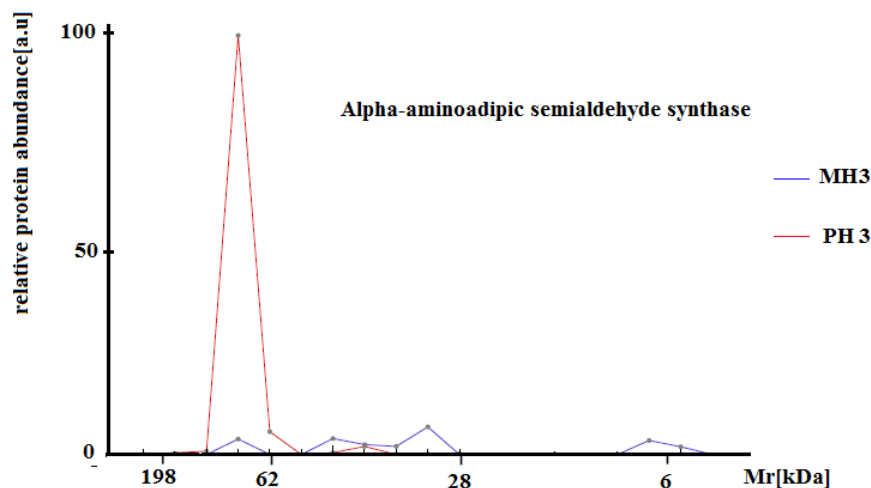


Figure 19: SDS-PAGE-migration profiles of Alpha-aminoadipic semialdehyde synthase constructed from the relative quantities of its species, identified by tryptic digestion and following LC-MS/MS analysis in the individual SDS-PAGE bands of the lanes of the protein extracts from the third rat pancreas sample obtained by mechanical homogenization and PIRL-DIVE homogenization. PH3: PIRL homogenate of the third rat pancreas sample, MH3: mechanical homogenate of the third rat pancreas sample.

For protein Biliverdin reductase A (Gene: BIEA, m=33.6 kDa) SDS-PAGE-migration profiles were generated from the third rat pancreas (Figure 20). The Biliverdin reductase A protein was identified in the PH of rat pancreas no. 3 at band no.14 at a molecular weight around the 38 kDa marker, whereas in the MH of rat pancreas no.3 it was identified at band no. 21 at a molecular weight around 6 kDa (Figure 11).

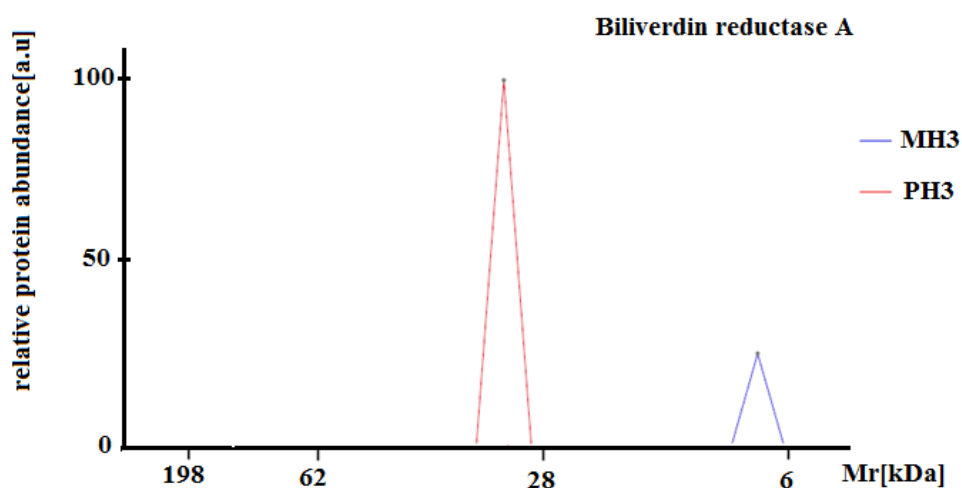


Figure 20: SDS-PAGE-migration profiles of Biliverdin reductase A constructed from the relative quantities of its species, identified by tryptic digestion and following LC-MS/MS analysis in the individual SDS-PAGE bands of the protein extracts from rat pancreas sample obtained by mechanical homogenization and PIRL-DIVE homogenization (PH). PH3: PIRL homogenate of the third rat pancreas sample, MH3: mechanical homogenate of the third rat pancreas sample.

SDS-PAGE-migration profiles of the 28S ribosomal protein S7 (Gene: RTO7, m=28.2 kDa) (Figure 21) showed that this protein was identified in the PH of rat pancreas no. 3 at molecular weight of 28 kDa at band no. 16 (Figure 11), whereas this protein was identified at molecular weight around 14 at band no.19 in MH of rat pancreas no. 3 (Figure 16).

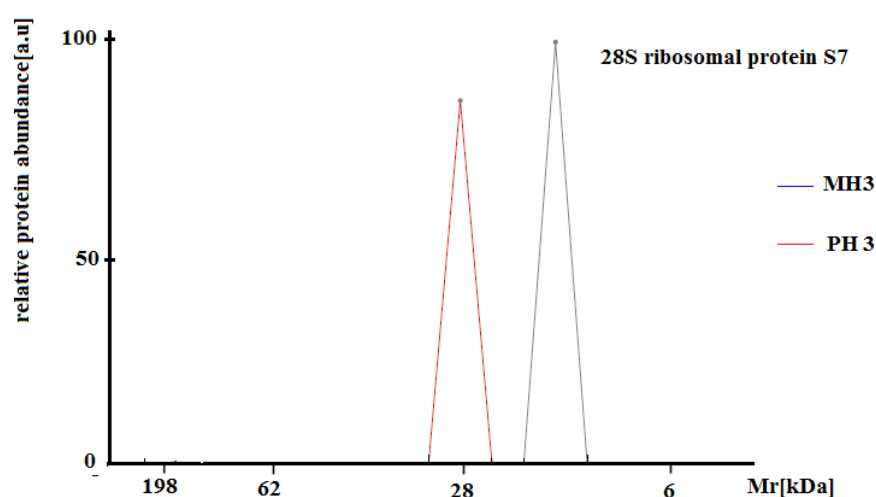


Figure 21: SDS-PAGE-migration profiles of 28S ribosomal protein S7 constructed from the relative quantities of its species, identified by tryptic digestion and following LC-MS/MS analysis in the individual SDS-PAGE bands of the protein extracts from rat pancreas sample obtained by mechanical homogenization and PIRL-DIVE homogenization. PH3: PIRL homogenate of the third rat pancreas sample, MH3: mechanical homogenate of the third rat pancreas sample.

SDS-PAGE-migration profiles in figure 22 represent the distribution of the protein species of Long-chain-fatty-acid-CoA ligase 5 (Gene: ACSL5, m=76.4 kDa) from the first rat pancreas after PH, which was identified at the intense band no. 9 slightly above the 62 kDa marker (Figure 11). This protein species was not found in the corresponding area in the SDS-PAGE of MH from rat pancreas no. 1 nor in any other area in the whole lane (MH1, Figure 10). This situation is indicated in SDS-PAGE-migration profiles where the signal of this protein species from MH1 is missing (Figure 22).

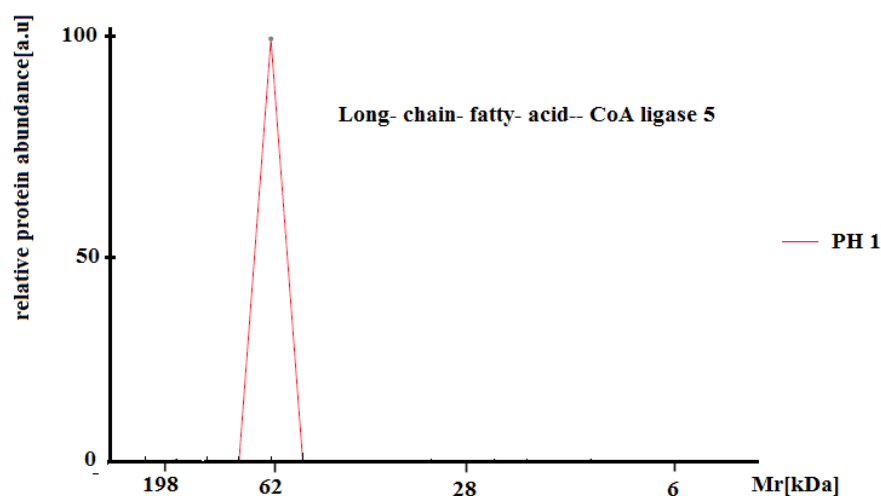


Figure 22: SDS-PAGE-migration profiles of Long-chain-fatty-acid-CoA ligase 5 constructed from the relative quantities of its species, identified by tryptic digestion and following LC-MS/MS analysis in the individual SDS-PAGE bands of the protein extracts from rat pancreas sample obtained by mechanical homogenization and PIRL-DIVE homogenization. PH1: PIRL homogenate of the first rat pancreas sample.

For the protein species of Amyloid beta A4 (Gene: App, m=86.7 kDa), SDS-PAGE migration profiles were built from the three biological replicate samples (Figure 23). The protein species were identified in bands no. 6 and no.7 which are located between the molecular weight markers at 98 kDa and 62 kDa (Figure 11), whereas this protein species was not identified in all SDS-PAGE of the MH samples of the three biological replicates (Figure 10).

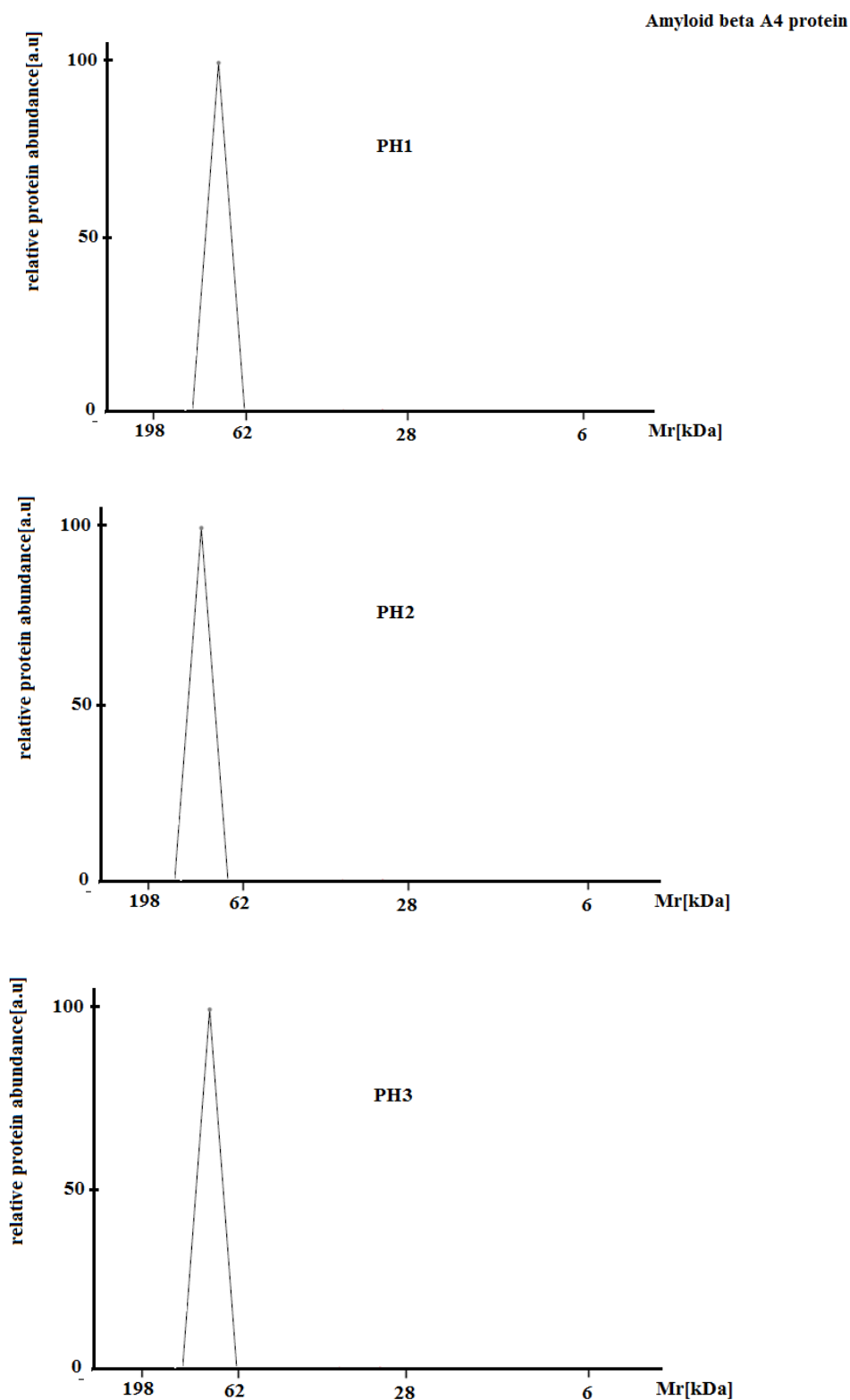


Figure 23: SDS-PAGE-migration profiles of the Amyloid beta A4 protein constructed from the relative quantities of their species, identified by tryptic digestion and following LC-MS/MS analysis in the individual SDS-PAGE bands of the protein extracts from rat pancreas yielded by PIRL-DIVE homogenization. PH1: PIRL homogenate of the first rat pancreas sample, PH2: PIRL homogenate of the second rat pancreas sample, PH3: PIRL homogenate of the third rat pancreas sample.

The same results as for the Amyloid beta A4 (Figure 23) were obtained for the protein species of the Pyruvate dehydrogenase (acetyl-transferring) kinase isozyme 2 (Gene: PDK2, m=46.1 kDa) (Figure 24). As shown in the SDS-PAGE migration profiles of the Pyruvate dehydrogenase (acetyl-transferring) kinase isozyme 2 protein species, the protein species were identified at bands no. 11 and 12 which is located approximately at the 49 kDa marker in the PH samples of the three biological replicates (Figure 11), whereas this protein was not found in all SDS-PAGE of the MH samples in the three biological replicates of MH (Figure 10).

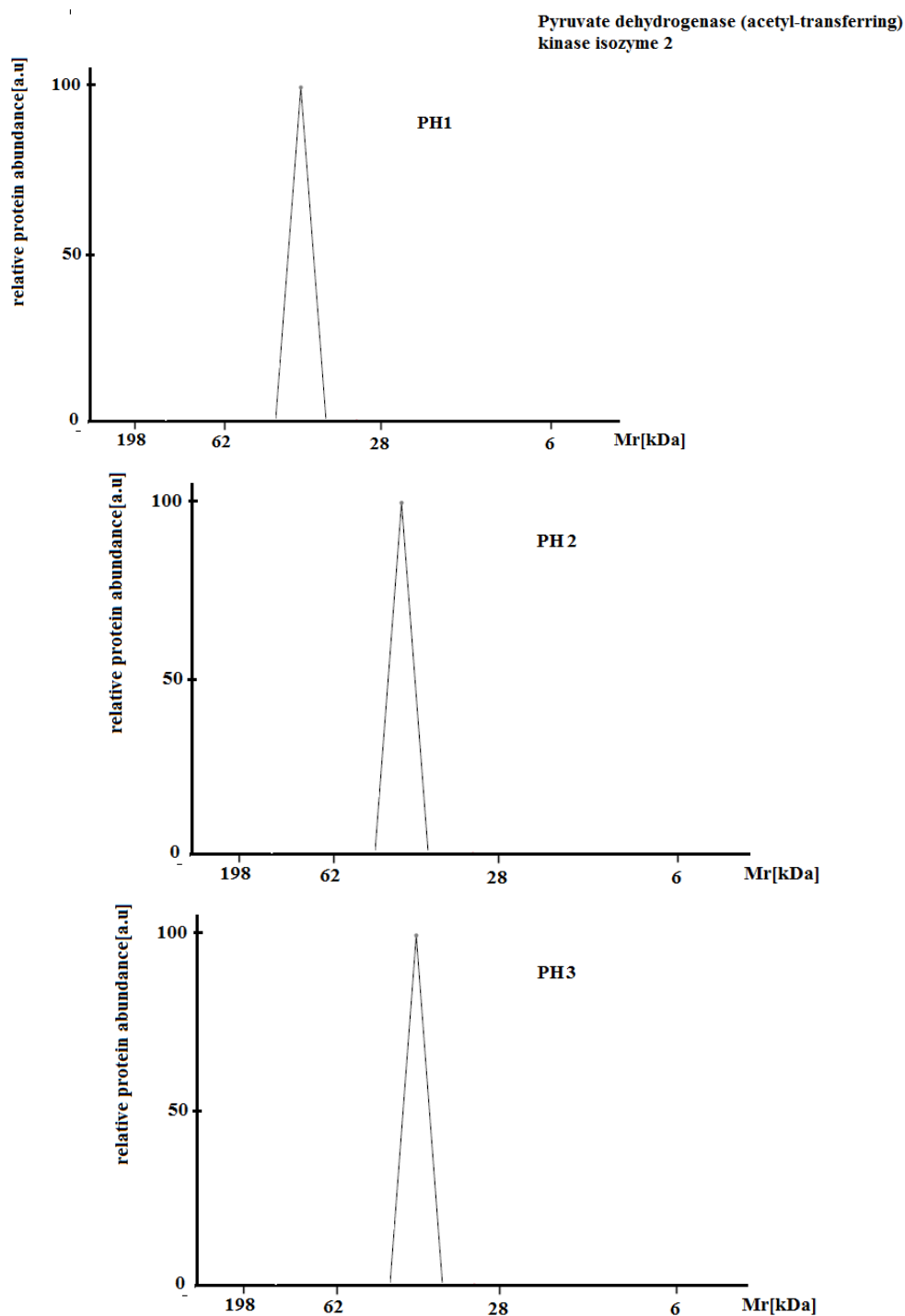


Figure 24: SDS-PAGE-migration profiles of Pyruvate dehydrogenase (acetyl-transferring) kinase isozyme 2 constructed from the relative quantities of their species, identified by tryptic digestion and following LC-MS/MS analysis in the individual SDS-PAGE bands of the protein extracts from rat pancreas obtained by PIRL-DIVE homogenization. PH1: PIRL homogenate of the first rat pancreas sample, PH2: PIRL homogenate of the second rat pancreas sample, PH3: PIRL homogenate of the third rat pancreas sample.

In addition, protein species of Heat shock 70 kDa protein 1 B (HS71B, m=70.2 kDa) were missing in all three biological replicates in the mechanical homogenates according to its SDS-PAGE migration profiles (Figure 25). In PIRL homogenates of all biological replicates, the protein species of protein Heat shock 70 kDa protein 1 B were identified at bands no. 8 and 9 which were slightly above the 62 kDa marker (Figure 11).

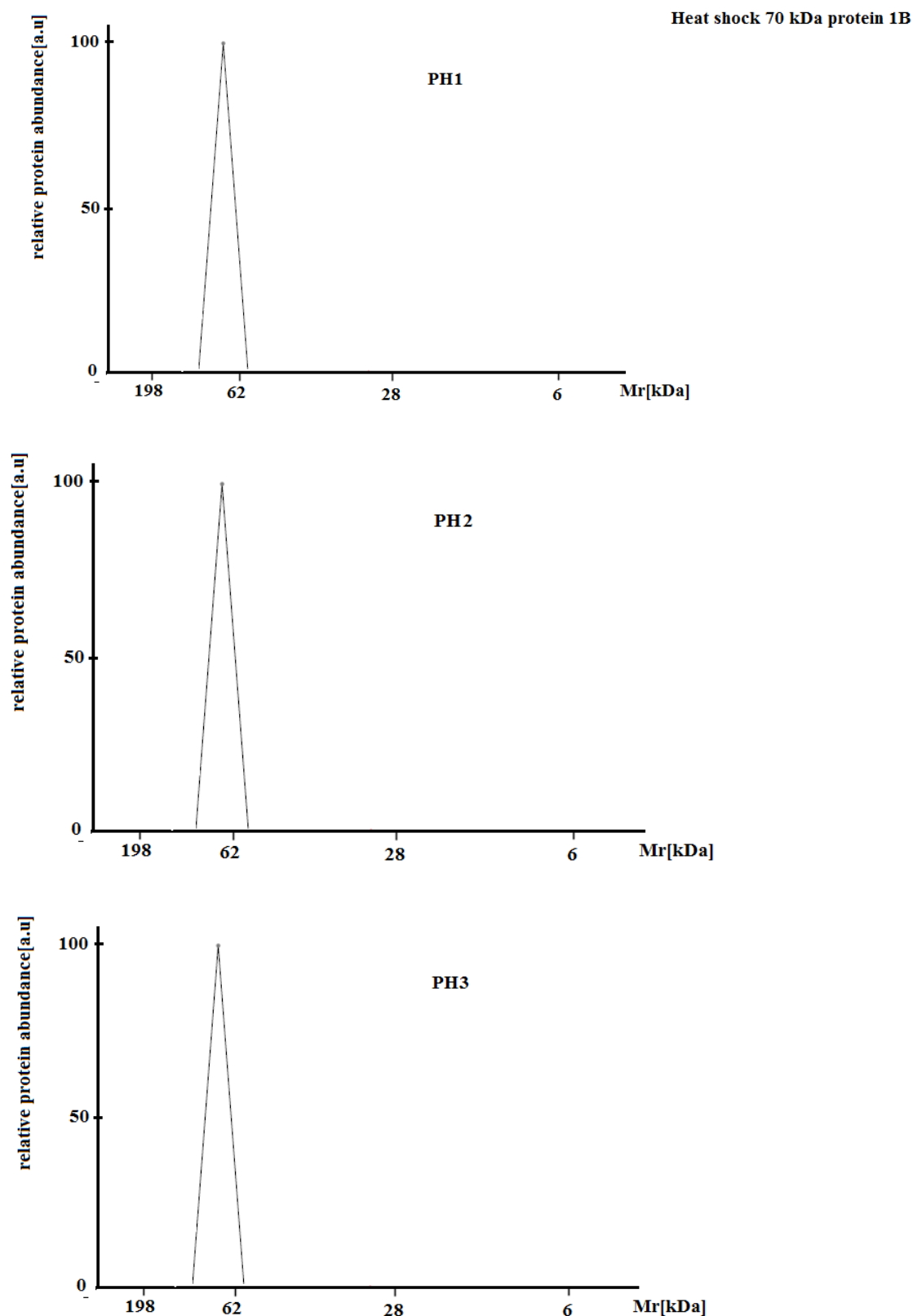


Figure 25: SDS-PAGE-migration profiles of Heat shock 70 kDa protein 1 B constructed from the relative quantities of its species, identified by tryptic digestion and following LC-MS/MS analysis in the individual SDS-PAGE bands of the protein extracts from rat pancreas obtained by PIRL-DIVE homogenization . PH1: PIRL homogenate of the first rat pancreas sample, PH2: PIRL homogenate of the second rat pancreas sample, PH3: PIRL homogenate of the third rat pancreas sample.

SDS-PAGE-migration profiles of Cyclin-G-associated kinase (Gene: GAK, m=143.7 kDa) from the first rat pancreas obtained by PIRL-DIVE and mechanical homogenization (Figure 26 top) revealed the protein species of this protein at bands no.5 at a molecular weight level slightly below 198 kDa in SDS-PAGE of PH of rat pancreas no.1 (Figure 10,11). The protein species of this protein was not identified in the SDS-PAGE of protein homogenates obtained by mechanical homogenization from rat pancreas no.1 (Figure 10, MH1).

A similar observation in the distribution of Cyclin-G-associated kinase protein species is shown in figure 26 (bottom) for the SDS-PAGE migration profile of the Chromodomain-helicase-DNA-binding protein 5 (Gene: CHD5, m=222.3) obtained by PIRL-DIVE homogenization from the second rat pancreas. In the SDS-PAGE of protein homogenates obtained by mechanical homogenization from rat pancreas no.2 this protein could not be identified (Figure 5, MH2) (Figure 6).

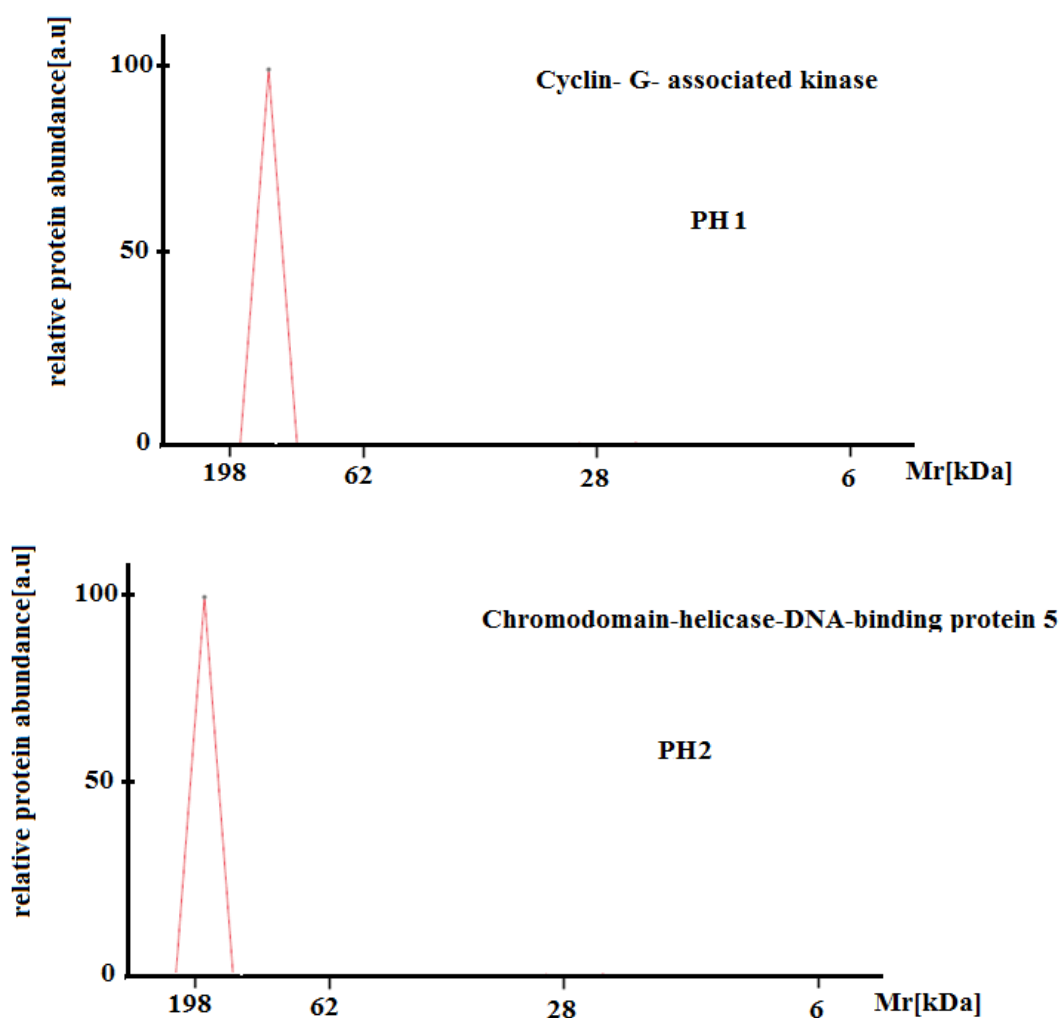


Figure 26: SDS-PAGE-migration profiles of Cyclin-G-associated kinase (top) and Chromodomain-helicase-DNA-binding protein 5 (bottom) constructed from the relative quantities of their species, identified by tryptic digestion and following LC-MS/MS analysis in the individual SDS-PAGE bands of the protein extracts from rat pancreas sample obtained by mechanical homogenization (MH) and PIRL-DIVE homogenization. PH2: PIRL homogenate of the second rat pancreas sample. PH3: PIRL homogenate of the third rat pancreas sample.

The proteins Regulator complex protein LAMATOR3 (Gene: LAMTOR3, m=13.6 kDa) and Protein preY (Gene: PYURF, m=12.7 kDa) shared similar migration profiles in the SDS-PAGE analysis (Figure 27). Both proteins were not found in the SDS-PAGE of protein homogenates obtained by mechanical homogenization from rat pancreas no.1 (Figure 10, MH1). Therefore the signals of these proteins from MH are missing in their SDS-PAGE migration profiles (Figure 27). In contrast, the protein species of Regulator complex protein LAMATOR3 and preY protein were identified in the PH samples of rat pancreas sample no.1. in band no. 19 at a molecular weight slightly below 14 kDa marker (Figure 11). The SDS-PAGE migration profiles of these proteins in the PH samples are shown in figure 27.

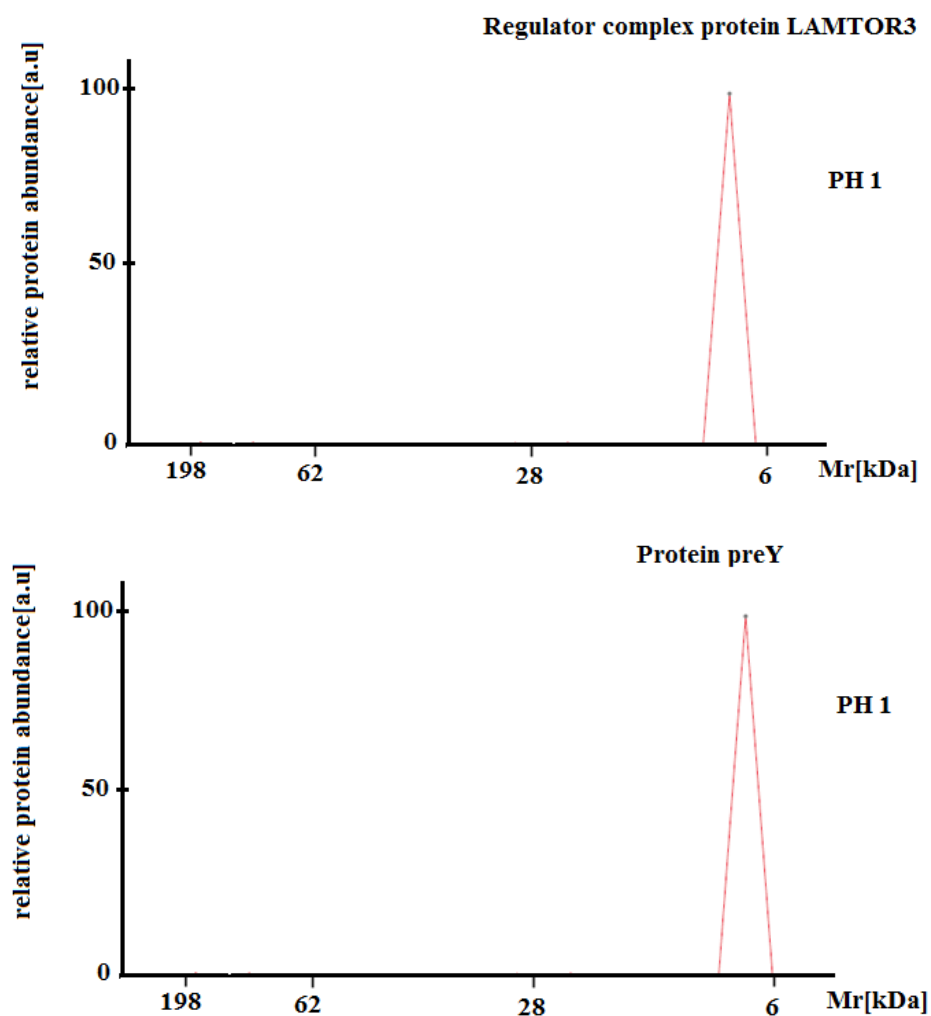


Figure 27: SDS-PAGE-migration profiles of Regulator complex protein LAMATOR3 and Protein preY constructed from the relative quantities of their species, identified by tryptic digestion and following LC-MS/MS analysis in the individual SDS-PAGE bands of the protein extracts from rat pancreas sample obtained by mechanical homogenization and PIRL-DIVE homogenization. PH1: PIRL homogenate of the first rat pancreas sample.

3.2.5 Global statistical analysis of the LC-MS/MS data from the SDS-PAGE of the PIRL homogenates (PH) and the mechanical homogenates (MH) from rat pancreas (n=3)

In order to estimate the global degree of proteolysis between mechanical homogenate (MH) and PIRL homogenate (PH), SDS-PAGE-migration shift peak histograms were constructed depending on SDS-PAGE migration profiles. These migration profiles (examples shown in the previous section) were constructed from the relative quantities of the protein species, identified by tryptic digestion and subsequent LC-MS/MS analysis in the SDS-PAGE bands of the protein extracts from rat pancreas samples obtained by mechanical homogenization and PIRL-DIVE homogenization.

From the SDS-PAGE migration profiles SDS-PAGE migration peak shift histograms were produced for three biological replicates of rat pancreas samples (Figure 28-30) showing the relative migration peak shifts of proteins between mechanical and PIRL homogenate.

For the construction of the migration peak shift histograms only the most abundant signal of a protein was taken into account to build this histogram. In the migration peak shift analysis no proteolysis was considered if the most abundant signal of a protein was detected in both the SDS-PAGE migration profile of MH and PH in the same (migration shift=0) or an adjacent band (migration shift +1, -1). If the most abundant signal of protein was shifted towards lower molecular weights in the SDS-PAGE-migration profile of PH (negative migration distance) or MH (positive migration distance) by at least two bands, the protein was considered as proteolytically degraded.

In the rat pancreas no.1, the SDS-PAGE-migration peak shift histogram (Figure 28, Table 4) shows 1177 proteins with a migration shift distance equal 0. Twenty proteins show migration shift distances greater than or equal to 2 in PH, whereas in the mechanical homogenate sample (MH) 33 proteins were detected with migration shift distances greater than or equal to 2. The relative degree of proteolysis was in the first rat pancreas for PH 1.63% and for MH 2.68% (Table 5).

The SDS-PAGE migration peak shift histogram for rat pancreas no. 2 shows 1144 proteins with no migration shift distances. Fourteen proteins with a migration shift distance greater than or equal 2 were observed in the PIRL homogenate (PH) sample, whereas 24 proteins in the MH sample were observed with differences greater than or equal 2 (Figure 29, Table 4). The relative degree of proteolysis was in the second rat pancreas for PH 1.2% and MH 2.03% (Table 5).

1367 proteins were demonstrated in SDS-PAGE-migration peak shift analysis for rat pancreas no. 3 with migration shift distances equal 0. In the case of PIRL homogenate (PH) 15 proteins with migration shift distances greater than or equal 2 were observed and in the case of mechanical homogenate, 28 proteins with migration distances greater than or equal 2 were detected (Figure 30, Table 4). The relative degree of proteolysis in the third rat pancreas was for PH 1.1% and MH 2.0% (Table 5).

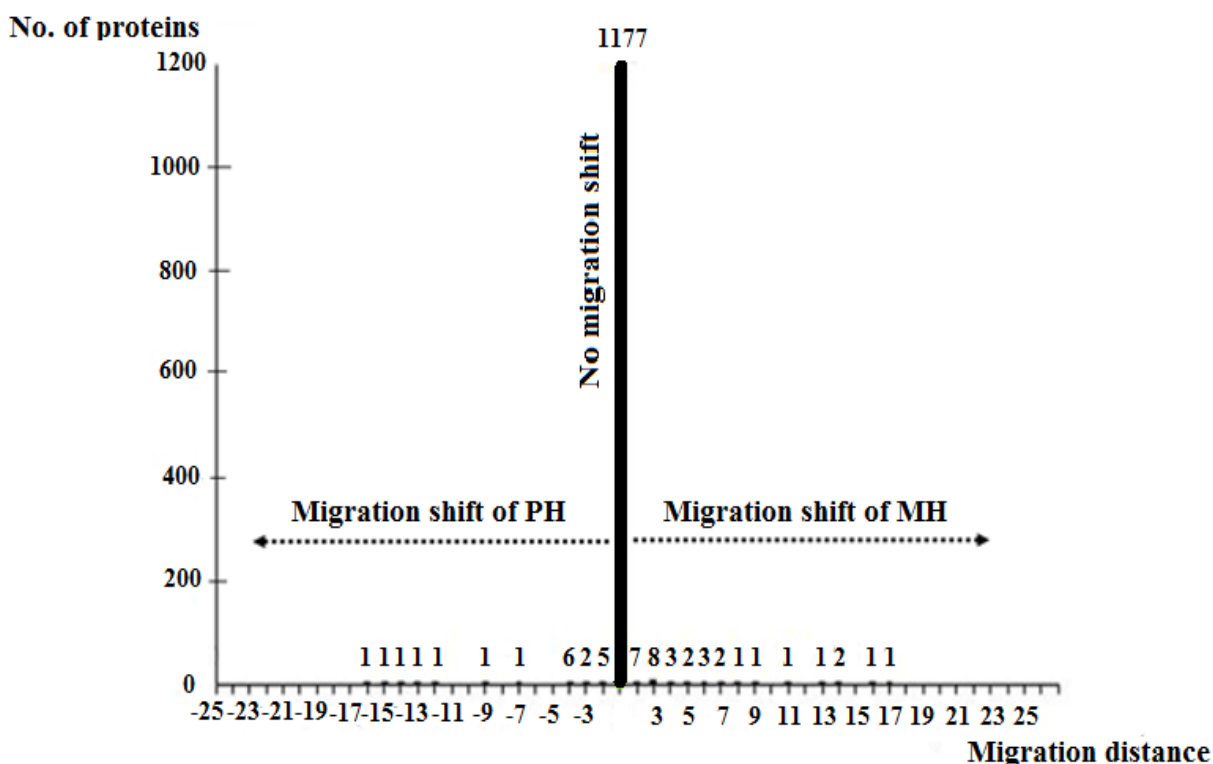


Figure 28: SDS-PAGE-migration peak shift histogram of proteins of rat pancreas 1.

The histogram shows the relative migration peak shifts of proteins between mechanical homogenate (MH) and PIRL homogenate (PH). If the most intense signal of a protein was detected in both the SDS-PAGE migration profile of MH and PH in the same or adjacent band (migration peak shift 0, +1, -1), the migration distance in the histogram is 0 indicating no migration shift due to proteolysis. If the most intense signal of protein was shifted towards lower molecular weights in the SDS-PAGE-migration profile of PH (negative migration distance) or MH (positive migration distance) by at least two bands, they were considered proteolysed. The numbers represent the number of proteins in PH and MH with a corresponding migration distance.

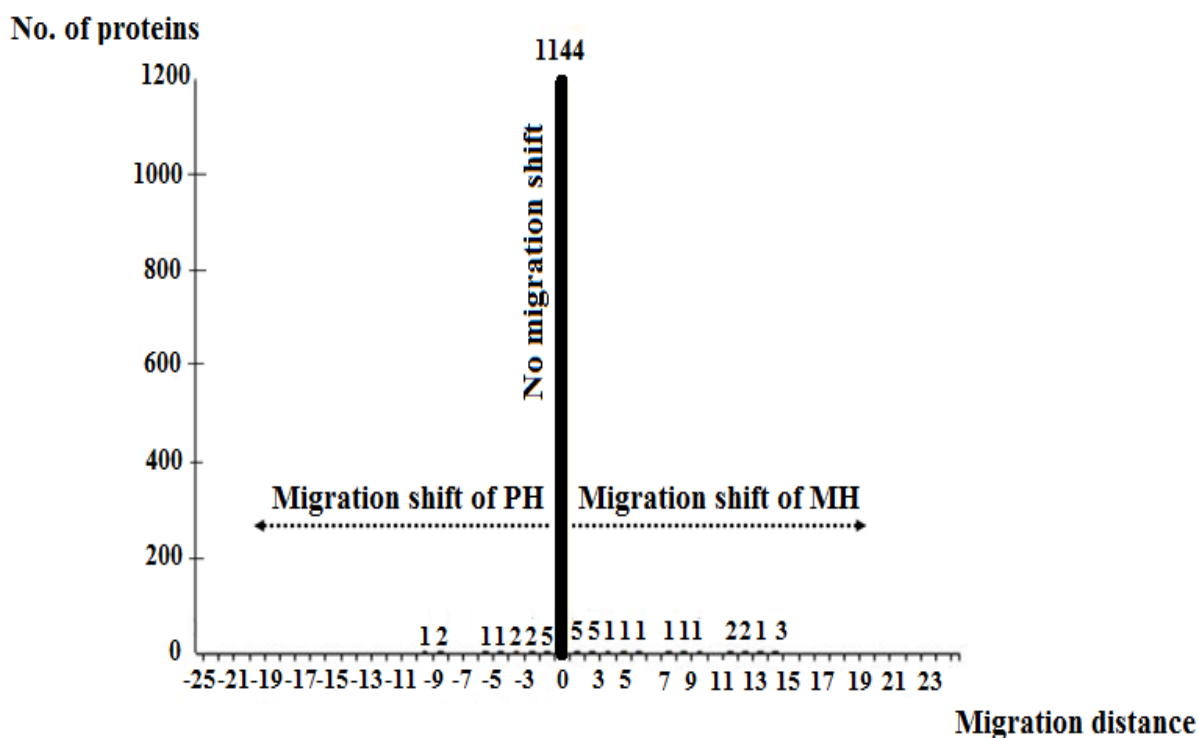


Figure 29: SDS-PAGE-migration peak shift histogram of proteins of rat pancreas 2.

The histogram shows the relative migration peak shifts of proteins between mechanical homogenate (MH) and PIRL homogenate (PH). If the most intense signal of a protein was detected in both the SDS-PAGE migration profile of MH and PH in the same or adjacent band (migration peak shift 0, +1, -1), the migration distance in the histogram is 0 indicating no migration shift due to proteolysis. If the most intense signal of protein was shifted towards lower molecular weights in the SDS-PAGE-migration profile of PH (negative migration distance) or MH (positive migration distance) by at least two bands, they were considered proteolysed. The numbers represent the number of proteins in PH and MH with a corresponding migration distance.

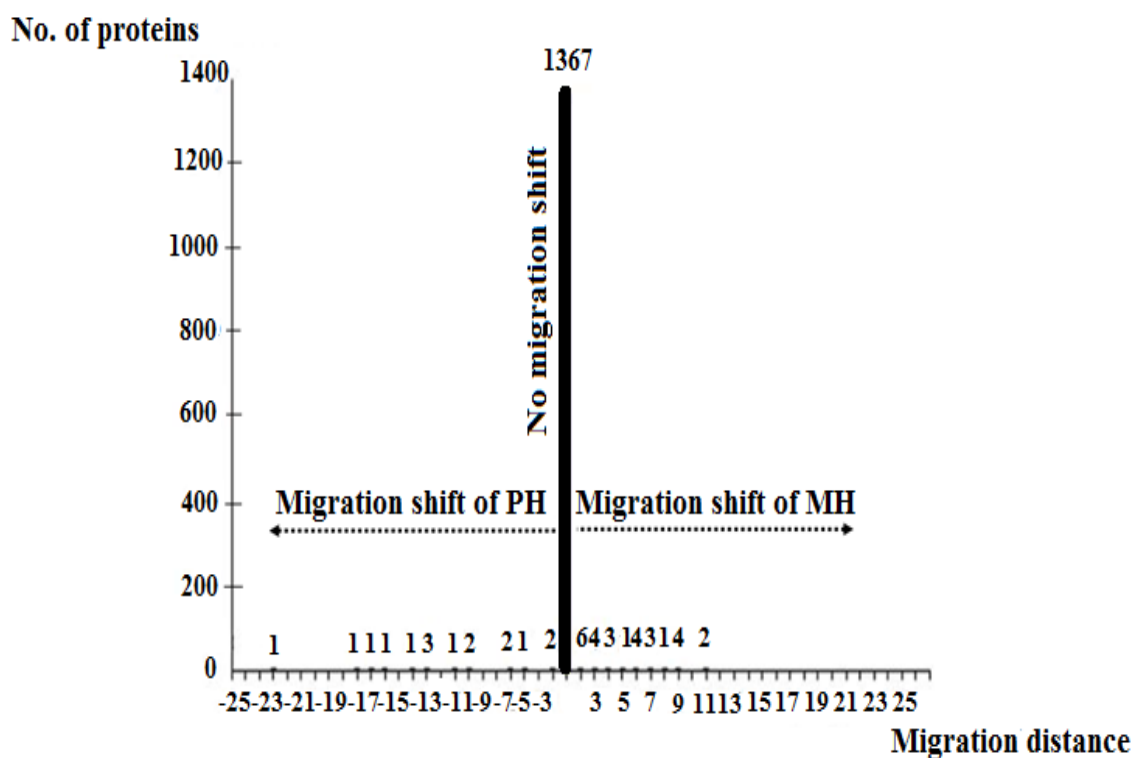


Figure 30: SDS-PAGE-migration peak shift histogram of proteins of rat pancreas 3.

The histogram shows the relative migration peak shifts of proteins between mechanical homogenate (MH) and PIRL homogenate (PH). If the most intense signal of a protein was detected in both the SDS-PAGE migration profile of MH and PH in the same or adjacent band (migration peak shift 0, +1, -1), the migration distance in the histogram is 0 indicating no migration shift due to proteolysis. If the most intense signal of protein was shifted towards lower molecular weights in the SDS-PAGE-migration profile of PH (negative migration distance) or MH (positive migration distance) by at least two bands, they were considered proteolysed. The numbers represent the number of proteins in PH and MH with a corresponding migration distance.

Table 4: Number of proteins that show relative migration peak shifts or no migration shift between mechanical (MH) and PIRL homogenization (PH) in the three rat pancreas samples derived from the SDS-PAGE-migration peak shift histograms (Figure 28-30).

	No. Of proteins with migration shift= 0	PH: no. Of proteins with migration shift ≥ 2	MH: no. of proteins with migration shift ≥ 2
Rat pancreas 1	1177	20	33
Rat pancreas 2	1144	14	24
Rat pancreas 3	1367	15	28

Table 5: Degree of relative proteolysis [%] in PIRL homogenate (PH) and mechanical homogenate (MH) of rat pancreas samples:

	Degree of relative proteolysis in PH [%]	Degree of relative proteolysis in MH [%]
Rat pancreas 1	1.63	2.68
Rat pancreas 2	1.20	2.03
Rat pancreas 3	1.10	2.00

The analysis of the SDS-PAGE-migration peak shift histograms of proteins in the three biological replicates (Figure 28-30) gave an average degree of relative proteolysis of 1.31% (+/- 0.28%) in the PIRL homogenate (PH) and 2.24% (+/- 0.38%) in the mechanical homogenate (MH) (Figure 31, Table 5). According to the calculated p-value from t-test (T-test: $p = 0.028$), the results from the average degree of relative proteolysis illustrated a significantly higher degree of proteolysis in the case of MH compared to PH.

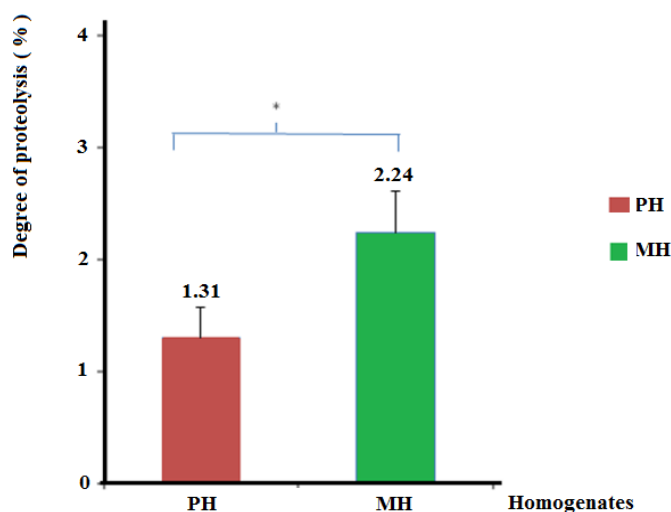


Figure 31: Bar graph (mean with SD) showing the global degree of proteolysis in the three biological replicates in PIRL homogenates (PH) and mechanical homogenates (MH), *: $p=0.028$ (t-test). At least two unique peptides had to be identified for a protein to be taken into account.

On average 1743 proteins (+/- 173 proteins, PH) in the PH-SDS-PAGE of the three rat pancreas samples were identified and in MH-SDS-PAGE of the three rat pancreas samples 1467 proteins (+/- 138 proteins, MH) were identified on average (Figure 32 A, Table 6).

In all three biological replicates, 1418 proteins were identified in the PIRL homogenate (PH), and 1116 proteins were identified in the mechanical homogenate (MH) (Figure 32 A).

Comparing the number of proteins in all the three biological replicates in MH and in PH samples a total of 1092 proteins (75.7 %) were identified in both homogenates. A total of 326 proteins (22.6%) were exclusively identified in the PIRL homogenates (PH), and 24 proteins (1.7%) were identified only in the mechanical homogenates (MH) (Figure 32 A).

The Venn diagram constructed from the proteins identified in PIRL homogenate (PH) (Figure 32 B) showed that 1418 proteins were identified in all three rat pancreas samples, 105 proteins (7.4%) were identified in the first biological replicate, 35 proteins (2.5%) were identified in the second biological replicate, and 176 proteins (12.4%) were identified in the third biological replicate. In both first and second samples in PH 37 proteins (2.6%) were identified, in the first and third sample 232 proteins (16.4%) were found, and in both second and third sample 61 proteins (4.3%) were found.

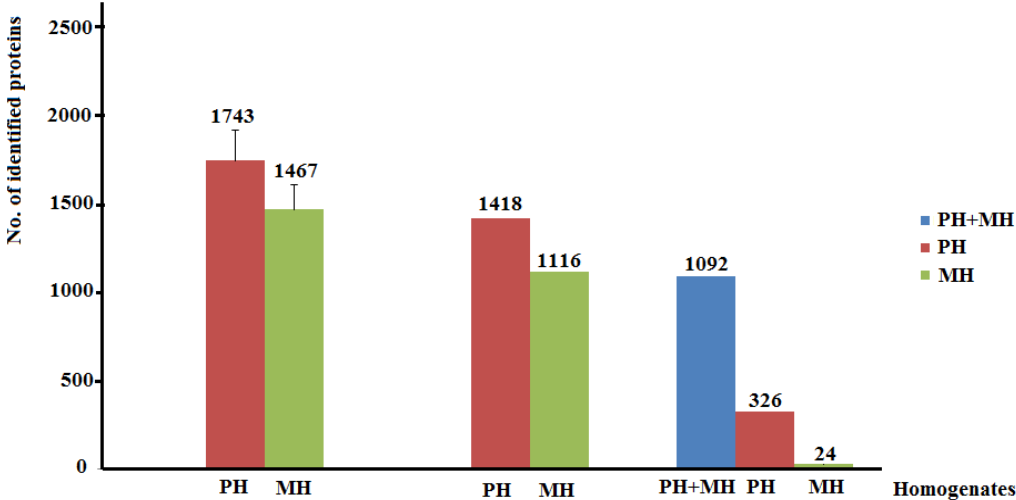
In the case of the Venn diagram from the proteins identified in the mechanical homogenates (MH) (Figure 32 C) 1116 proteins were identified in all the three, 60 proteins (5.4%) were identified in the first biological replicate, 78 proteins (7.0%) were identified in the second

biological replicate, and 239 proteins (21.4%) were identified in the third biological replicate. 68 proteins (6.1%) were found in both the first and second rat pancreas sample in MH, 161 proteins (14.4%) were found in both the first and third rat pancreas sample, and 109 proteins (9.8%) were found in both second and third rat pancreas sample.

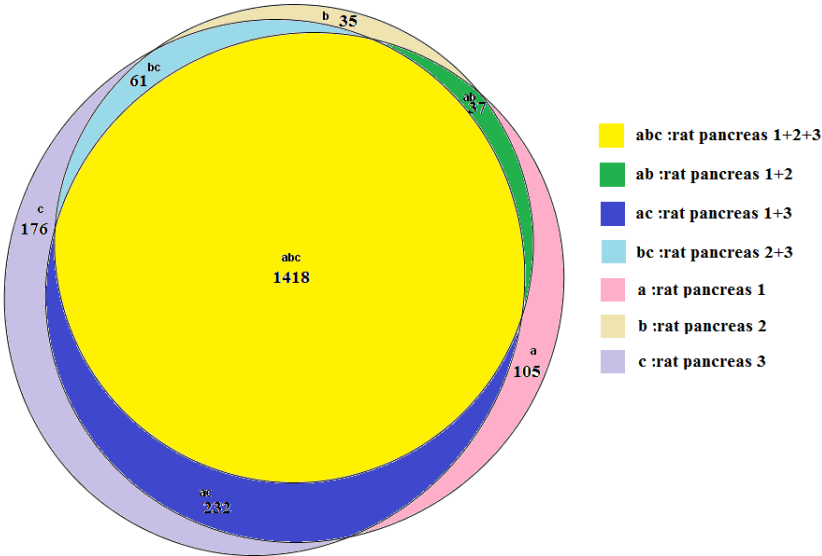
Table 6: Number of proteins identified in each rat pancreas sample obtained by mechanical and by PIRL-DIVE homogenization.

	No. of identified proteins obtained via PIRL-DIVE homogenization	No. of identified proteins obtained via mechanical homogenization
Rat pancreas 1	1792	1405
Rat pancreas 2	1551	1371
Rat pancreas 3	1887	1625

A)



B)



C)

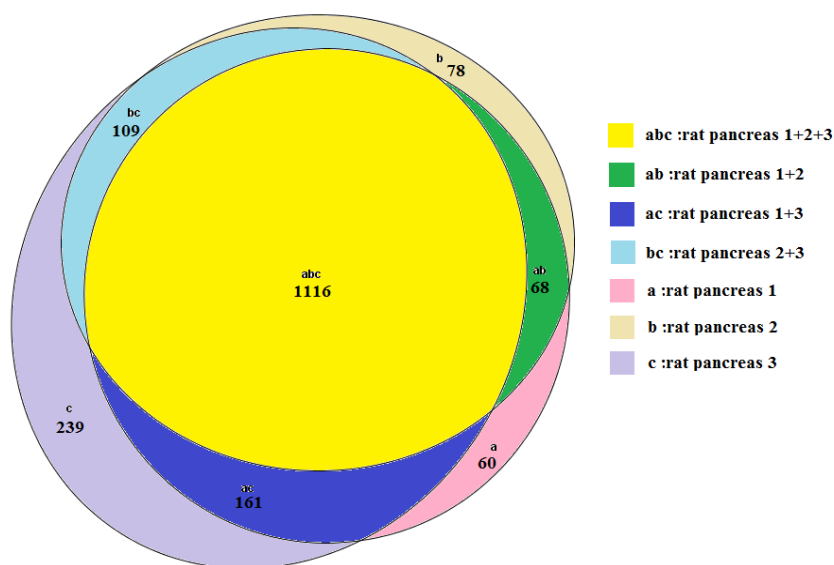


Figure 32: Statistical analysis of the LC-MS/MS data from the SDS-PAGE of the PIRL homogenates (PH) and the mechanical homogenates (MH) from rat pancreas (n=3).

A: Bar graph (mean with standard deviation) showing the total number of proteins identified in the three biological replicates.

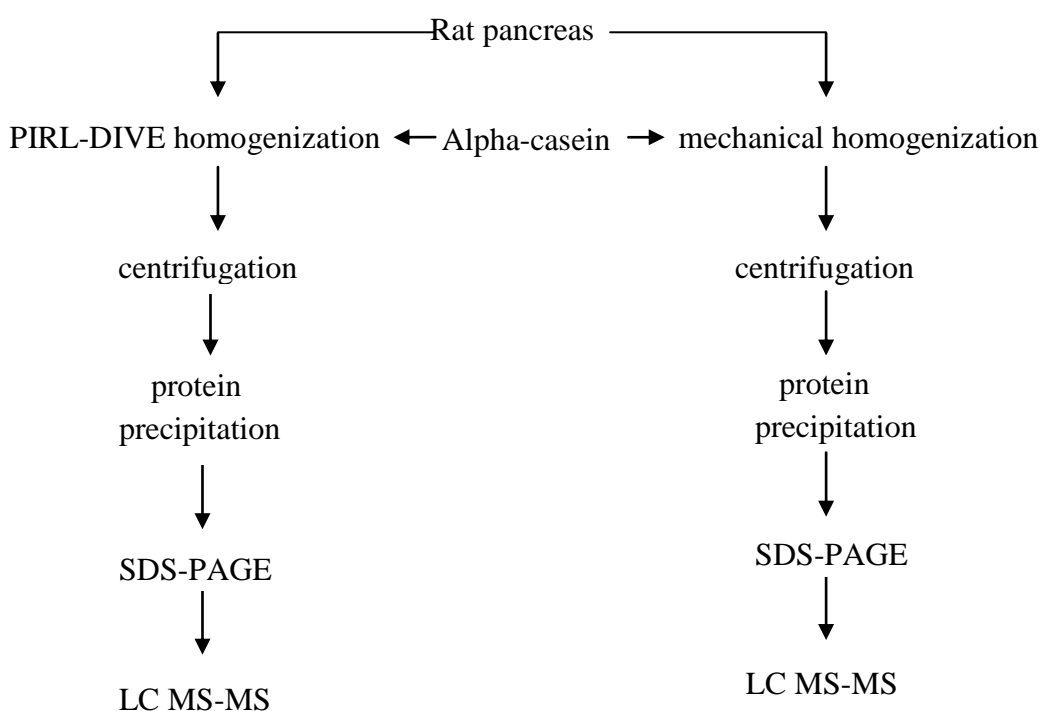
Bar graph showing the number of proteins identified in all three biological replicates in both PH and MH, only in PH and only in MH.

B: Venn diagram showing the number of proteins identified in the PIRL homogenates (PH) in all three biological replicates (abc), in biological replicates one and two (ab), in biological replicates one and three (ac), in biological replicates two and three, only in biological replicate one (a), only in biological replicate two (b) and only in biological replicate three (c).

C: Venn diagram showing the number of proteins identified in the mechanical homogenates (MH) in all three biological replicates (abc), in biological replicates one and two (ab), in biological replicates one and three (ac), in biological replicates two and three, only in biological replicate one (a), only in biological replicate two (b) and only in biological replicate three (c).

3.3 Comparison of the recovery rate of alpha casein spiked in rat pancreas and homogenized via PIRL-DIVE and mechanical in the presence of urea and thiourea as lysis buffer

Rat pancreas samples were spiked with alpha casein and homogenized by either PIRL-DIVE according to Kwiatkowski et al. [111] or with the mechanical homogenization method. Both homogenates were centrifuged to get rid of particles, equal amounts of protein ($m= 30 \mu\text{g}$) were applied to the SDS-PAGE gel and the bands from the gel analyzed by liquid chromatography-mass spectrometry/mass spectrometry (LC-MS/MS) (Scheme 2).



Scheme 3: Experimental workflow (details in material and methods section). SDS-PAGE: sodium dodecyl sulfate- polyacrylamide gel electrophoresis.

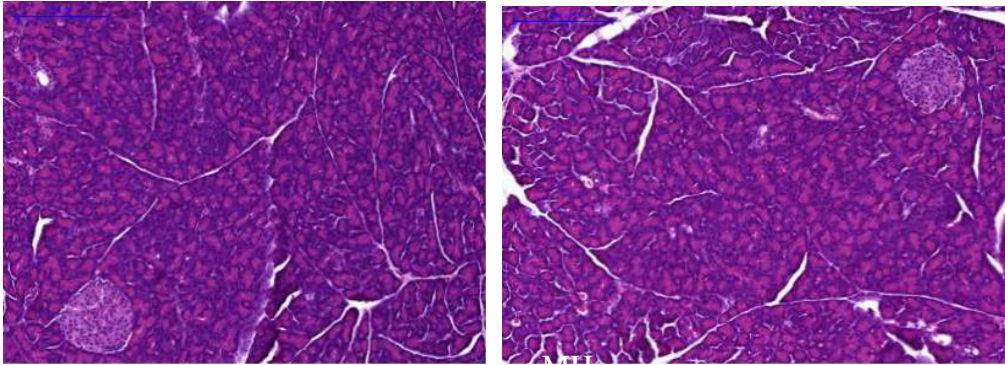
3.3.1 Histological examination, comparison between tissue samples used for PIRL-DIVE and mechanical tissue homogenization

For this part of the experiment, three rat pancreas samples were obtained. From each tissue, two equal pieces were cut out for PIRL-DIVE and mechanical homogenization.

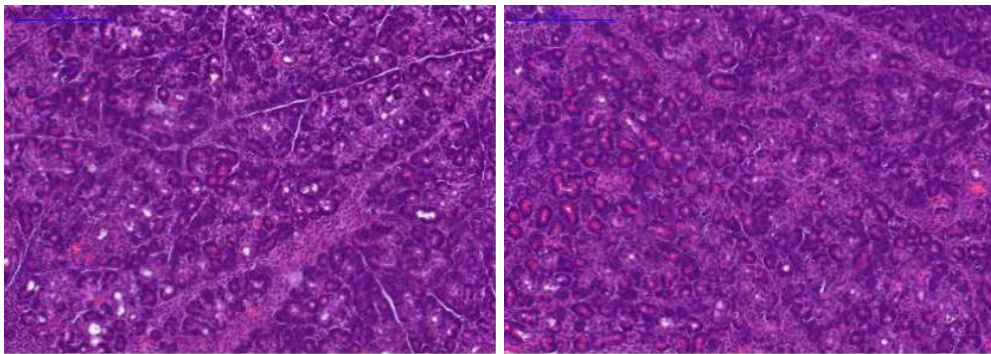
To investigate whether the rat pancreas tissue used for PIRL and mechanical homogenization were comparable, a small section was cut from each of the two pieces for PIRL and mechanical homogenization and used for histological staining. Histological examination (Figure 33) showed all main components of pancreatic tissue, such as endocrine cells surrounded by exocrine glandular tissue, the parenchyma, divided into lobes and lobules by

septa of connective tissue, blood vessels, excretory ducts, and lymph. Therefore the histological inspection indicated, that the tissue samples used for mechanical and PIRL-DIVE homogenization were comparable, with no hint of the presence of different components.

A)



B)



C)

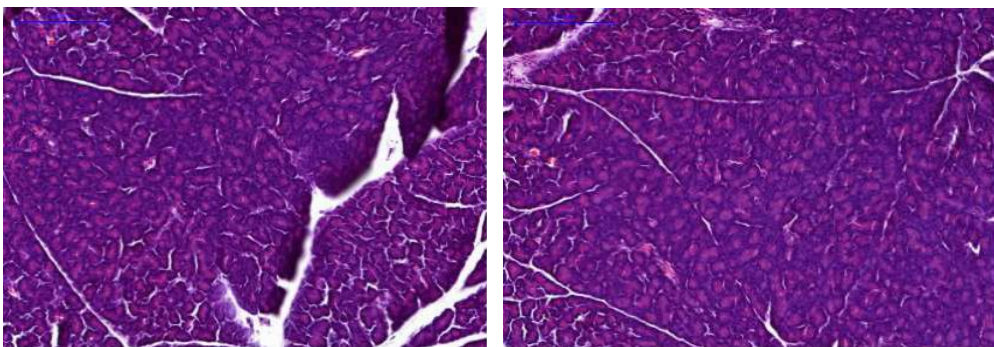


Figure 33: Hematoxylin and Eosin staining (10 x magnification) of pancreas tissue from three rats (A-C), which were used for homogenization by PIRL-DIVE or mechanically. PH: tissue used for PIRL-DIVE homogenization. MH: tissue used for mechanical homogenization.

3.3.2 Separation of proteins in PIRL homogenate (PH) and mechanical homogenate (MH) by one-dimensional gel electrophoresis

The protein alpha casein was spiked in equal amounts in PH and MH and subjected to gel electrophoresis (SDS-PAGE). Three biological replicates were used. The PIRL and mechanical homogenates were captured in a bottle contains alpha-casein and lysis buffer (see materials and methods section for more details)

The proteins from the three biological replicates of PIRL homogenate (PH) and mechanical homogenate (MH) migrated from a molecular weight above 200 kDa down to 6 kDa.

Also, the bands were comparable in all three biological replicates of MH and PH with the same intense color (Figure 34).

The Lanes were divided into comparable slices; slices were cut out of the gel from about 24 kDa where the intact alpha casein protein was expected down to the bottom of the gel. For each biological replicate, identical slices were cut out and the proteins in these bands were digested with trypsin (Figure 35).

The resulting tryptic peptide mixtures from proteins in the marked SDS-PAGE bands (Figure 35) were analyzed by LC MS-MS, the protein composition in every band down to 24 kDa was determined and the huge number of proteomics data thus obtained was used to calculate the number of identified phosphopeptides, the degree of degradation and the recovery rate.

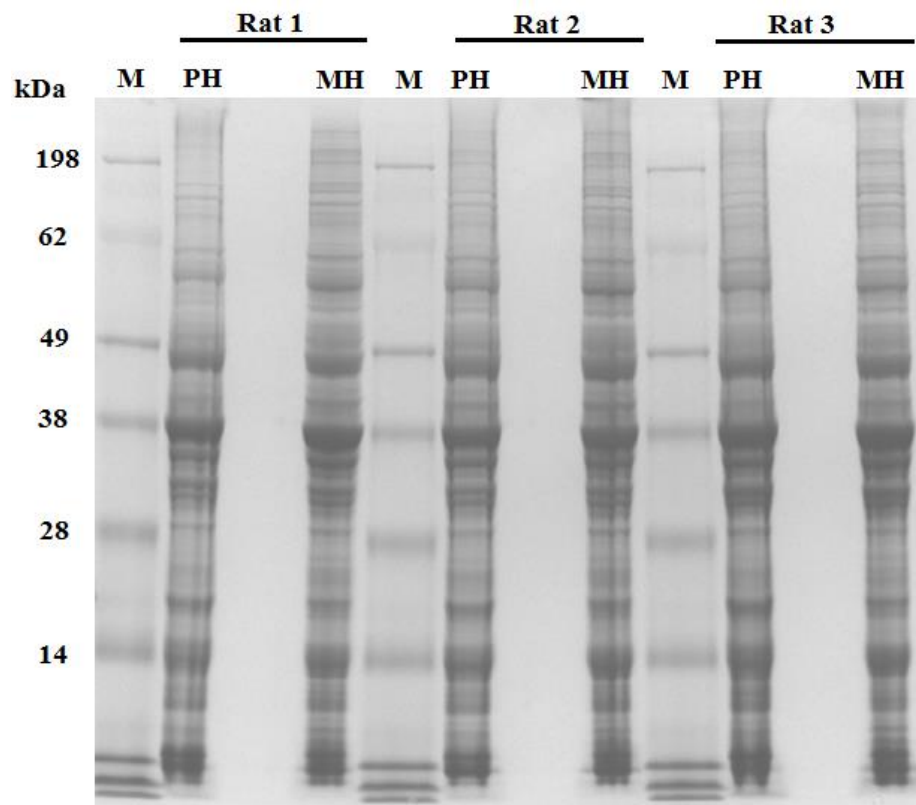


Figure 34: SDS-PAGE of protein homogenates from rat pancreas spiked with alpha casein. M: protein marker. MH: Protein sample of rat pancreas yielded by mechanical homogenization (MH, m= 30 μ g). PH: Protein sample of rat pancreas obtained by PIRL-DIVE homogenization (PH, m= 30 μ g).

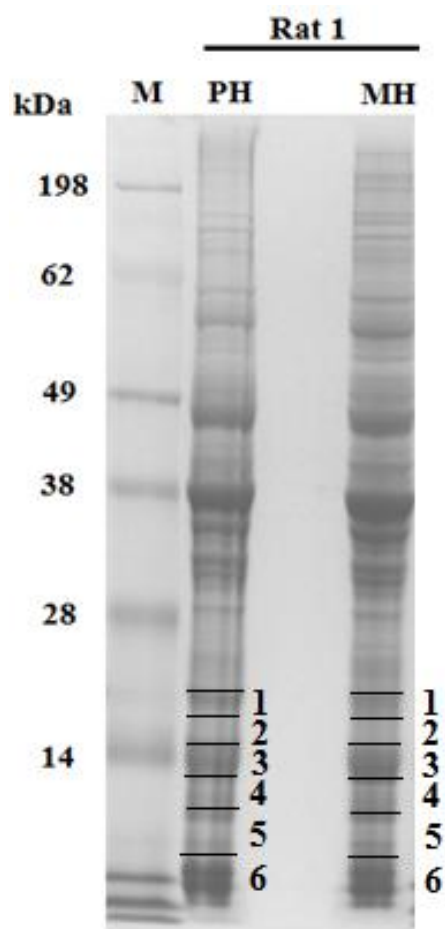


Figure 35: SDS-PAGE of protein homogenates from rat pancreas no. 1 spiked with alpha casein. M: protein marker. MH: Protein sample of rat pancreas no. 1 spiked with alpha casein obtained by mechanical homogenization (MH, $m=30\ \mu\text{g}$). PH: Protein sample of rat pancreas no. 1 spiked with alpha casein obtained by PIRL-DIVE homogenization (PH, $m=30\ \mu\text{g}$). Cut bands for in-gel digestion marked with a line and a number.

3.3.3 Comparison of the degradation, recovery rate and the number of identified phosphopeptides between PIRL homogenates (PH) and in mechanical homogenates (MH)

The LC-MS raw data from SDS-PAGE bands of alpha casein spiked equally in PIRL homogenates (PH), and mechanical homogenates (MH) (Figure 34) were processed in MaxQuant (version 1.5.2.8) [119].

Table 7 shows the sum of label-free quantification (LFQ) intensities determined with MaxLFQ [120] of alpha S1-casein protein species detected in the incised bands (1-2) in the SDS-PAGE (Figure 35) from PIRL homogenates (PH) and mechanical homogenates (MH) of three replicates of rat pancreas samples.

The average relative protein abundance of intact alpha-S1-casein protein species detected in the incised bands (1-2) in the SDS-PAGE of PIRL homogenates (PH) $3.5 \times 10^9 (+/- 1.0 \times 10^9)$

whereas in mechanical homogenates (MH) 1.0×10^9 ($\pm 0.6 \times 10^9$) (numbers are given in arbitrary units) (Table 7, Figure 36). The results show that in the homogenates of PIRL (PH) compared to the mechanical homogenates (MH) a significantly higher relative protein abundance of intact alpha-S1-casein was detected (T-test: $p = 0.02$) (Figure 36).

Table 7: Sum of the label-free quantification (LFQ) intensities (arbitrary units) of the intact alpha-S1-casein protein species detected in the incised bands (1-2) in SDS-PAGE (Figure 34,35) of protein homogenates from rat pancreas spiked with alpha casein obtained by mechanical homogenization and PIRL-DIVE homogenization.

	Homogenate type	
	PH	MH
Rat pancreas 1	4.2×10^9	0.3×10^9
Rat pancreas 2	2.4×10^9	1.4×10^9
Rat pancreas 3	4.1×10^9	1.3×10^9

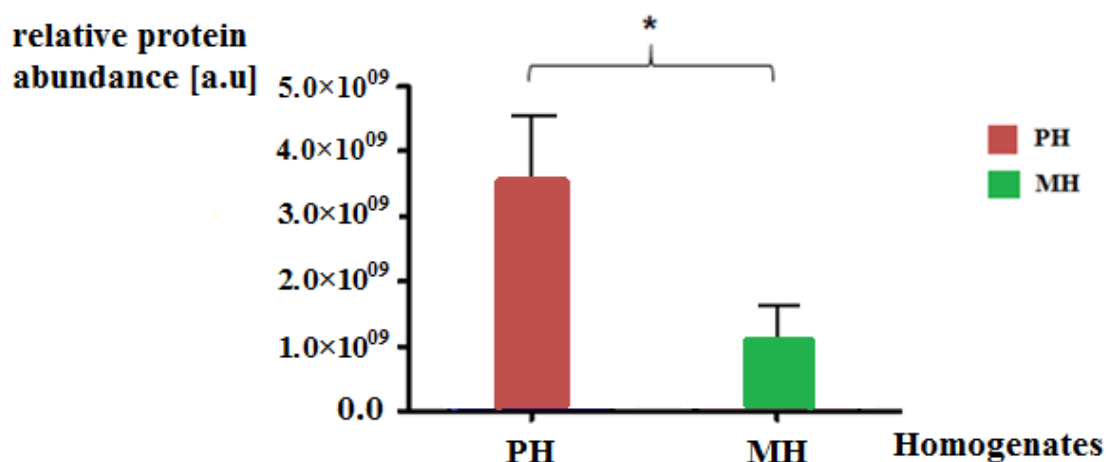


Figure 36: Graph bars (mean with standard deviation) showing the average relative protein abundance of intact alpha-S1-casein protein species detected in the SDS-PAGE bands 1-2 (Figure 34-35) of PH and MH, *: $p=0.02$ (t-test).

Table 8 shows the sum of the label-free quantification (LFQ) intensities determined with MaxLFQ [120] of alpha S1-casein protein species detected in the whole incised bands 1-6 in the SDS-PAGE of PIRL homogenates (PH) and mechanical homogenates (MH) from the three biological replicates (figure 35). In the PIRL homogenates (PH) an average intensity of 3.7×10^9 ($\pm 1.1 \times 10^9$) and in the case of the mechanical homogenates (MH) of 1.2×10^9 ($\pm 0.8 \times 10^9$) (a.u.) was detected.

In addition, for the area at a molecular weight less than 14 kDa (incised bands 3-6 in the SDS-PAGE) the sum of the intensities for the alpha S1-casein protein species (determined by label-free quantification (LFQ) with MaxLFQ [120] the following intensities for the three biological replicates (Figure 35) of the PIRL homogenates (PH) and mechanical homogenates (MH) were shown in table 9.

Based on the sum of the label-free quantification (LFQ) intensities of the alpha S1-casein protein species, which are shown in table 8 and table 9, the percentage of alpha-S1-casein species with molecular weight less than 14 kDa was calculated (Table 10, Figure 37). The percentage of alpha-S1-casein species with a molecular weight less than 14 kDa was in the PIRL homogenates (PH) 6.2 % (± 3.3 %) and in case of the mechanical homogenates (MH) 17.2 % (± 4.9 %) (Table 10, Figure 37).

Table 8: Sum of the label-free quantification (LFQ) intensities of the alpha-S1-casein protein species detected in the whole incised bands (1-6) in the SDS-PAGE (Figure 34, 35) of protein homogenates from rat pancreas spiked with alpha casein obtained by mechanical homogenization and PIRL homogenization.

	Homogenate type	
	PH	MH
Rat pancreas 1	4.5×10^9	0.3×10^9
Rat pancreas 2	2.5×10^9	1.6×10^9
Rat pancreas 3	4.1×10^9	1.7×10^9

Table 9: Sum of the label-free quantification (LFQ) intensities of the alpha-S1-casein protein species detected in the incised bands (3-6) below 14 kDa in the SDS-PAGE (Figure 34, 35) of protein homogenates from rat pancreas spiked with alpha casein obtained by mechanical homogenization and PIRL homogenization.

	Homogenate type	
	PH	MH
Rat pancreas 1	3.7×10^8	0.7×10^8
Rat pancreas 2	2.1×10^8	1.8×10^8
Rat pancreas 3	1.0×10^8	3.3×10^8

Table 10: The percentage of alpha-S1-casein species with a molecular weight less than 14 kDa detected in the appropriate SDS-PAGE bands no.3-6 (Figure 34, 35) of protein homogenates from rat pancreas spiked with alpha casein obtained by mechanical homogenization and PIRL homogenization.

	Homogenate type	
	PH	MH
Rat pancreas 1	8.1 %	20.3 %
Rat pancreas 2	8.0 %	11.6 %
Rat pancreas 3	2.4 %	19.7 %

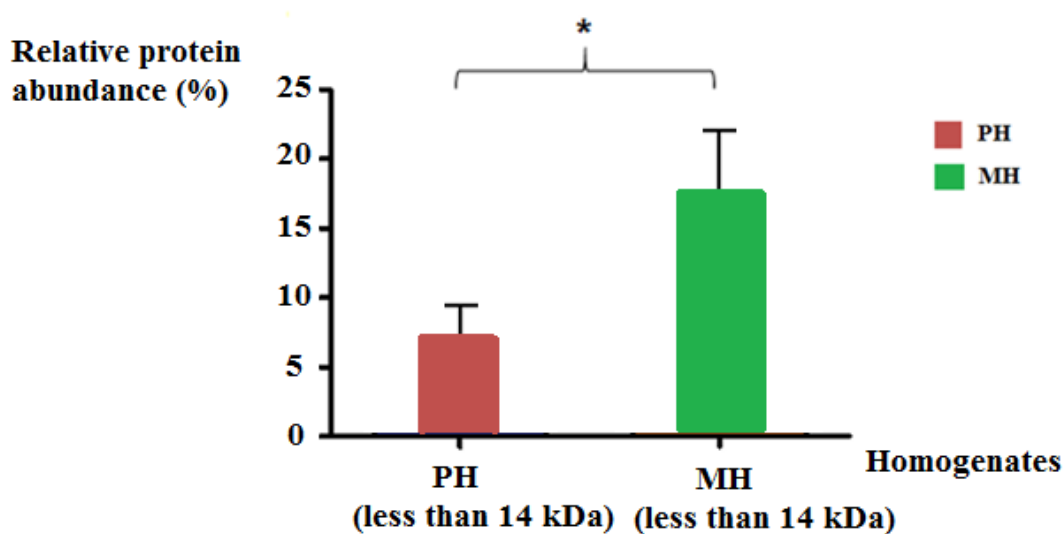


Figure 37: Graph bars (mean with standard deviation) showing the percentage of alpha-S1-casein species with a molecular weight less than 14 kDa detected in the belonging SDS-PAGE bands 3-6 (Figure 34,35) of PH and MH, *: p= 0.031 (t-test).

The number of alpha-S1- casein phosphopeptides detected in the three biological replicates of PH and MH is shown in figure 38. The average number of phosphopeptides in PH was 5.67 (+/- 1.53), which is considerably higher than in MH 3.67 (+/- 1.53).

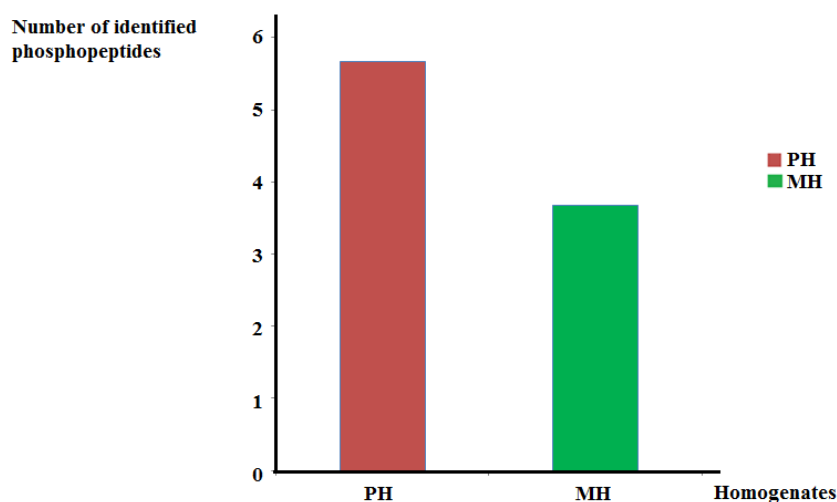


Figure 38: Graph bars are showing the number of identified alpha-S1-casein phosphopeptides in PIRL homogenate (PH) and in mechanical homogenate (MH)

For the alpha-S2-casein protein species, the sum of label-free quantification (LFQ) intensities was determined in the incised bands (1-2) in SDS-PAGE (Figure 35) from the PIRL homogenate (PH) and mechanical homogenate (MH) of three biological samples. A considerably higher relative protein abundance of intact alpha-S2-casein was detected in PIRL homogenates (PH) 16.6×10^8 (+/- 8.1×10^8) compared to the mechanical homogenates (MH) 3.3×10^8 (+/- 1.9×10^8) (Table 11, Figure 39).

Table 11: Sum of the label-free quantification (LFQ) intensities of the intact alpha-S2-casein protein species detected in the incised bands (1-2) in SDS-PAGE (Figure 34,35) of protein homogenates from rat pancreas spiked with alpha casein obtained by mechanical homogenization and PIRL homogenization

	Homogenate type	
	PH	MH
Rat pancreas 1	7.4×10^8	1.5×10^8
Rat pancreas 2	22.9×10^8	5.3×10^8
Rat pancreas 3	19.5×10^8	3.2×10^8

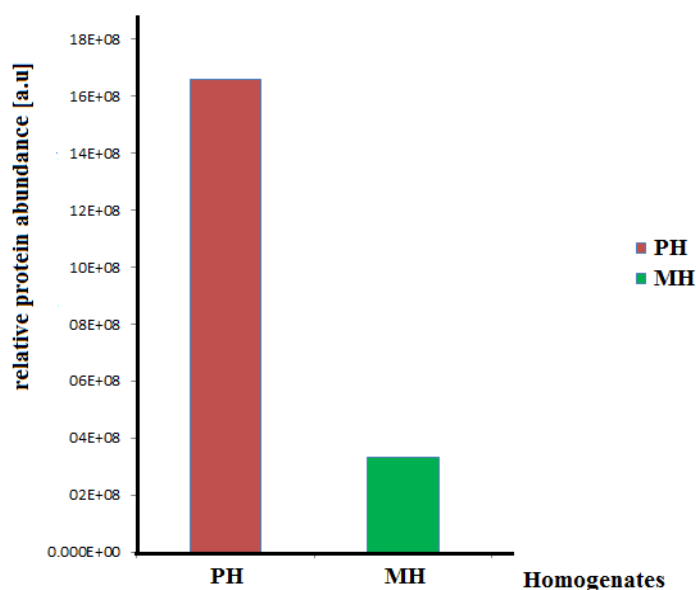


Figure 39: Graph bars showing the average relative protein abundance of intact alpha-S2-casein protein species detected in the appropriate SDS-PAGE bands 1-2 (Figure 34, 35) of PH and MH.

In addition, the label-free quantification (LFQ) intensities of alpha S2-casein protein species detected in the whole incised bands 1-6 in SDS-PAGE (Figure 35) of PIRL homogenates (PH) and mechanical homogenates (MH) from the three biological replicates were determined (Table 12). The sum of the label-free quantification (LFQ) intensities of whole alpha-S2-

casein in PIRL homogenates (PH) is 17.9×10^8 ($\pm 8.3 \times 10^8$) and in the mechanical homogenates (MH) 4.8×10^8 ($\pm 2.7 \times 10^8$).

The sum of the label-free quantification (LFQ) intensities of alpha-S2-casein from incised bands 3-6 in SDS-PAGE (Figure 35) of PIRL homogenates (PH) and mechanical homogenates (MH) from the three biological replicates was calculated. In the PIRL homogenates (PH) the sum of the label-free quantification intensities is 1.3×10^8 ($\pm 6.9 \times 10^7$), whereas in the mechanical homogenates (MH) it is 1.5×10^8 ($\pm 1.3 \times 10^8$) (Table 13).

Based on the intensity values in table 12 & 13, the percentage of alpha-S2-casein species with molecular weight less than 14 kDa was determined. In PIRL homogenates (PH) this percentage was 8.6 % (± 5.7 %) and in case of mechanical homogenates (MH) 26.3 % (± 18.5 %) (Table 14, Figure 40).

Table 12: Sum of the label-free quantification (LFQ) intensities of alpha-S2-casein protein species detected in the whole incised bands (1-6) in SDS-PAGE (Figure 34, 35) of protein homogenates from rat pancreas spiked with alpha casein obtained by mechanical homogenization and PIRL homogenization.

	Homogenate type	
	PH	MH
Rat pancreas 1	8.7×10^8	1.7×10^8
Rat pancreas 2	24.9×10^8	6.7×10^8
Rat pancreas 3	20.2×10^8	6.0×10^8

Table 13: Sum of the label-free quantification (LFQ) intensities of the alpha-S2-casein protein species detected in the incised bands (3-6) below 14 kDa in SDS-PAGE (Figure 34, 35) of protein homogenates from rat pancreas spiked with alpha casein obtained by mechanical homogenization and PIRL homogenization.

	Homogenate type	
	PH	MH
Rat pancreas 1	1.3×10^8	0.2×10^8
Rat pancreas 2	2.0×10^8	1.4×10^8
Rat pancreas 3	0.7×10^8	2.8×10^8

Table 14: The percentage of alpha-S2-casein species with a molecular weight less than 14 kDa detected in the appropriate SDS-PAGE bands no.3-6 (Figure 34, 35) of protein homogenates from rat pancreas spiked with alpha casein obtained by mechanical homogenization and PIRL homogenization.

	Homogenate type	
	PH	MH
Rat pancreas 1	14.5 %	10.5 %
Rat pancreas 2	8.2 %	21.6 %
Rat pancreas 3	3.2 %	46.7 %

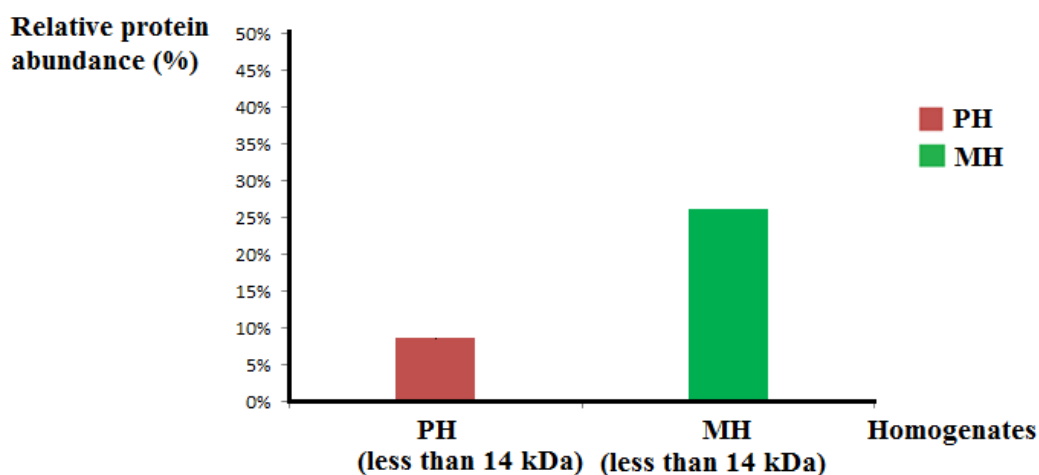


Figure 40: Graph bars are showing the percentage of alpha-S2-casein species with a molecular weight less than 14 kDa detected in the belonging SDS-PAGE bands no.3-6 (Figure 34, 35) of PH and MH.

The number of identified alpha-S2-casein phosphopeptides in both PH and MH in the three biological replicates was calculated as demonstrated in figure 41. In average, the number of phosphopeptides in PH was 11.3 (+/- 3.8) and in MH was 3.7 (+/- 2.5). These results (Figure 41) revealed that a significantly higher number of phosphopeptides was identified in PH compared to MH (T-test: $p = 0.04$).

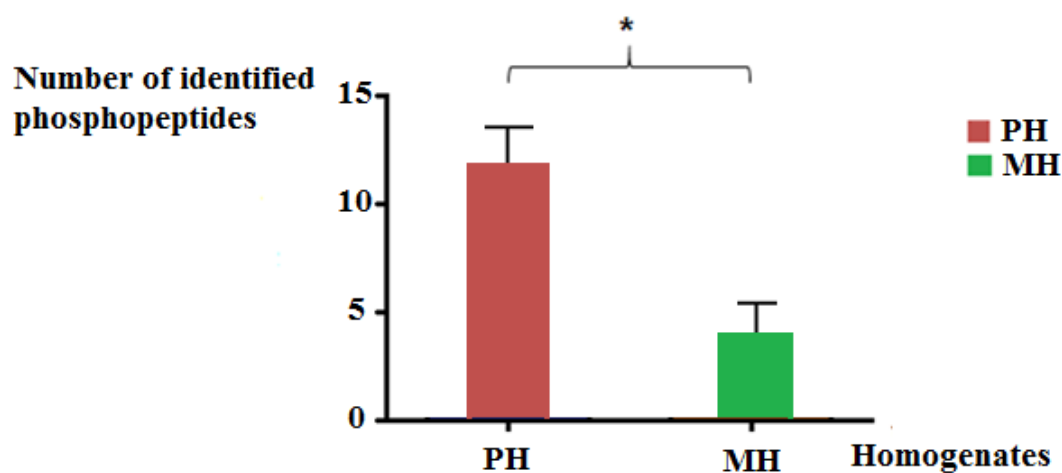


Figure 41: Graph bars (mean with standard deviation) showing the number of identified alpha-S2-casein phosphopeptides after PIRL homogenization and mechanical homogenization. *: $p = 0.04$ (t-test).

4 Discussion

The term “protein species” was introduced in 1996 by Jungblut et al. to describe a protein by its chemical structure [47] and was further outlined in 2009 [49]. Protein species is defined by the exact chemical structure as a smallest functional unit in a proteome [48, 49]. The ability to access the protein species level will open the way for proteomic scientist to understand the proteome at a functional level [121].

The change in the exact chemical composition of the protein will generate new protein species which may occur during sample preparation like in the homogenization of the tissue and protein extraction. Therefore, new technologies and protocols for proteomics sample preparation are an essential demand in proteomics to preserve the intact protein species.

Maintaining protein integrity and minimizing a loss of proteins during sample preparation in proteomics remains one of the challenging tasks in a proteomics workflow.

The aim of this study is to investigate the hypothesis that because of the ultrafast homogenization process of the tissues via PIRL, proteins are exposed to enzymatic actions of proteases only for a very short time which enables soft distribution of proteins from tissues.

The integrity of proteins *in vivo* is conserved due to compartmentalization. In the homogenization process, organelles are disrupted, proteases are released from their intracellular compartments and they come in contact with cellular proteins. By increasing the contact time between endogenous enzymes and cellular proteins, these endogenous enzymes are given a chance to degrade and modify cellular proteins. Thereby tissue homogenization leads to proteolytic degradation and post-translational modifications of these proteins. As products, new protein species will be generated which are different in their chemical composition in comparison to the exact *in vivo* fundamental structure of the proteins. Ahmed et.al [122] compared changes in protein profiles in mouse hippocampus and cortex following three methods of preparing the tissue: immediate lysate preparation, rapid heating to 95°C and standard snap freezing in liquid nitrogen, prior to lysate preparation. They found in this study, specific differences in the levels of phosphorylation and proteolytic degradation in a very short time.

By using a new technology, PIRL for ablation of different types of tissues [1, 111, 123-125] and bone [108] as described in the material and methods section, it became possible to reduce the time for the homogenization of the tissue and accordingly reduce the time of exposure of cellular proteins to the endogenous enzymes.

In the first block of the experiment, porcine muscle tissue was chosen as model tissue to investigate our hypothesis because this tissue is more or less homogenous. The porcine muscle tissue samples were homogenized by either PIRL-DIVE or with a mechanical procedure. Equal amounts of proteins ($m=90 \mu\text{g}$) from both PIRL and mechanical homogenates were applied to high-resolution two-dimensional gel electrophoresis (2DE, Figure 6 and 7) to achieve an optimal comparison between the two homogenates. The workflow for preparing both homogenates was identical except for the method of homogenization as a variable in the preparation workflow. The 2DE approach was used in this experiment in order to separate proteins at high resolution and easily compare different spot pattern in the gel with respect to modifications and proteolytic degradation [28, 126, 127].

The comparison between the 2DE protein patterns from both PH and MH revealed that more spots were detected in the molecular weight region lower than 29 kDa in the MH gel than in the PH gel. In the corresponding region, adenylate kinase isoenzyme 1 protein (Gene: AK1) which has a theoretical molecular weight of 21.6 kDa, is a protein which catalyses the phosphorylation of AMP by using ATP or GTP as phosphate donor, plays a role in cellular energy homeostasis and in adenine nucleotide metabolism [128, 129]. It was identified by LC-MS/MS in spot no. 9 in PH (Figure 6, Table 2). The theoretical molecular weight of this protein matches with the experimental molecular weight, whereas this protein is totally missing at the same position in the MH gel. Obviously, degradation has occurred for the adenylate kinase isoenzyme 1 protein [130, 131] during the mechanical homogenization process, the organelles were opened, and the proteases which were safely packed in the organelles, released outside these organelles and then the proteases come into contact with the cellular proteins. This contact between proteases and cellular proteins was drastically shorter in the case of PH compared to MH. Therefore, this protein was in MH much more susceptible to degradation by proteases compared to the PH.

Creatine kinase (Gene: CKM, $m=43.3\text{kDa}$), an enzyme associated with energy transduction in tissues such as skeletal muscle, heart, and brain [132], was identified by LC-MS/MS in spot

no. 6 in the MH gel (Figure 7). The experimental molecular weight of this protein according to its position in the MH gel was < 29 kDa, which is considerably lower than the correct molecular weight. This effect is obviously due to the action of the endogenous enzymes on this protein leading to its proteolytic degradation. A similar effect was observed for this protein according to a study by Lametsch et.al identifying proteins that change during post-mortem storage of porcine meat [133].

In addition, spots no. 7 and 8 in MH gel (Figure 7) were attributed to the protein Fructose-bisphosphate aldolase A(m=39.4 kDa), which plays a critical role in the reversible conversion of fructose-1,6-bisphosphate to glyceraldehydes 3-phosphate and dihydroxyacetone phosphate [134]. This protein was detected in the lower molecular weight area <20 kDa by LC-MS/MS (spots no. 7-8 in the MH gel, figure 7). This discrepancy between theoretical and experimental molecular weight for this protein in MH indicated proteolytic degradation because of the action of endogenous enzymes.

Four protein species of Fructose-bisphosphate aldolase A(m=39.4 kDa) were detected in spot no.1-4 in the PIRL homogenate (PH) (Figure 6, Table 2) whereas only two protein species of Fructose-bisphosphate aldolase A were detected in spot no.1-2 in the mechanical homogenate (MH) (Figure 7, Table 3). Furthermore, four protein species of creatine kinase were detected in spot no.5-8 in PH (Figure 6, Table 2), and only three protein species from this protein were detected in spots no.3-5 in MH (Figure 7, Table 3).

Several modifications were described in Fructose-bisphosphate aldolase A and creatine kinase [135-137]. These protein modifications change the chemical composition of these proteins and thereby are responsible for a generation of new protein species. The number of identified protein species was higher for both proteins in the case of PH compared to MH. This reduction in the number of modified species during the homogenization of the tissue is most likely due to the action of endogenous enzymes.

In general, the results obtained from this experiment demonstrated increased proteolytic degradation and decrease of protein species in the mechanical compared to the PIRL homogenate by the action of endogenous enzymes. Because of the ultrafast release of proteins from tissue via PIRL, these proteins are expected to be exposed to enzymatic degradation reactions for shorter time window compared to the mechanical homogenization method and because of this, we expected in the 2DE PAGE of PIRL homogenates (PH) less proteolysis

and higher identification number of protein species compared to the mechanical homogenates (MH).

These findings in our first experiment validated the results from Kwiatkowski et al.[1] where human tonsils were homogenized via PIRL-DIVE and mechanically. The proteins in both homogenates were separated by 2DE. By identification of several spots in both gels by LC-MS/MS it was shown that in summary more protein species were detected in the PH rather than in the mechanically homogenized samples. For example, eleven glyceraldehyde-3-phosphate dehydrogenase species were identified on the 2DE gel of the PH. In contrast, only one glyceraldehyde-3-phosphate dehydrogenase was identified in MH.

There are several reasonable explanations for these results. One possible reason may be that during PIRL tissue homogenization (PTH), protein species are exposed to enzymatic reactions for a very short time compared to the mechanical tissue homogenization (MTH). This short time of exposure of cellular proteins to endogenous enzymes results in less impact of proteases and phosphatases to degrade cellular proteins and cleave phosphate from phosphoprotein in case of PH compared to MH. This effect is most likely responsible for the lower number of protein species detected in MH compared to PH. Another reason is the loss of material during tissue homogenization and preparation steps in the case of mechanical tissue homogenization prior mass spectrometer measurement which also might result in protein species losses [77].

A further study was performed to investigate how PIRL and mechanical homogenates behave in the hot Laemmli buffer and to determine the degree of differences between both homogenates.

In order to answer these two questions, both PIRL homogenate (PH) and mechanical homogenate (MH) from rat pancreas samples were compared after treatment with hot Laemmli buffer.

The hot Laemmli buffer was used in this experiment to make sure that enzymatic degradation was stopped at the earliest time point possible and to analyze if we still see differences regarding proteolytic degradation between both homogenization methods.

Rat pancreas tissue was chosen because it contains a high level of degrading enzymes, especially proteases [138, 139] which directly start to degrade proteins after the animal is killed.

Histological studies from incised rat pancreas were performed in this experimental section (Figure 9). This is important to assure that we have used comparable tissue parts for PTH and MTH experiments with respect to the type of tissue taken during incision and to exclude contamination of the sample with tissue of a different type. The composition of the tissue will have an effect on the protein composition and therefore significant variations between various types of tissue in the list of identified proteins would have to be expected.

The hot Laemmli buffer was used to minimize the degree of proteolytic degradation. Using Laemmli buffer in combination with heat [140] has been shown to be highly effective in stopping enzymatic degradation. The pancreas tissues were homogenized via the PIRL-DIVE and the mechanical method, extraction was performed in the same buffer composition, and the same protein amount was loaded onto the SDS-PAGE. Subsequently, the bands from both homogenates were cut in a comparable fashion (Figure 11). All steps in the workflow were comparable except the method of homogenization in order to achieve a reliable comparison between two homogenates (Scheme 2).

As SDS-PAGE is a qualitative approach and gives only a rough overview about the composition of the proteins in the cell, in order to more deeply determine the protein composition in the bands the samples were further analysed by LC-MS/MS.

The quantitative and qualitative data obtained from the LC-MS/MS analysis were used to generate SDS-PAGE migration profiles (Figure 13), which can easily illustrate the distribution of a specific protein all over the gel and determine the proteolytic degradation.

The SDS-PAGE migration profiles of the proteins EH domain-containing protein 1 (Gene: EHD 1, $m=60.6$ kDa) and Isocitrate dehydrogenase (NAD) subunit beta (Gene: IDH3B, $m=42.4$ kDa) (Figure 14 & 15) represent nice examples for a fit between the theoretical and the experimental molecular weight. The distribution of these protein species in all the three biological replicates are at the correct molecular weight as shown in their migration profiles. EH domain-containing protein 1 was distributed between bands 9-10 (Figure 11), which approximately correspond to its theoretical molecular weight of 60.6 kDa. The other protein, Isocitrate dehydrogenase (NAD) subunit beta was detected in bands 11-13 at the level of 38-49 kDa (Figure 11), which almost fits the theoretical molecular weight of this protein. These two examples demonstrate clearly and nicely how precise and reproducible these SDS-PAGE gels could be cut and how accurate the run distance of the proteins in the SDS-PAGE

correlate with their theoretical molecular weight, which is an important aspect in the reliable comparison between PH and MH.

The migration profile of the protein Nucleoside diphosphate kinase A protein (Gene: NDKA, m=17.2 kDa) (Figure 16) shows that in the SDS-PAGE band no. 18 of a third rat pancreas sample obtained by PIRL-DIVE homogenization only one signal was apparent from the identification by LC-MS/MS analysis after tryptic digestion. In contrast, MH from the third replicate of the same protein which shows two signals due to the distribution of this protein between bands no.18 and 22 (Figure 11). The signal intensity generated from band no.18 at a molecular weight of 17 kDa matched with the theoretical molecular weight of this protein while the signal from band no.22, at a lower molecular weight region in the SDS-PAGE, represents a degradation species of this protein. Thus, in principle, there is a migration shift toward lower molecular weight according to SDS-PAGE migration profiles of the protein Nucleoside diphosphate kinase A in the MH sample, showing one signal shifted toward the lower molecular weight area in migration profile. However, only the most abundant species was considered in the calculation of the migration shift profile. In this case, the most abundant signal was generated from the protein species in band 18 at a molecular weight around 17 kDa, and the shifted signal, which represents band no. 22 at a molecular weight of 6 kDa is the less abundant signal (Figure 16).

Similar effects were demonstrated in figure 17 and 18 for the proteins tRNA-slicing ligase RtcB homolog (Gene: RTCB, m=55.2 kDa) and Septin-2 (Gene: SEPT2, m=41.6 kDa) respectively. The SDS-PAGE migration profiles of the PH from these two proteins showed that the most abundant signal is in agreement with the theoretical molecular weight of these proteins with no detectable shift toward a lower molecular weight. Even though signals from both proteins appeared in their migration profiles toward lower molecular weight, these signals had a low intensity and the most abundant species were detected at the correct theoretical molecular weight. Thus, these two proteins are nice examples where no migration shifts were recorded for the most abundant protein species.

Figure 19 shows the SDS-PAGE- migration profile of the protein Alpha-aminoadipic semialdehyde synthase (Gene: Aass, m=103.1 kDa), which illustrates an example of different degrees of enzymatic degradation between PH and MH. Only one signal from one species of this protein was apparent in the PH sample, detected in band no.7. On the opposite, several protein species were detected all over the entire SDS-PAGE in the MH sample due to proteolytic degradation. The most abundant species shown in the SDS-PAGE migration

profile of MH belonged to the band no.13 at an approximate molecular weight of 28 kDa. Therefore in the migration profile this can be considered as a migration shift toward lower molecular weight. The results for Alpha-amino adipic semialdehyde synthase revealed that the intact protein species were partially degraded by proteases in the case of MH after longer time exposure to these endogenous enzymes compared to PH. This phenomenon leads to the generation of different protein species distributed at lower molecular weight in SDS-PAGE in MH.

The effect of the proteolytic enzymes was shown in the protein Biliverdin reductase A (Gene: *Blvra*, m=33.6 kDa). The SDS-PAGE migration profile of this protein (Figure 20) in PH illustrates a signal of this protein that is correlated to its correct molecular weight at band no.14 located beneath the 38 kDa marker (Figure 11). One protein species of Biliverdin reductase A was identified in the MH gel at band no.21 corresponding to a molecular weight around 6 kDa. The ultrafast process of PTH in contrast to MTH might again play a crucial role in preserving Biliverdin reductase A in the intact state because of short snapshot time of exposure to the endogenous enzymes whereas the longer time of exposure to these enzymes can be interpreted as the cause of the proteolytic degradation seen in MH.

The SDS-PAGE-migration profiles of 28S the ribosomal protein S7 (Gene: *RTO7*, m=28.2 kDa) (Figure 21) showed that this protein was identified in PH at a molecular weight of 28 kDa in band no. 16 (Figure 6). In MH this protein was identified at a molecular weight around 14 kDa in band no. 19 (Figure 16). Again the action of proteases degraded the intact protein species in the MH sample and as result these degradation products shifted to the lower molecular weight as displayed in the SDS-PAGE migration profiles for this protein (Figure 16).

During the investigation and analysis of the SDS-PAGE migration profiles for the proteins identified in PH and MH for the three biological replicates the phenomenon of a total loss of protein species in the entire gel was observed mostly in case of the MH samples. Later in this discussion chapter, this observation will be discussed based on the statistical numbers we obtained. Below a few examples of this observation are given:

Protein Long-chain-fatty-acid-CoA ligase 5 (Gene: *ACSL5*, m=76.4 kDa) was identified in the PH rat pancreas no. 1 gel in band no. 9 slightly above the 62 kDa marker (Figure 11), corresponding to the theoretical molecular weight of this protein. On the contrary, this protein was not detected in the entire SDS-PAGE from the MH of rat pancreas no.1. This

phenomenon of the total loss of the protein species in all three biological replicates in MH compared to PH is shown in figures 23-25, which represent the SDS-PAGE migration profiles of the following proteins: Amyloid beta A4 (Gene: App, m=86.7 kDa), Pyruvate dehydrogenase (acetyl-transferring) kinase isozyme 2 (Gene: PDK2, m=46.1 kDa), and Heat shock 70 kDa protein 1 B (HS71B, m=70.2 kDa), respectively. In PH in all biological replicates, these proteins were found as intact species, whereas in MH in all of the biological replicates these proteins were totally absent. The results for these proteins shown above implied that intact protein species were completely degraded by proteases in the case of MH. As a consequence of the ultrafast ablation process in the tissue via PIRL, which lead to fast transfer of the intact species from the tissue directly into the trap (a wash bottle immersed in liquid nitrogen) the number of identified intact protein species is higher in the case of PH compared to MH. this assumption brings to mind a new important aspect concerning tissue homogenization methods and protocols in sample preparation, which is “reproducibility”. This will be discussed later in this chapter.

A large cytosolic protein, Cyclin-G-associated kinase (Gene: GAK, m=143.7 kDa), which has a role in uncoating clathrin-coated vesicles from non-neuronal cells [141], was detected in intact form in bands no.5 at molecular weight level slightly below 198 kDa in SDS-PAGE of PH from rat pancreas 1 (Figure 10, 11). This signal was shown in SDS-PAGE migration profile for this protein (Figure 26 top). In contrast, this protein was totally missing in MH of the same rat pancreas sample. This result implicates that this large protein is exposed in the MH process to proteases in a time frame that enables a fully proteolytic degradation. Another possible explanation might be, that it is lost during centrifugation of the samples due to the presence of particles in MH, which lead to adsorption of some of the proteins and thereby to their loss during the centrifugation process.

Another example demonstrating the effect of proteases on large proteins is illustrated by the SDS-PAGE migration profiles from the second rat pancreas sample of the protein Chromodomain-helicase-DNA-binding protein 5 (Gene: CHD5, m=222.3) (Figure 26 down). This protein is associated with nervous system development [142] and may act as a tumor suppressor [143]. The protein was detected intact in PH, whereas it was totally missing in the MH. In agreement with these results, the study from Kwiatkowski et al. at mouse muscle showed that in the PIRL homogenization from mouse muscle tissue large proteins, myosin-4 (M=222.7 kDa) and titin (m=3.9 MDa), were desorbed intact in case of PTH [111]. In human tonsil tissue a Collagen alpha-3(VI) chain (Mr =343.7 kDa) was identified at molecular

weight above 200 kDa, whereas different species were identified at lower molecular weight in MH [1]. These two examples in previous studies demonstrated the ability to detect even large proteins in intact form in PH samples and can represent one of a great promising advantages of using PIRL to ablate and homogenize tissue for the study of large proteins.

The Regulator complex protein LAMATOR3 (Gene: LAMTOR3, m=13.6 kDa) associated with amino acid sensing and activation of mTORC1 [144, 145] and the protein preY (Gene: PYURF, m=12.7 kDa), which plays a role in the glycosylphosphatidylinositol (GPI) anchor biosynthetic process and is involved in the positive regulation of metabolic processes [145, 146], were studied as examples of small proteins. Both were identified as intact species in PH from rat pancreas no.1 while they were missing in MH (Figure 27).

According to SDS-PAGE migration profiles, the SDS-PAGE-migration shift peak histograms were constructed and then the global degree of proteolysis between MH and PH was estimated. The average degree of relative proteolysis was 1.31% (+/- 0.28%) in PIRL homogenates (PH) and 2.24% (+/- 0.38%) in mechanical homogenates (MH) (Figure 31, Table 5). This result revealed a significantly lower degree of proteolysis (T-test: $p = 0.028$) in PH compared to MH samples. These results are also in a good accordance with previously reported results from Kwiatkowski et al. [1], which was showed a higher degree of proteolysis in human tonsils samples in MH (22.41%) compared to PH samples (1.92 %).

No differences regarding proteolytic degradation between PIRL and the mechanical homogenization process were expected when hot Laemmli buffer was used in this experiment. However, significant differences were still seen even though they were rather low. According to a study of Stingl et al. [147] the proteolytic activity was observed regardless of treated samples with different conditions such as temperature and different concentration of urea. Stingl et al. studied the proteolytic degradation by applying 6 different protocols to stop this action on rat brain tissue using oxygen -18 labelling to assess the degree of degradation. The authors found that the degradation still occurs even after treating the samples with different protocols, with minimal degree of degradation by using heat method.

The use of Laemmli buffer in combination with heating prevents the application of isoelectric focusing or tryptic digestion. For isoelectric focusing the charge of the proteins must be conserved and for tryptic digestion SDS denaturation must be avoided. Therefore uncharged chemicals for extracting and denaturing the proteins must be used to apply to isoelectric focusing or tryptic digestion approaches according to Rabilloud T et.al. [148]. Also reagents

incompatible with reversed-phase liquid chromatography and mass spectrometry must be avoided [149]. PIRL homogenates (PH), on the other hand, can directly be applied for these approaches. Thus one of the benefits behind the use of PIRL-DIVE for homogenization of tissues consists in overcoming the problem of having to use different kinds of buffer and their incompatibility to different proteomics approaches. Also diluting the samples to reduce the concentration of these buffers to an acceptable level to be compatible with a specific approach can be avoided by the application of PH. The otherwise necessary diluting steps could cause an imbalance between the denaturing agents necessary to stop the activity of endogenous proteases on the one hand and the tryptic digestion on the other hand [91].

The number of proteins identified by LC-MS/MS analysis of the SDS-PAGE of the three biological rat pancreas replicates showed a higher number of proteins identified in the PH samples: 1743 proteins (+/- 173 proteins) compared to 1467 proteins (+/- 138 proteins) identified in the MH sample (Figure 32 A).

Moreover, a considerably higher number of proteins was identified in all the three rat pancreas samples in PH: 1418 proteins, compared to those identified in MH: 1116 proteins. Of these proteins 1092 (75.7 %) were identified in both PH and MH, 24 proteins (1.7%) were identified only in MH, and a considerably higher number of proteins (326 proteins, 22.6 %) were exclusively identified in PH (Figure 32 A). These results were supported by previous findings by Kwiatkowski et al., where a higher number of proteins were identified from human tonsils in PH compared to MH (Figure 8 A).

These results show that by using PIRL-DIVE for homogenization the tissue samples we were able to identify a higher number of proteins compared to mechanical tissue homogenization. This is considered as another advantage of using PTH.

Several steps in the tissue homogenization tissue and protein extraction process can introduce variability in the outcome of the protein identification because of the action of endogenous enzymes. Therefore one of the main challenges in the sample preparation approaches is the reproducibility. In spite of the availability of various methods to stop the action of proteases such as using proteases inhibitors cocktails, pH adjustment, precipitation as well as heating [63, 86, 150], still these methods are not effectively preserving the entire proteome from the actions of these endogenous enzymes. This lack of reproducibility was demonstrated in the study of Jizu Yi et.al for serum and plasma proteins by using three different anticoagulants [151]. New methods in tissue homogenization and protein extraction which

can minimize the loss in the integrity of proteins during sample preparation is urgently demanded.

The reproducibility of the protein identification in our experiments was checked depending on the number of proteins identified in the all three rat pancreas samples for both PIRL and mechanical homogenates. For this purpose, the Venn diagram was constructed from the proteins identified in PIRL homogenates (PH) (Figure 32 B) showing that 1418 proteins (69%) were identified in all three rat pancreas samples in PH compared to 1116 proteins (61%) in case of the MH (Figure 32 C). These results are in agreement with the results obtained for human tonsil samples where the percentage of protein identification in all three biological replicates in PH was 46 % (Figure 8 B) whereas it was 34 % in MH (Figure 8 C) [1].

Using PIRL for tissue homogenization results in a considerably higher reproducibility of identifying proteins (Figure 8 B and C, tonsils, and Figure 32 B and C, pancreas). This is most probably due to the absence of particles in the PIRL homogenate, thus minimizing losses based on surface adsorption [77], and the significantly lower degree of proteolytical degradation of intact protein species (Figure 31).

Because of the effect of proteases, resulting in proteolytic degradation of the proteins during tissue homogenization, and the inability to reproduce enzymatic degradation all the time to the same amount, it is often difficult or impossible to validate diagnostic protein markers. The higher reproducibility with a lower degree of proteolytic degradation in case of PTH holds a significant advantage in biomarkers validation.

Based on these remarkable properties of PTH resulting in improved reproducibility and the identification of more proteins in intact form, new disease-associated protein species could be identified and validated by using PTH in pre-analytical sample preparation to achieve a higher reproducibility and preserve the intact chemical composition of the protein.

The reproducibility is a fundamental aspect to success in diagnostic protein biomarker research as in the last 20 years only a few biomarkers were validated and accepted by the US food and drug administration (FDA) to use as a clinical marker [152, 153].

In a recent review by Anderson et.al [152] it is shown that only 22 tests were approved as a diagnostic marker since 1993. Yi et al. implied as the reason of this problem that these protein biomarker has not passed the validation [151]. According to Obuchowski et.al and Sackett

et.al these diagnostic biomarkers should be validated in an independent study before approved for clinical use [154, 155].

To validate the previous results regarding degradation rate, determine a recovery rate, and to have the first hint about phosphorylation, rat pancreas was spiked with alpha casein homogenized via PIRL-DIVE and mechanical homogenization in the presence of urea and thiourea as lysis buffer.

Using urea in this experiment for unfolding and denaturation the proteins [156] has limitations. Firstly does trypsin, which is widely used in protein digestion protocols, not tolerate harsh solubilizing condition as 8 M urea for example [157], and secondly can the heating of proteins above 37 °C in the presence of urea induce carbamylation, an artificial modification of protein amino groups [158]. In contrary to this, if we ablate tissue via PIRL then we can apply the PIRL homogenates (PH) directly to different proteomics approaches without further sample preparation.

Top-down proteomics is one approach of choice to apply the condensate after ablation of the sample via PIRL directly. The intact protein analyses in this approach without tryptic digestion and with the ability to detect post-translation modifications represent the main advantages of using this approach [159]. However, the lack of robust data analysis tools and the solubility issue of the intact proteins is one of the main challenges which this approach still faces [60, 159, 160].

In order to perform reproducible and comparable experiments, the tissue type plays an important role in determining the protein list we obtained. Therefore an histological examination from both cuts of the rat pancreas used for PTH and MTH was performed as described in previous experiment section (Figure 33).

A standard protein, alpha casein, was chosen as a model to spike the rat pancreas tissue used for the homogenization experiment, because alpha casein is rich in phosphorylated amino acids [161] and has been thoroughly characterized previously.

An equal protein amount of PH and MH was subjected to SDS-PAGE in order to compare samples obtained by PH and MH (Figure 34).

The bands in SDS-PAGE were cut starting from a molecular weight of 24 kDa, because this is the theoretical molecular weight of the intact alpha-casein protein. All bands were cut in equal fashion to assure a reliable comparison between both PH and MH (Figure 35).

A higher yield of intact alpha-S1-casein species in the sample obtained by PH compared to MH was demonstrated after LC-MS/MS analysis (Figure 36). In addition, a considerably higher yield of intact alpha-S2-casein species was obtained in PH compared to MH (Figure 39).

Furthermore, the results indicated that the yield of alpha-S1-casein species with a molecular weight less than 14 kDa was significantly higher in the MH sample compared to PH (Figure 37). Regarding alpha-S2-casein, the results also illustrated a higher amount of degradation products with a molecular weight of less than 14 kDa in MH compared to PH (Figure 40). The number of identified phosphopeptides in alpha-S1-casein was significantly higher in PH than those detected in MH (Figure 38). A considerably higher number of phosphopeptides in alpha-S2-casein was detected in PH compared to MH (Figure 41).

To summarize the results obtained in this experiment, a significantly higher yield of intact alpha-casein species and a higher number of phosphopeptides were identified in PH compared to MH. The most probable reason for that is the much shorter exposure time to enzymatic degradation reactions and the minimal sample loss during PTH, because almost no particles were present in homogenates obtained by PH. In contrast samples obtained by MH contained undissolved particles, which may adsorb some proteins, which are then lost after the centrifugation step. Another reason for the higher yield of intact alpha-casein species in case of PH compared to MH is the reduction in experimental steps involved in PTH compared to MTH [111].

Upon homogenization of the tissue, the endogenous enzymes are liberated and come in direct contact with the cellular proteins, leading to protein degradation and loss of phosphate groups by the action of phosphatases. The longer the time of exposure to phosphatases the larger is the chance of losing phosphate groups from phosphopeptides. This would explain the lower number of phosphopeptides identified in case of MH. The importance of such findings here concerning the number of phosphopeptides lies in the development of pre-analytical sample preparation protocols, which ensure the highest possible integrity of the proteins for the study of post-translational modifications. This is one of the essential demands in proteomics due to the vital role of PTMs in cellular processes and in many diseases [162, 163].

Another reason is the adsorptive loss of phosphopeptides on surfaces during sample preparation which was clearly demonstrated in the study of Stewart et.al [164] and Speicher et.al. [165].

Based on previous results in chapter 1, chapter 2, and the tonsils results [1] (Kwiatkowski et al.,2016), a higher yield of intact alpha-casein protein species, a higher recovery rate and a higher number of phosphopeptides was expected in the case to PIRL homogenate compared to mechanical homogenates. This could be expected, since in the PIRL homogenates (PH) almost no particles were detected, which could have caused loss of proteins and since in the PH experiment the proteins were exposed to the action of proteases for a shorter time, compared to the mechanical homogenates (MH). The results in this chapter fully matched our expectations in the case of alpha-S1-casein and still considerably matched in case of alpha-S2-casein.

Finally, this work was confirmed the hypothesis that due to the ultrafast homogenization process of tissues via PIRL-DIVE the cellular proteome exposed to endogenous enzymes in a minimal time frame compared to mechanical homogenization method. This very short time exposure lead to reduce the effect of these endogenous enzymes on the proteins in PH ,and make the investigation of the proteome at exact chemical composition more close than previous.

5 Summary-Zusammenfassung

a) Summary

One of the main goals of proteomics is to develop diagnostic and therapeutic applications. The smallest functional unit of the proteome is the protein species. The exact chemical composition of any protein species determines their function. The alteration of the exact chemical composition of the protein will form new different protein species. Changing of the exact chemical composition of the protein in vitro consider one of the challenging face the study of protein at their in vivo state. During homogenization, the disruption of cellular membranes via tissue homogenization disrupts compartmentation, so endogenous enzymes will get in contact with cellular proteins. In this case, the time of contact enables these endogenous enzymes to degrade the proteins and alter in their in vivo modifications. Many procedures have been taken place to stop the action of these endogenous enzymes. With the new PIRL-DIVE technology, the homogenization process occurs in milliseconds. Our hypothesis came to light that because of this ultrafast process of homogenization the tissue via PIRL-DIVE the time frame of exposure of cellular proteins to endogenous enzymes is minimized which enables soft desorption of proteins from tissues. The results obtained from separation both PH and MH from porcine muscle tissue in 2DE and analysis via LC-MS/MS indicated a lower number of intact protein species, much more proteolysis products detected in mechanical homogenate (MH) compared to PIRL homogenate (PH). Based on these results, it was shown that the action of the endogenous enzymes such as proteases and phosphatases cause alterations in the exact chemical composition of proteins, and the impact of these endogenous enzymes was clearly seen in MH rather than in PH. Furthermore, a significantly higher number of proteins in the three biological replicates of rat pancreas and considerably higher number of all the three biological replicates were identified in PH. From spiked rat pancreas with alpha casein experiment, a significantly larger number of intact Alpha-S1casein was detected in the case of PH compared to MH. Moreover, the recovery rate of phosphopeptides of Alpha-S2-casein was significantly higher in PH compared to MH. Summing up the results, it can be concluded that due to the ultrafast homogenization process of tissues via PIRL-DIVE, the cellular proteome exposed to endogenous enzymes in a minimal time frame compared to mechanical. This leads to reduced effects of these endogenous enzymes on the proteins in PH. The absence of particles in PH reduces the loss of protein via adsorption compared to MH. From one sample, several PH aliquots can apply to different proteomic approaches without further sample preparation and without caring about

buffer compatibility to each approach unlike in MH. Using PIRL-DIVE for homogenization of tissues in the future will enable studying of the proteome in their exact chemical composition. This will help to understand the molecular mechanisms in healthy and diseased situations and to design new protein biomarkers that can reach the clinical market successfully.

b) Zusammenfassung

Eines der wesentlichen Ziele der Proteomforschung ist die Entwicklung neuer diagnostischer und therapeutischer Anwendungen. Die kleinste Einheit des Proteoms ist die Proteinspezies. Die exakte chemische Zusammensetzung einer Proteinspezies bestimmt deren Funktion. Verändert sich die chemische Zusammensetzung, ergibt dies eine neue Proteinspezies. Die Veränderung der exakten chemischen Zusammensetzung der Proteine *in vitro* ist eine der wesentlichen Probleme bei der Untersuchung ihres *in vivo*-Zustandes. Bei der Homogenisierung von Geweben werden die Zellmembranen zerstört und somit die Kompartimentierung aufgehoben, so dass endogene Enzyme mit den zellulären Proteinen in Kontakt treten. Die endogenen Enzyme können dabei die Proteine degradieren oder auf andere Art chemisch verändern. Es existieren mehrere Möglichkeiten, diese Enzyme zu inhibieren. Mit der PIRL-DIVE-Technologie findet die Homogenisierung innerhalb von Millisekunden statt. Unserer Hypothese nach wird der Kontakt der zellulären Proteine mit den endogenen Enzymen durch den extrem schnellen Homogenisierungsschritt stark minimiert. Die Ergebnisse der 2D-Gelelektrophorese und der LC-MS/MS-Analyse deuteten auf eine niedrigere Anzahl intakter Proteine sowie eine höhere Menge an Proteolyseprodukten in den mechanisch homogenisierten (MH) im Vergleich zu den PIRL-homogenisierten (PH) Proben. Diese Ergebnisse lassen darauf schließen, dass die exakte chemische Zusammensetzung der Proteine durch die endogenen Enzyme in den MH-Proben verändert wurde. In den PH-Proben des Rattenpankreas wurde eine signifikant höhere Zahl an Proteinen als in den MH-Proben identifiziert. Gleichzeitig war der Anteil der reproduzierbaren Identifizierungen (drei biologische Replikate) höher. In den mit alpha-Casein gespickten Rattenpankreasproben wurde eine signifikant größere Menge alpha-S1-Casein im PIRL-Homogenat nachgewiesen. Weiterhin war die Wiederfindungsrate von Phosphopeptiden des alpha-S2-Casein signifikant höher. Zusammengefasst kann festgestellt werden, dass das zelluläre Proteom durch die ultraschnelle Homogenisierung mit PIRL-DIVE weniger den Veränderungen durch endogene Enzyme unterliegt als bei der mechanischen Homogenisierung. Da das PIRL-Homogenat frei von Partikeln ist, treten weniger Adsorptionsverluste auf. Von einer PIRL-homogenisierten Probe können diverse Aliquots für verschiedene Analysen genutzt werden, ohne dass Komplikationen durch bei der mechanischen Homogenisierung genutzte Puffer und Lösungen auftreten. Die PIRL-DIVE-Homogenisierung von Gewebeproben wird in Zukunft die Analyse der exakten chemischen Zusammensetzung des Proteoms erleichtern und damit zum besseren Verständnis der molekularen Mechanismen von Krankheitsbildern sowie zur Entwicklung neuer Proteinbiomarker beitragen.

6 Abbreviations

2DE	Two-Dimensional Electrophoresis
ACN	Acetonitrile
AGC	Automatic Gain Control
ACE	Angiotensin-Converting Enzyme
a.u.	Arbitrary Units
BPC	Base Peak Chromatogram
BCA	Bicinchoninic Acid
BSA	Bovine serum albumin
BEH	Ethylene Bridged Hybrid
°C	Celsius
cm ²	Square Centimeter
DDA	Data Dependant Acquisition
DTT	Dithiothreitol
DIVE	Desorption by Impulsive Vibrational Excitation
DNA	Deoxyribonucleic Acid
EIC	Extracted Ion Chromatogram
ESI	Electrospray Ionization
eV	Electron-Volt
et al.	et alii
FDA	Food and Drug Administration
FA	Formic Acid
H ₂ O	Water
HCL	Hydrochloric Acid
HPLC	High pressure liquid chromatography
Hz	Hertz
IR	Infrared
J	Joule
kDa	Kilo Dalton
kV	Kilovolt
Q	Quadrupole
Laser	Light Amplification by Stimulated Emission of Radiation
LC	Liquid Chromatography
LFQ	Label-free Quantitation

L	Liter
min	Minutes
MW	Molecular Weight
MS	Mass Spectrometry
MS/MS	Tandem Mass Spectrometry
MTH	Mechanical Tissue Homogenization
MH	Mechanical Homogenate
MeOH	Methanol
Mr	Molecular Mass
m/z	Mass to Charge Ratio
M	Molar
mg	Milligrams
nm	Nanometre
mm	Millimetre
mA	Milliampere
nanoUPLC	nano-Ultra Pressure Liquid Chromatography
nanoESI	nano-Electrospray ionisation
NH ₄ HCO ₃	Ammonium Bicarbonate
Nd:YLF	Neodymium-Doped Yttrium Lithium Fluoride
Nd:YAG	Neodymium-Doped Glass
OPA	Optical Parametric Amplifier
PMSF	Phenylmethylsulfonyl Fluoride
PIRL	Picosecond-Infrared-Laser
PH	PIRL-Homogenate
PTH	PIRL-Tissue-Homogenization
PBS	Phosphate Buffered Saline
RP	Reverse Phase
ps	Picosecond
pMol	Picomole
RNA	Ribonucleic Acid
RT	Room Temperature
rpm	Revolutions per Minute
SDS-PAGE	Sodium Dodecyl Sulphate-Polyacrylamide Gel Electrophoresis
SDS	Sodium Dodecyl Sulfate

Sec	Second
TOF	Time of flight
Tris	Tris (hydroxymethyl) aminomethane
T	Temperature
UV	Ultra Violet
V	Volt
W	Watt
μ	Micro-
μg	Microgram
μm	Micrometre

7 References

1. Kwiatkowski, M., et al., *Homogenization of tissues via picosecond-infrared laser (PIRL) ablation: Giving a closer view on the in-vivo composition of protein species as compared to mechanical homogenization*. J Proteomics, 2016. **134**: p. 193-202.
2. Berg, J.M., J. Tymoczko, and L. Stryer, *Biochemistry*. New York, 2006.
3. Cooper, G.M., *The central role of enzymes as biological catalysts*. 2000.
4. Lodish, H., et al., *Overview of Membrane Transport Proteins*. 2000.
5. Bean, A.J., *Protein trafficking in neurons*. 2006: Academic Press.
6. O'Farrell, P.H., *High resolution two-dimensional electrophoresis of proteins*. J Biol Chem, 1975. **250**(10): p. 4007-21.
7. Graves, P.R. and T.A. Haystead, *Molecular biologist's guide to proteomics*. Microbiol Mol Biol Rev, 2002. **66**(1): p. 39-63; table of contents.
8. Klose, J., *Protein mapping by combined isoelectric focusing and electrophoresis of mouse tissues. A novel approach to testing for induced point mutations in mammals*. Humangenetik, 1975. **26**(3): p. 231-43.
9. Wilkins, M.R., et al., *Progress with proteome projects: why all proteins expressed by a genome should be identified and how to do it*. Biotechnol Genet Eng Rev, 1996. **13**: p. 19-50.
10. Wasinger, V.C., et al., *Progress with gene-product mapping of the Mollicutes: Mycoplasma genitalium*. Electrophoresis, 1995. **16**(7): p. 1090-4.
11. Anderson, N.L. and N.G. Anderson, *Proteome and proteomics: new technologies, new concepts, and new words*. Electrophoresis, 1998. **19**(11): p. 1853-61.
12. Tyers, M. and M. Mann, *From genomics to proteomics*. Nature, 2003. **422**(6928): p. 193-7.
13. Fields, S., *Proteomics. Proteomics in genomeland*. Science, 2001. **291**(5507): p. 1221-4.
14. Twyman, R.M., *Principles of proteomics*. 2013: Garland Science.
15. Pandey, A. and M. Mann, *Proteomics to study genes and genomes*. Nature, 2000. **405**(6788): p. 837-46.
16. Periago, P.M., et al., *Identification of proteins involved in the heat stress response of Bacillus cereus ATCC 14579*. Applied and Environmental Microbiology, 2002. **68**(7): p. 3486-3495.
17. Patterson, S.D. and R.H. Aebersold, *Proteomics: the first decade and beyond*. Nat Genet, 2003. **33 Suppl**: p. 311-23.

18. Olsen, J.V. and M. Mann, *Status of large-scale analysis of post-translational modifications by mass spectrometry*. Mol Cell Proteomics, 2013. **12**(12): p. 3444-52.
19. Ren, R.J., et al., *Proteomics of protein post-translational modifications implicated in neurodegeneration*. Transl Neurodegener, 2014. **3**(1): p. 23.
20. Witze, E.S., et al., *Mapping protein post-translational modifications with mass spectrometry*. Nat Methods, 2007. **4**(10): p. 798-806.
21. Abu-Farha, M., F. Elisma, and D. Figeys, *Identification of protein-protein interactions by mass spectrometry coupled techniques*. Adv Biochem Eng Biotechnol, 2008. **110**: p. 67-80.
22. Gingras, A.C., et al., *Analysis of protein complexes using mass spectrometry*. Nat Rev Mol Cell Biol, 2007. **8**(8): p. 645-54.
23. Boersema, P.J., A. Kahraman, and P. Picotti, *Proteomics beyond large-scale protein expression analysis*. Curr Opin Biotechnol, 2015. **34**: p. 162-70.
24. Freeman, W.M. and S.E. Hemby, *Proteomics for protein expression profiling in neuroscience*. Neurochem Res, 2004. **29**(6): p. 1065-81.
25. Patel, S., *Role of proteomics in biomarker discovery: prognosis and diagnosis of neuropsychiatric disorders*. Adv Protein Chem Struct Biol, 2014. **94**: p. 39-75.
26. Johann, D.J., Jr., et al., *Clinical proteomics and biomarker discovery*. Ann N Y Acad Sci, 2004. **1022**: p. 295-305.
27. Yates, J.R., C.I. Ruse, and A. Nakorchevsky, *Proteomics by mass spectrometry: approaches, advances, and applications*. Annu Rev Biomed Eng, 2009. **11**: p. 49-79.
28. Aebersold, R. and M. Mann, *Mass spectrometry-based proteomics*. Nature, 2003. **422**(6928): p. 198-207.
29. Eidhammer, I., et al., *Computational methods for mass spectrometry proteomics*. 2008: John Wiley & Sons.
30. Fenn, J.B., et al., *Electrospray ionization for mass spectrometry of large biomolecules*. Science, 1989. **246**(4926): p. 64-71.
31. Karas, M., D. Bachmann, and F. Hillenkamp, *Influence of the wavelength in high-irradiance ultraviolet laser desorption mass spectrometry of organic molecules*. Analytical Chemistry, 1985. **57**(14): p. 2935-2939.
32. Cottrell, J.S., *Protein identification using MS/MS data*. J Proteomics, 2011. **74**(10): p. 1842-51.
33. Mann, M., R.C. Hendrickson, and A. Pandey, *Analysis of proteins and proteomes by mass spectrometry*. Annu Rev Biochem, 2001. **70**: p. 437-73.

34. Chait, B.T., *Chemistry. Mass spectrometry: bottom-up or top-down?* Science, 2006. **314**(5796): p. 65-6.
35. Breuker, K., et al., *Top-down identification and characterization of biomolecules by mass spectrometry.* J Am Soc Mass Spectrom, 2008. **19**(8): p. 1045-53.
36. Aebersold, R. and M. Mann, *Mass-spectrometric exploration of proteome structure and function.* Nature, 2016. **537**(7620): p. 347-55.
37. Bogdanov, B. and R.D. Smith, *Proteomics by FTICR mass spectrometry: top down and bottom up.* Mass Spectrom Rev, 2005. **24**(2): p. 168-200.
38. Hondermarck, H., *Proteomics: Biomedical and Pharmaceutical Applications.* 2004: Springer.
39. Gundry, R.L., et al., *Preparation of proteins and peptides for mass spectrometry analysis in a bottom-up proteomics workflow.* Curr Protoc Mol Biol, 2009. **Chapter 10**: p. Unit10.25.
40. Patterson, S.D., *Proteomics: evolution of the technology.* Biotechniques, 2003. **35**(3): p. 440-4.
41. Eriksson, J. and D. Fenyo, *Improving the success rate of proteome analysis by modeling protein-abundance distributions and experimental designs.* Nat Biotechnol, 2007. **25**(6): p. 651-5.
42. Anderson, N.L. and N.G. Anderson, *The human plasma proteome: history, character, and diagnostic prospects.* Mol Cell Proteomics, 2002. **1**(11): p. 845-67.
43. Chandramouli, K. and P.Y. Qian, *Proteomics: challenges, techniques and possibilities to overcome biological sample complexity.* Hum Genomics Proteomics, 2009. **2009**.
44. Rifai, N., M.A. Gillette, and S.A. Carr, *Protein biomarker discovery and validation: the long and uncertain path to clinical utility.* Nat Biotechnol, 2006. **24**(8): p. 971-83.
45. Righetti, P.G., et al., *How to bring the "unseen" proteome to the limelight via electrophoretic pre-fractionation techniques.* Biosci Rep, 2005. **25**(1-2): p. 3-17.
46. Hodge, K., et al., *Cleaning up the masses: exclusion lists to reduce contamination with HPLC-MS/MS.* Journal of proteomics, 2013. **88**: p. 92-103.
47. Jungblut, P., et al., *Resolution power of two-dimensional electrophoresis and identification of proteins from gels.* Electrophoresis, 1996. **17**(5): p. 839-47.
48. Jungblut, P.R., et al., *The speciation of the proteome.* Chem Cent J, 2008. **2**: p. 16.
49. Schluter, H., et al., *Finding one's way in proteomics: a protein species nomenclature.* Chem Cent J, 2009. **3**: p. 11.

50. Jungblut, P.R., B. Thiede, and H. Schluter, *Towards deciphering proteomes via the proteoform, protein speciation, moonlighting and protein code concepts*. *J Proteomics*, 2016. **134**: p. 1-4.
51. He, Q.Y. and J.F. Chiu, *Proteomics in biomarker discovery and drug development*. *J Cell Biochem*, 2003. **89**(5): p. 868-86.
52. Zimny-Arndt, U., et al., *Classical proteomics: two-dimensional electrophoresis/MALDI mass spectrometry*. *Methods Mol Biol*, 2009. **492**: p. 65-91.
53. Braun, R.J., et al., *Two-dimensional electrophoresis of membrane proteins*. *Analytical and bioanalytical chemistry*, 2007. **389**(4): p. 1033-1045.
54. Ong, S.E. and A. Pandey, *An evaluation of the use of two-dimensional gel electrophoresis in proteomics*. *Biomol Eng*, 2001. **18**(5): p. 195-205.
55. Bunai, K. and K. Yamane, *Effectiveness and limitation of two-dimensional gel electrophoresis in bacterial membrane protein proteomics and perspectives*. *J Chromatogr B Analyt Technol Biomed Life Sci*, 2005. **815**(1-2): p. 227-36.
56. Gygi, S.P., et al., *Evaluation of two-dimensional gel electrophoresis-based proteome analysis technology*. *Proc Natl Acad Sci U S A*, 2000. **97**(17): p. 9390-5.
57. Jungblut, P.R., et al., *Comparative proteome analysis of Helicobacter pylori*. *Mol Microbiol*, 2000. **36**(3): p. 710-25.
58. Rosal-Vela, A., et al., *Identification of multiple transferrin species in the spleen and serum from mice with collagen-induced arthritis which may reflect changes in transferrin glycosylation associated with disease activity: The role of CD38*. *J Proteomics*, 2016. **134**: p. 127-37.
59. Jungblut, P.R., *The proteomics quantification dilemma*. *J Proteomics*, 2014. **107**: p. 98-102.
60. Doerr, A., *Top-down mass spectrometry*. *Nature Methods*, 2008. **5**(1): p. 24-24.
61. Zhang, H. and Y. Ge, *Comprehensive analysis of protein modifications by top-down mass spectrometry*. *Circ Cardiovasc Genet*, 2011. **4**(6): p. 711.
62. Armirotti, A. and G. Damonte, *Achievements and perspectives of top-down proteomics*. *Proteomics*, 2010. **10**(20): p. 3566-76.
63. Bodzon-Kulakowska, A., et al., *Methods for samples preparation in proteomic research*. *J Chromatogr B Analyt Technol Biomed Life Sci*, 2007. **849**(1-2): p. 1-31.
64. Sciences, G.H.L., *Protein Sample Preparation Handbook*. Vol. 28-9887-41 AB.
65. Huber, L.A., K. Pfaller, and I. Vietor, *Organelle proteomics: implications for subcellular fractionation in proteomics*. *Circ Res*, 2003. **92**(9): p. 962-8.

66. Chaiyarit, S. and V. Thongboonkerd, *Comparative analyses of cell disruption methods for mitochondrial isolation in high-throughput proteomics study*. Analytical biochemistry, 2009. **394**(2): p. 249-258.
67. Weiss, W. and A. Görg, *Sample solubilization buffers for two-dimensional electrophoresis*. 2D PAGE: Sample Preparation and Fractionation, 2008: p. 35-42.
68. Burden, D.W., *Guide to the homogenization of biological samples*. Random Primers, 2008. **7**: p. 1-14.
69. Wu, Q., et al., *Proteome studies on liver tissue in a phenobarbital-induced rat model*. European journal of pharmacology, 2011. **670**(2): p. 333-340.
70. D'Souza, R., et al., *Detection and characterization of interleukin-1 in human dental pulps*. Arch Oral Biol, 1989. **34**(5): p. 307-13.
71. Canas, B., et al., *Trends in sample preparation for classical and second generation proteomics*. J Chromatogr A, 2007. **1153**(1-2): p. 235-58.
72. Kim, J., et al., *Proteome analysis of human liver tumor tissue by two-dimensional gel electrophoresis and matrixassisted laser desorption/ionization-mass spectrometry for identification of disease-related proteins*. Electrophoresis, 2002. **23**(24): p. 4142-4156.
73. Howell, K.E., E. Devaney, and J. Gruenberg, *Subcellular fractionation of tissue culture cells*. Trends in biochemical sciences, 1989. **14**(2): p. 44-47.
74. Gruenberg, J. and K.E. Howell, *Fusion in the endocytic pathway reconstituted in a cell-free system using immuno-isolated fractions*. Prog Clin Biol Res, 1988. **270**: p. 317-31.
75. Jiang, L., L. He, and M. Fountoulakis, *Comparison of protein precipitation methods for sample preparation prior to proteomic analysis*. J Chromatogr A, 2004. **1023**(2): p. 317-20.
76. von Hagen, J., *Proteomics sample preparation*. 2008: John Wiley & Sons.
77. Feist, P. and A.B. Hummon, *Proteomic challenges: sample preparation techniques for microgram-quantity protein analysis from biological samples*. Int J Mol Sci, 2015. **16**(2): p. 3537-63.
78. Hashemitabar, G.R., G.R. Razmi, and A. Naghibi, *Trials to induce protective immunity in mice and sheep by application of protoscolex and hydatid fluid antigen or whole body antigen of Echinococcus granulosus*. J Vet Med B Infect Dis Vet Public Health, 2005. **52**(5): p. 243-5.

79. Ryan, E.D. and W.H. Walker, *Influence of tissue homogenization techniques on levels of estrogen and progesterone receptors measured in calf uterus and human breast tumors*. J Immunoassay, 1980. **1**(4): p. 463-74.
80. Oda, K., *New families of carboxyl peptidases: serine-carboxyl peptidases and glutamic peptidases*. J Biochem, 2012. **151**(1): p. 13-25.
81. Skehel, J.M., *Preparation of extracts from animal tissues*. Methods Mol Biol, 2004. **244**: p. 15-20.
82. Olivieri, E., B. Herbert, and P.G. Righetti, *The effect of protease inhibitors on the two-dimensional electrophoresis pattern of red blood cell membranes*. Electrophoresis, 2001. **22**(3): p. 560-5.
83. Botker, H.E., et al., *Analytical evaluation of high energy phosphate determination by high performance liquid chromatography in myocardial tissue*. J Mol Cell Cardiol, 1994. **26**(1): p. 41-8.
84. McNulty, D.E. and J.R. Slemmon, *Peptide proteomics*. Protein Purification Protocols, 2004: p. 411-423.
85. Clynen, E., et al., *Peptidomics of the pars intercerebralis-corpora cardiacum complex of the migratory locust, Locusta migratoria*. Eur J Biochem, 2001. **268**(7): p. 1929-39.
86. Svensson, M., et al., *Heat stabilization of the tissue proteome: a new technology for improved proteomics*. J Proteome Res, 2009. **8**(2): p. 974-81.
87. Scopes, R., *Protein Purification Principles and Practice 3rd Edition (Cantor CR ed) pp. 270-277 Springer-Verlag*. New York, 1994.
88. Fágáin, C.Ó., *Storage of pure proteins*. Protein Purification Protocols, 1996: p. 339-356.
89. J, S.R., *Purifying Proteins from Proteomics: A Laboratory Manual*. 2004, CSHL Press, New York.
90. Minamino, N., et al., *Determination of endogenous peptides in the porcine brain: possible construction of peptidome, a fact database for endogenous peptides*. J Chromatogr B Analyt Technol Biomed Life Sci, 2003. **792**(1): p. 33-48.
91. Beynon, R.J. and J.S. Bond, *Proteolytic enzymes: a practical approach*. 1989: IRL Press at Oxford University Press.
92. Kawasaki, H. and K. Suzuki, *Separation of peptides dissolved in a sodium dodecyl sulfate solution by reversed-phase liquid chromatography: removal of sodium dodecyl sulfate from peptides using an ion-exchange precolumn*. Anal Biochem, 1990. **186**(2): p. 264-8.

93. Diaz, J.I., L.H. Cazares, and O.J. Semmes, *Tissue sample collection for proteomics analysis*. *Methods Mol Biol*, 2008. **428**: p. 43-53.
94. Emmert-Buck, M.R., et al., *Laser capture microdissection*. *Science*, 1996. **274**(5289): p. 998-1001.
95. Ornstein, D.K., et al., *Proteomic analysis of laser capture microdissected human prostate cancer and in vitro prostate cell lines*. *Electrophoresis*, 2000. **21**(11): p. 2235-42.
96. Best, C.J. and M.R. Emmert-Buck, *Molecular profiling of tissue samples using laser capture microdissection*. *Expert Rev Mol Diagn*, 2001. **1**(1): p. 53-60.
97. Espina, V., et al., *Laser capture microdissection*. *Methods Mol Biol*, 2006. **319**: p. 213-29.
98. Vandermoere, F., et al., *Proteomics in Oncology: the Breast Cancer Experience*, in *Proteomics: Biomedical and Pharmaceutical Applications*. 2004, Springer. p. 139-161.
99. Solon, L.R., R. Aronson, and G. Gould, *Physiological implications of laser beams*. *Science (New York, NY)*, 1961. **134**(3489): p. 1506-1508.
100. McGuff, P.E., et al. *STUDIES OF THE SURGICAL APPLICATIONS OF LASER (LIGHT AMPLIFICATION BY STIMULATED EMISSION OF RADIATION)*. in *Surg. Forum, 14: 143-5 (1963)*. 1963. Tufts-New England Center Hospital, Boston.
101. Franjic, K. and D. Miller, *Vibrationally excited ultrafast thermodynamic phase transitions at the water/air interface*. *Phys Chem Chem Phys*, 2010. **12**(20): p. 5225-39.
102. Franjic, K., et al., *Laser selective cutting of biological tissues by impulsive heat deposition through ultrafast vibrational excitations*. *Opt Express*, 2009. **17**(25): p. 22937-59.
103. Amini-Nik, S., et al., *Ultrafast mid-IR laser scalpel: protein signals of the fundamental limits to minimally invasive surgery*. *PLoS One*, 2010. **5**(9).
104. Miller, R.D., *Mapping atomic motions with ultrabright electrons: The chemists' Gedanken experiment enters the lab frame*. *Annual review of physical chemistry*, 2014. **65**: p. 583-604.
105. Ren, L., et al., *Towards instantaneous cellular level bio diagnosis: laser extraction and imaging of biological entities with conserved integrity and activity*. *Nanotechnology*, 2015. **26**(28): p. 284001.

106. Kwiatkowski, M., et al., *Ultrafast extraction of proteins from tissues using desorption by impulsive vibrational excitation*. *Angew Chem Int Ed Engl*, 2015. **54**(1): p. 285-8.
107. Linke, S.J., et al., *A New Technology for Applanation Free Corneal Trephination: The Picosecond Infrared Laser (PIRL)*. *PloS one*, 2015. **10**(3): p. e0120944.
108. Jowett, N., et al., *Bone ablation without thermal or acoustic mechanical injury via a novel picosecond infrared laser (PIRL)*. *Otolaryngol Head Neck Surg*, 2014. **150**(3): p. 385-93.
109. Böttcher, A., et al., *A novel tool in laryngeal surgery: preliminary results of the picosecond infrared laser*. *The Laryngoscope*, 2013. **123**(11): p. 2770-2775.
110. Mulisch M., W.U., *18 ed. Spektrum Akademischer Verlag; Heidelberg: 2010. Romeis Mikroskopische Technik*.
111. Kwiatkowski, M., et al., *Ultrafast extraction of proteins from tissues using desorption by impulsive vibrational excitation*. *Angewandte Chemie International Edition*, 2015. **54**(1): p. 285-288.
112. Smith, P.K., et al., *Measurement of protein using bicinchoninic acid*. *Anal Biochem*, 1985. **150**(1): p. 76-85.
113. Desjardins, P., J.B. Hansen, and M. Allen, *Microvolume spectrophotometric and fluorometric determination of protein concentration*. *Curr Protoc Protein Sci*, 2009. **Chapter 3**: p. Unit 3.10.
114. Scientific, T.F., <http://www.nanodrop.com/library/nd-1000-v3.7-users-manual-8.5x11.pdf>.
115. Fanun, M., S. Makharza, and M. Sowwan, *UV-Visible and AFM Studies of Nonionic Microemulsions*. *Journal of Dispersion Science and Technology*, 2010. **31**(4): p. 501-511.
116. Healthcare, G. *2-D quant kit*.
https://www.gelifesciences.com/gehcls_images/GELS/Related%20Content/Files/1314729545976/litdoc28954714AE_20110830215136.pdf.
117. Klose, J. and U. Kobalz, *Two-dimensional electrophoresis of proteins: an updated protocol and implications for a functional analysis of the genome*. *Electrophoresis*, 1995. **16**(6): p. 1034-59.
118. Shevchenko, A., et al., *In-gel digestion for mass spectrometric characterization of proteins and proteomes*. *Nat Protoc*, 2006. **1**(6): p. 2856-60.

119. Cox, J. and M. Mann, *MaxQuant enables high peptide identification rates, individualized p.p.b.-range mass accuracies and proteome-wide protein quantification*. Nat Biotechnol, 2008. **26**(12): p. 1367-72.
120. Cox, J., et al., *Accurate proteome-wide label-free quantification by delayed normalization and maximal peptide ratio extraction, termed MaxLFQ*. Mol Cell Proteomics, 2014. **13**(9): p. 2513-26.
121. Jungblut, P.R., *Back to the future--the value of single protein species investigations*. Proteomics, 2013. **13**(21): p. 3103-5.
122. Ahmed, M.M. and K.J. Gardiner, *Preserving protein profiles in tissue samples: differing outcomes with and without heat stabilization*. J Neurosci Methods, 2011. **196**(1): p. 99-106.
123. Jowett, N., et al., *Heat generation during ablation of porcine skin with erbium:YAG laser vs a novel picosecond infrared laser*. JAMA Otolaryngol Head Neck Surg, 2013. **139**(8): p. 828-33.
124. Petersen, H., et al., *Comparative study of wound healing in rat skin following incision with a novel picosecond infrared laser (PIRL) and different surgical modalities*. Lasers Surg Med, 2016. **48**(4): p. 385-91.
125. Bottcher, A., et al., *Reduction of thermocoagulative injury via use of a picosecond infrared laser (PIRL) in laryngeal tissues*. Eur Arch Otorhinolaryngol, 2015. **272**(4): p. 941-8.
126. Anderson, N.L., et al., *Global approaches to quantitative analysis of gene-expression patterns observed by use of two-dimensional gel electrophoresis*. Clin Chem, 1984. **30**(12 Pt 1): p. 2031-6.
127. Rogowska-Wrzesinska, A., et al., *2D gels still have a niche in proteomics*. J Proteomics, 2013. **88**: p. 4-13.
128. Heil, A., et al., *The amino-acid sequence of sarcosine adenylate kinase from skeletal muscle*. Eur J Biochem, 1974. **43**(1): p. 131-44.
129. Fry, D.C., S.A. Kuby, and A.S. Mildvan, *ATP-binding site of adenylate kinase: mechanistic implications of its homology with ras-encoded p21, F1-ATPase, and other nucleotide-binding proteins*. Proc Natl Acad Sci U S A, 1986. **83**(4): p. 907-11.
130. Di Luca, A., et al., *Centrifugal drip is an accessible source for protein indicators of pork ageing and water-holding capacity*. Meat Sci, 2011. **88**(2): p. 261-70.

131. Di Luca, A., et al., *Monitoring post mortem changes in porcine muscle through 2-D DIGE proteome analysis of Longissimus muscle exudate*. Proteome Sci, 2013. **11**(1): p. 9.
132. Wallimann, T., et al., *Intracellular compartmentation, structure and function of creatine kinase isoenzymes in tissues with high and fluctuating energy demands: the 'phosphocreatine circuit' for cellular energy homeostasis*. Biochem J, 1992. **281** (Pt 1): p. 21-40.
133. Lametsch, R., P. Roepstorff, and E. Bendixen, *Identification of protein degradation during post-mortem storage of pig meat*. J Agric Food Chem, 2002. **50**(20): p. 5508-12.
134. Lin, L., et al., *Radiation hybrid mapping of the pig ALDOA, ALDOB and ALDOC genes to SSC3, SSC1 and SSC12*. Anim Genet, 2004. **35**(1): p. 66-7.
135. Lundby, A., et al., *Quantitative maps of protein phosphorylation sites across 14 different rat organs and tissues*. Nat Commun, 2012. **3**: p. 876.
136. Huttlin, E.L., et al., *A tissue-specific atlas of mouse protein phosphorylation and expression*. Cell, 2010. **143**(7): p. 1174-89.
137. Zhang, X., et al., *Novel tyrosine phosphorylation sites in rat skeletal muscle revealed by phosphopeptide enrichment and HPLC-ESI-MS/MS*. J Proteomics, 2012. **75**(13): p. 4017-26.
138. Watanabe, T., et al., *Three trypsinogens from rat pancreas*. FEBS Lett, 1980. **121**(2): p. 369-71.
139. Schick, J., H. Kern, and G. Scheele, *Hormonal stimulation in the exocrine pancreas results in coordinate and anticoordinate regulation of protein synthesis*. J Cell Biol, 1984. **99**(5): p. 1569-74.
140. Laemmli, U.K., *Cleavage of structural proteins during the assembly of the head of bacteriophage T4*. Nature, 1970. **227**(5259): p. 680-5.
141. Greener, T., et al., *Role of cyclin G-associated kinase in uncoating clathrin-coated vesicles from non-neuronal cells*. J Biol Chem, 2000. **275**(2): p. 1365-70.
142. Potts, R.C., et al., *CHD5, a brain-specific paralog of Mi2 chromatin remodeling enzymes, regulates expression of neuronal genes*. PLoS One, 2011. **6**(9): p. e24515.
143. Bagchi, A. and A.A. Mills, *The quest for the Ip36 tumor suppressor*. Cancer Res, 2008. **68**(8): p. 2551-6.
144. Rebsamen, M., et al., *SLC38A9 is a component of the lysosomal amino acid sensing machinery that controls mTORC1*. Nature, 2015. **519**(7544): p. 477-81.

145. Gerhard, D.S., et al., *The status, quality, and expansion of the NIH full-length cDNA project: the Mammalian Gene Collection (MGC)*. *Genome Res*, 2004. **14**(10b): p. 2121-7.
146. Strausberg, R.L., et al., *Generation and initial analysis of more than 15,000 full-length human and mouse cDNA sequences*. *Proc Natl Acad Sci U S A*, 2002. **99**(26): p. 16899-903.
147. Stingl, C., et al., *Uncovering effects of ex vivo protease activity during proteomics and peptidomics sample extraction in rat brain tissue by oxygen-18 labeling*. *J Proteome Res*, 2014. **13**(6): p. 2807-17.
148. Rabilloud, T. and C. Lelong, *Two-dimensional gel electrophoresis in proteomics: a tutorial*. *J Proteomics*, 2011. **74**(10): p. 1829-41.
149. Chen, E.I., et al., *Optimization of mass spectrometry-compatible surfactants for shotgun proteomics*. *J Proteome Res*, 2007. **6**(7): p. 2529-38.
150. RK, S., *Protein Purification: Principles and Practice*. 3 ed. 1994, New York: Springer-Verlag.
151. Yi, J., C. Kim, and C.A. Gelfand, *Inhibition of intrinsic proteolytic activities moderates preanalytical variability and instability of human plasma*. *J Proteome Res*, 2007. **6**(5): p. 1768-81.
152. Anderson, N.L., *The clinical plasma proteome: a survey of clinical assays for proteins in plasma and serum*. *Clin Chem*, 2010. **56**(2): p. 177-85.
153. Fuzery, A.K., et al., *Translation of proteomic biomarkers into FDA approved cancer diagnostics: issues and challenges*. *Clin Proteomics*, 2013. **10**(1): p. 13.
154. Obuchowski, N.A., M.L. Lieber, and F.H. Wians, Jr., *ROC curves in clinical chemistry: uses, misuses, and possible solutions*. *Clin Chem*, 2004. **50**(7): p. 1118-25.
155. Sackett, D.L. and R.B. Haynes, *The architecture of diagnostic research*. *Bmj*, 2002. **324**(7336): p. 539-41.
156. Pace, C.N., *Determination and analysis of urea and guanidine hydrochloride denaturation curves*. *Methods Enzymol*, 1986. **131**: p. 266-80.
157. Giansanti, P., et al., *Six alternative proteases for mass spectrometry-based proteomics beyond trypsin*. 2016. **11**(5): p. 993-1006.
158. Cole, E.G. and D.K. Mecham, *Cyanate formation and electrophoretic behavior of proteins in gels containing urea*. *Anal Biochem*, 1966. **14**(2): p. 215-22.
159. Lane, N.M., Z.R. Gregorich, and Y. Ge, *Top-Down Proteomics*, in *Manual of Cardiovascular Proteomics*. 2016, Springer. p. 187-212.

160. Aebersold, R. and M. Mann, *Mass-spectrometric exploration of proteome structure and function*. Nature, 2016. **537**(7620): p. 347-355.
161. Jensen, S.S. and M.R. Larsen, *Evaluation of the impact of some experimental procedures on different phosphopeptide enrichment techniques*. Rapid Commun Mass Spectrom, 2007. **21**(22): p. 3635-45.
162. Karve, T.M. and A.K. Cheema, *Small changes huge impact: the role of protein posttranslational modifications in cellular homeostasis and disease*. J Amino Acids, 2011. **2011**: p. 207691.
163. Murray, C.I., et al., *Post-translational Modifications in the Cardiovascular Proteome*, in *Manual of Cardiovascular Proteomics*. 2016, Springer. p. 293-320.
164. Stewart, II, T. Thomson, and D. Figeys, *¹⁸O labeling: a tool for proteomics*. Rapid Commun Mass Spectrom, 2001. **15**(24): p. 2456-65.
165. Speicher, K.D., et al., *Systematic analysis of peptide recoveries from in-gel digestions for protein identifications in proteome studies*. J Biomol Tech, 2000. **11**(2): p. 74-86.

8 Appendix

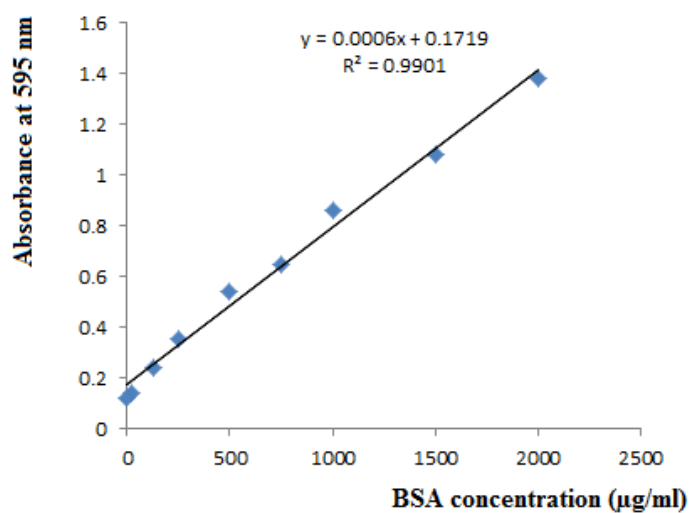


Figure 42: BSA standard curve for protein determination by BCA method of PIRL and mechanical homogenates from porcine muscle tissue. The absorbance of the protein from 10x diluted sample from PIRL homogenate was 0.2499, the protein concentration in PIRL homogenate according to the linear equation $c = 1.3 \mu\text{g}/\mu\text{L}$. The absorbance of the protein from 10x diluted sample from mechanical homogenate was 0.2397, the protein concentration in mechanical homogenate according to the linear equation $c = 1.1 \mu\text{g}/\mu\text{L}$.

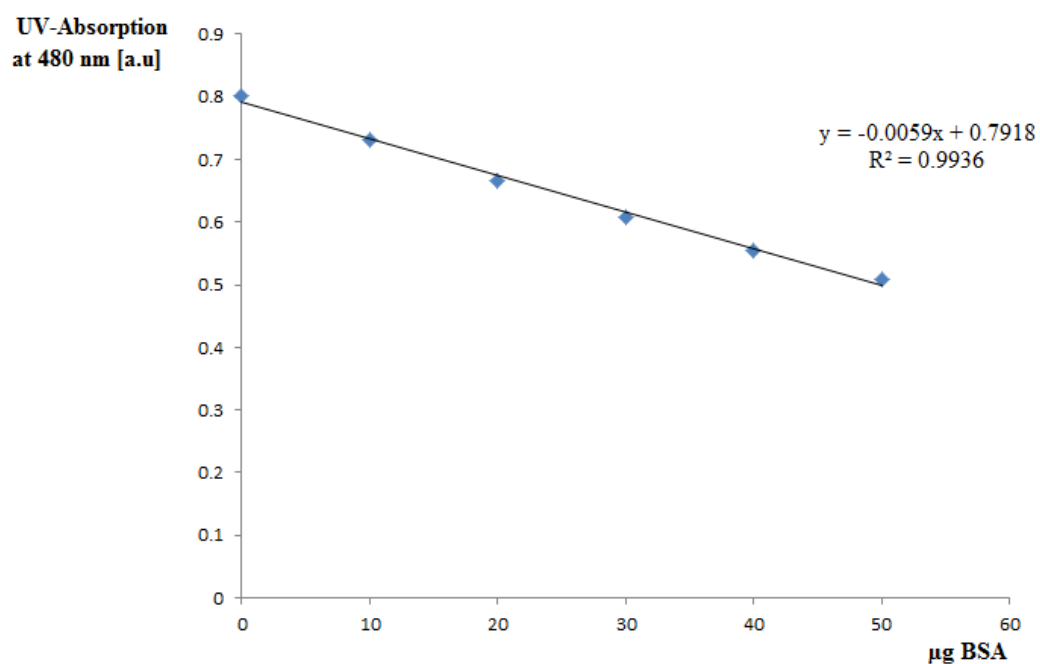


Figure 43: BSA calibration curve for protein determination by 2-D quant method of protein extracts from mechanical homogenates of the rat pancreas no.1 and 2. The UV-Absorption of 1 μL of mechanical homogenate from rat pancreas no.1 at 480 nm was 0.633, and the protein concentration was according to the linear equation $c = 26.9 \mu\text{g} / \mu\text{L}$. The UV-Absorption of 1 μL of mechanical homogenate from rat pancreas no.2 at 480 nm was 0.688, and the protein concentration was according to the linear equation $c = 17.6 \mu\text{g} / \mu\text{L}$.

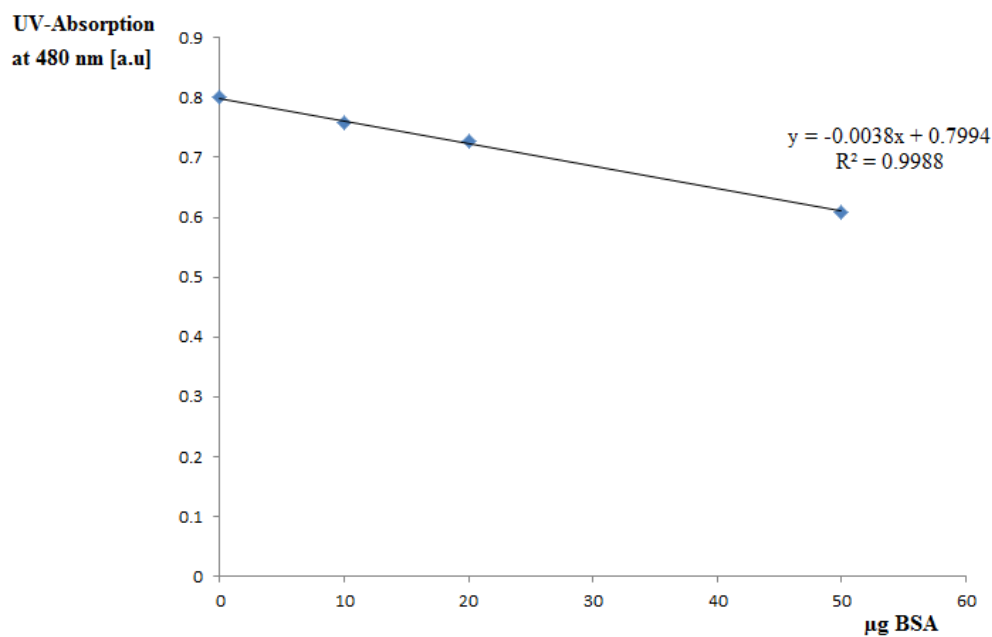
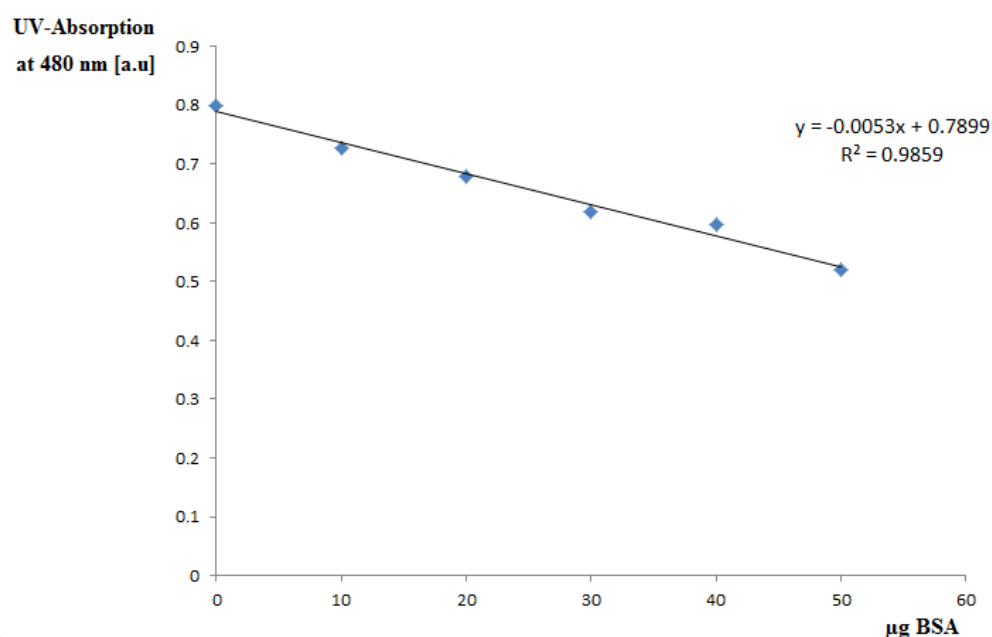


Figure 44: BSA calibration curve for protein determination by 2-D quant method of protein extracts from PIRL homogenates of the rat pancreas no.1 and 2. The UV-Absorption of 30 µL of PIRL homogenate from rat pancreas no.1 at 480 nm was 0.26, and the protein concentration was according to the linear equation $c = 4.7 \mu\text{g} / \mu\text{L}$. The UV-Absorption of 30 µL of PIRL homogenate from rat pancreas no.2 at 480 nm was 0.198 and the protein concentration was according to the linear equation $c = 5.3 \mu\text{g} / \mu\text{L}$.

A)



B)

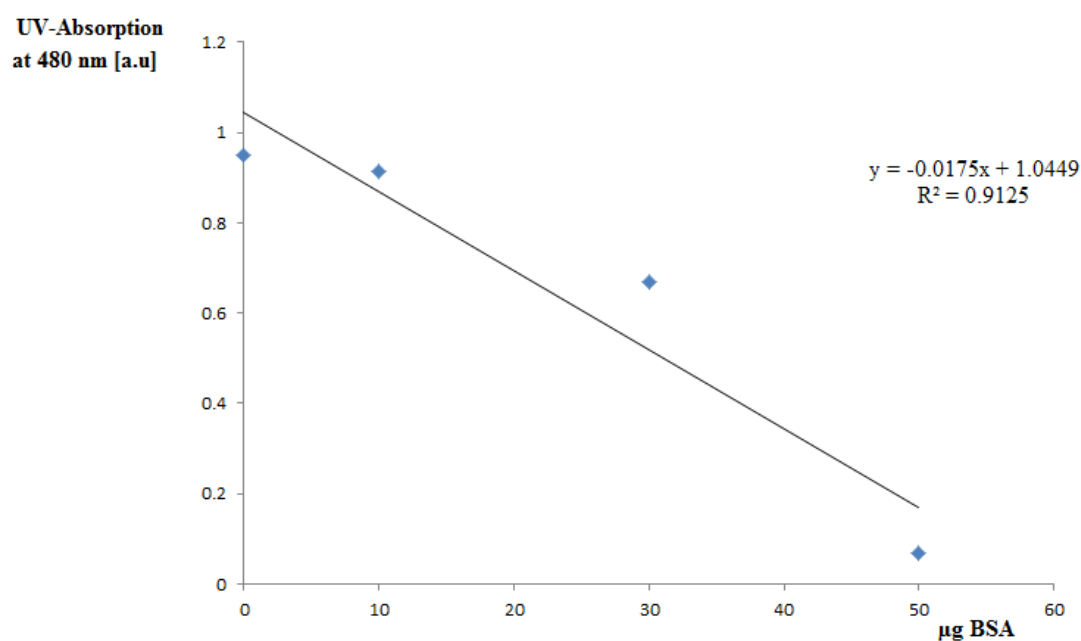


Figure 45: BSA calibration curve for protein determination by 2-D quant method of protein extracts from PIRL and mechanical homogenates of the rat pancreas no.3. A. BSA calibration curve for protein determination of protein extracts from mechanical homogenate. The UV-Absorption of 1 µL of mechanical homogenate from rat pancreas no.3 at 480 nm was 0.621, and the protein concentration was according to the linear equation $c = 31.7 \mu\text{g}/\mu\text{L}$. B. BSA calibration curve for protein determination of protein extracts from PIRL homogenate. The UV-Absorption of 10 µL of PIRL homogenate from rat pancreas no.3 at 480 nm was 0.7 and the protein concentration was according to the linear equation $c = 2.0 \mu\text{g}/\mu\text{L}$.

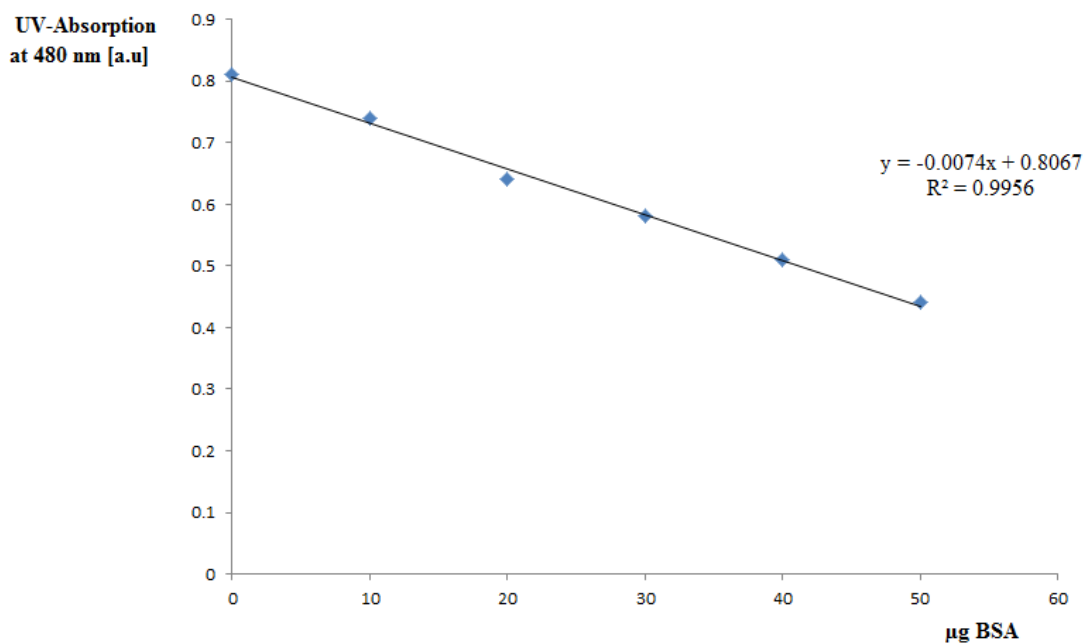


Figure 46: BSA calibration curve for protein determination by 2-D quant method of protein extracts from PIRL and mechanical homogenates of the three rat pancreas spiked with alpha-casein. The UV-Absorption of 15 μL of PIRL homogenate from rat pancreas spiked with alpha-casein no.1 at 480 nm was 0.571, and the protein concentration was according to the linear equation $c = 2.1 \mu\text{g} / \mu\text{L}$. The UV-Absorption of 15 μL of PIRL homogenate from rat pancreas spiked with alpha-casein no.2 at 480 nm was 0.431, and the protein concentration was according to the linear equation $c = 3.4 \mu\text{g} / \mu\text{L}$. The UV-Absorption of 15 μL of PIRL homogenate from rat pancreas spiked with alpha-casein no.3 at 480 nm was 0.421 and the protein concentration was according to the linear equation $c = 3.4 \mu\text{g} / \mu\text{L}$. The UV-Absorption of 5 μL of mechanical homogenate from rat pancreas spiked with alpha-casein no.1 at 480 nm was 0.471 and the protein concentration was according to the linear equation $c = 9.1 \mu\text{g} / \mu\text{L}$. The UV-Absorption of 5 μL of mechanical homogenate from rat pancreas spiked with alpha-casein no.2 at 480 nm was 0.431 and the protein concentration was according to the linear equation $c = 10.1 \mu\text{g} / \mu\text{L}$. The UV-Absorption of 5 μL of mechanical homogenate from rat pancreas spiked with alpha-casein no.3 at 480 nm was 0.471 and the protein concentration was according to the linear equation $c = 9.1 \mu\text{g} / \mu\text{L}$.

9 Acknowledgement

First of all, I pray and thank Almighty Allah who has given me the patience and insistence to complete this work.

I would like to express my deepest gratitude and thanks to my Supervisor Prof. Dr. Hartmut Schlüter, not only for giving me the opportunity to work under his supervision and providing me with a very interesting topic but because his support, kind supervision and patience. I learned a lot from discussing scientific issues, his way in generating ideas and simplifying concepts.

My deepest thanks to PD Dr. Friedrich Buck for his valuable discussions of the theoretical and practical issues in a friendly and understandable way, his assistance in QTOF measurements, and for editing and proofreading my thesis.

Many thanks also to my thesis committee: Prof.Dr.Dr.med. Udo Schumacher (Institute of Anatomy and Experimental Morphology) and Prof. Dr. med. Tobias Lange who gave me the opportunity to use some instruments and tools in the Anatomy department and for their supervision as members of my thesis committee.

I also want to thank Prof. Dr. Dwayne Miller, for giving me the opportunity to work with the impressive new technology “the picosecond infrared laser”.

Also, special thanks to the members in the working group of Prof. Miller: Dr. Nils-Owe Hansen, Sebastian Kruber , and Stephanie Uschold for their kind assistance during ablation experiments.

I also want to thank Dr. Hannes Petersen (Workgroup Prof. Dr. Rainald Knecht) for providing me with rat pancreas samples.

I want to thank Tobias Gosau (working group of Prof. Dr. Udo Schumacher) for his technical assistant in obtaining rat pancreas samples.

Thank you for Dr. Karola Lehmann of Proteome Factory Company in Berlin for making 2DE gels.

Special thanks to Dr. Marcel Kwiatkowski for extremely assisting me in the theoretical and practical aspects in this work.

Many thanks to my colleague Marcus Wurlitzer for his assistant in statistical and bioinformatical parts, his beneficial discussions, and for translating the summary part to German language.

Many thanks also to Sönke Harder, for spreading a nice lab work atmosphere and for his practical assistance.

I want to thank also Andrey Krutilin for our time working together in PIRL and for valuable discussions.

Many thanks to Marceline Manka Fuh for help editing the final draft of the dissertation.

To all my colleagues in the working group: Parnian Kiani, Maryam Omid, Pascal Steffen, Olga Krauss, Laura Heikaus, and Atef Manna thank you very much and best wishes to all of you.

Not forgetting my previous colleagues Dr. Diana Deterra and Dr. Verena Richter, thank you.

I express my appreciation also to The German Academic Exchange Service (DAAD) for funding my study and living expenses in Germany.

Finally, my deepest appreciation goes to my dear father and mother. Without them I could not reach this point, and to my wonderful wife Feda' for her love and support and to my sweet sons Laith & Omar.

Thank you very much

Refat Nimer

10 Curriculum Vitae

Mein Lebenslauf wird aus datenschutzrechtlichen Gründen in der elektronischen Version meiner Arbeit nicht veröffentlicht.

Publications

- Ultrafast extraction of proteins from tissues using desorption by impulsive vibrational excitation. Kwiatkowski M, Wurlitzer M, Omid M, Ling R, Kruber S, **Nimer R**, Robertson W, Horst A, Miller RJ Dwayne, Schlüter H. *Angew Chem Int Ed. Engl.* 2015 Jan 2;54(1):285-8
Desorption durch impulsive Anregung intramolekularer Vibrationszustände – eine Methode zur schnellen Extraktion von Proteinen aus intakten Geweben. *Angew. Chem.* 2015, 127, 287 –290
DOI: 10.1002/anie.201407669 (English Version)
DOI: 10.1002/ange.201407669 (German Version)
- Homogenization of tissues via picosecond-infrared laser (PIRL) ablation: Giving a closer view on the in-vivo composition of protein species as compared to mechanical homogenization. M. Kwiatkowski, M. Wurlitzer, A. Krutilin, P. Kiani, **R. Nimer**, M. Omid, A. Mannaa, T. Bussmann, K. Bartkowiak, S. Kruber, S. Uschold, P. Steffen, J. Lübberstedt, N. Küpker, H. Petersen, R. Knecht, N.O. Hansen, A. Zarrine-Afsar, W.D. Robertson, R.J.D. Miller, H. Schlüter. *Journal of proteomics* 134 (2016): 193-202.

Poster presentations

- Investigation of the composition of protein mixtures extracted from muscle tissue with a picoseconds infrared laser.
Refat Nimer, Marcel Kwiatkowski, Sebastian Kruber, R. J. Dwayne Miller, Hartmut Schlüter.
48th Annual Meeting of the German Society for Mass Spectrometry (DGMS), 01.03-04.03.2015, Wuppertal.
- Comparison by differential proteomics of protein extraction from muscle tissue by a picosecond-infrared-laser versus a classical method.
Refat Nimer, R.J.Dwayne Miller, Hartmut Schluter.
1st UKE Graduate Day, 26.02.2015, Hamburg.
- Efficiency of tissue homogenization via picosecond-infrared laser (PIRL) and classical homogenization as sample preparation step for proteomics.
Refat Nimer, Marcel Kwiatkowski, Nils-Owe Hansen, R.J.Dwayne Miller, Hartmut Schluter.
49th Annual Meeting of the German Society for Mass Spectrometry (DGMS), 28.02-02.03.2016, Hamburg.

Talks

- Comparison by differential proteomics of protein extraction from muscle tissue by a picosecond-infrared-laser versus a classical method.
Refat Nimer, 1st UKE Graduate Day, 26.02.2015, Hamburg.

11 Eidesstattliche Versicherung

Ich versichere ausdrücklich, dass ich die Arbeit selbständig und ohne fremde Hilfe verfasst, andere als die von mir angegebenen Quellen und Hilfsmittel nicht benutzt und die aus den benutzten Werken wörtlich oder inhaltlich entnommenen Stellen einzeln nach Ausgabe (Auflage und Jahr des Erscheinens), Band und Seite des benutzten Werkes kenntlich gemacht habe.

Ferner versichere ich, dass ich die Dissertation bisher nicht einem Fachvertreter an einer anderen Hochschule zur Überprüfung vorgelegt oder mich anderweitig um Zulassung zur Promotion beworben habe.

Ich erkläre mich einverstanden, dass meine Dissertation vom Dekanat der Medizinischen Fakultät mit einer gängigen Software zur Erkennung von Plagiaten überprüft werden kann.

Nimer, Refat

Hamburg, den 25.10.2016